EXPERIMENTAL STUDY OF SIMPLE AND MULTI-LEAF MASONRY SLENDER ELEMENTS UNDER COMPRESSIVE STRESS LOADED PARALLEL TO THE FACE

Joan Llorens Sulivera

DOCTORAL THESIS

Experimental study of simple and multi-leaf masonry slender elements under compressive stress loaded parallel to the face.

Joan Llorens Sulivera

2020

DOCTORAL THESIS

Experimental study of simple and multi-leaf masonry slender elements under compressive stress loaded parallel to the face.

Joan Llorens Sulivera

2020

Doctoral Programme in Technology

Supervised by:

Dr. Miquel Àngel Chamorro Trenado
Universitat de Girona

Dr. Miquel Llorens Sulivera
Universitat de Girona

Tutor:

Dr. Miquel Àngel Chamorro Trenado
Universitat de Girona

Presented to obtain the degree of PhD at the University of Girona

Universitat de Girona

Dr. Miquel Angel Chamorro Trenado, of Department of Architecture and Construction Engineering, University of Girona

and

Dr. Miquel Llorens Sulivera, Department of Mechanical Engineering and Industrial Construction, University of Girona.

WE DECLARE:

That the thesis titles *Experimental study of simple and multi-leaf masonry slender elements under compressive stress, loaded parallel to the face* presented by Joan Llorens Sulivera to obtain a doctoral degree, has been completed under our supervision

For all intents purposes, I hereby sign this document.

Dr. Miquel Angel Chamorro Trenado
Universitat de Girona

Dr. Miquel Llorens Sulivera
Universitat de Girona

Girona, March 2020

”

The devil is in the detail

(Anonymous)

Acknowledgement

This thesis would not have been possible without the collaboration and support of many people around me. I would like to thank the dedication and support received by my thesis supervisors Dr. Miquel Angel Chamorro and Dr. Miquel Llorens. Without your advice this thesis would never have seen daylight. I would also like to appreciate the indispensable collaboration of the laboratory staff, and in particular Mr. Pere Bellvehí, as well as Roman Demchuk, Albert Massegú, Ester Pérez, Alba Mallorquín, Carles Hernández, Pere Danés, Joaquim Romero, Sònia Sánchez, Adrián González, Llorenç Gironès and Aleix Costa, who had contributed to the demanding work in the laboratory.

I would also like acknowledge to Dra. Cristina Barris for her support and advice, as well as Mr. Jordi Gómez for their invaluable support in the DIC test.

To the Department of Architecture and Construction Engineering for the assistance in the laboratory work. To my colleagues in the Architectural Construction area for the continuous encouragement in the ups and downs experienced during this time.

I would like to thank of Col·legi d'Aparelladors, Arquitectes Tècnics i Enginers de l'Edificació de Girona for their contribution to the funding of this thesis

Finally, to my family for their understanding and esteem and especially to Lluc and Arlet for the stolen time.

List of Publications

Based on this thesis the following peer-reviewed journal papers have been prepared:

- J. Llorens, M. Llorens, M.A. Chamorro, J. Soler, Experimental Behavior of Brick Masonry under Uniaxial Compression on Parallel-to-Face Brick. Single-Leaf Case Study, International Journal of Architectural Heritage. 14 (2020) 23–37. doi:10.1080/15583058.2018.1503361. ISSN: 1558-3058, Impact Factor: 1.345/1.44, ranked 12/111 in Engineering Architecture (1st quartile) and ranked 35/63 in Construction and Building Technology (3st quartile).
- J. Llorens, M. Llorens, M.A. Chamorro, J. Gómez, C. Barris, Experimental study on the vertical interface of thin tile masonry. Submitted to Construction and Building Materials, 2020. ISSN: 0950:0618, Impact Factor: 4.046, ranked 9/63 in Construction and Building Technology (1st quartile).

List of Symbols

E_b	Young's modulus of the brick
E_{ci}	Young's modulus of the inner leaves
E_{co}	Young's modulus of the outer leaves
E_k	Young's modulus of the masonry computed at 1/3 of f_k
E_{kt}	Young's modulus of the thin-tile masonry computed at 1/3 of f_{kt}
$E_{m50\text{-}30}$	Young's modulus of the mortar computed as the value of slope linear interval within the 30-50% of the Ultimate stress
f_b	Compressive strength of the brick and tile
f'_b	Normalized compressive strength of the brick
$f_{c,e}$	Compressive strength of the outer leaves
$f_{c,i}$	Compressive strength of the inner leaves
f_k	Peak compressive strength of the masonry

f_{kt}	Peak compressive strength of the thin-tile masonry
f_{kti}	Compressive strength of the thin-tile masonry
f_{ktd}	Detachment compressive strength of the thin-tile masonry
f_m	Compressive strength of the mortar
$f_{wc,0}$	Compressive strength of the multi-leaf wall
k	Empirical corrective factor to take into account the influence of variations of the bonds of the masonry and the type of brick used in overall behaviour of the load-bearing brick masonry
t_{c1}	Thickness of the thin-tile leaf 1
t_{c2}	Thickness of the thin-tile leaf 2
t_m	Thickness of the mortar leaf
t_t	Total thickness of the specimen
V_e	Volume of the outer *leaf*
V_i	Volume of the inner *leaf*
V_w	Volume of the total wall
α	Empirical corrective factor to take into account the influence of brick used in overall behaviour of the load-bearing brick masonry
β	Empirical corrective factor to take into account the influence of mortar in overall behaviour of the load-bearing brick masonry

ε Strain corresponding to uniaxial compressive strength

σ Stress

θ_e Empirical corrective factor to take into account influence of outer leaves in overall behaviour of wall

θ_i Empirical corrective factor to take into account influence of inner leaves in overall behaviour of wall

Contents

List of Figures

List of Tables

Abstract

The thin-tile vault is a structural system widely used in the Mediterranean area that extends to the United States through the constructions carried out there by the Valencian architect Rafael Guastavino. Although there is evidence of the use of the thin-tile masonry vault as a main structure since the 14th century, probably the most spectacular development took place in the late 19th century through modernist-style buildings designed by architects such as Antonio Gaudí, Luís Domènech and Muntaner or Luís Muncunill to name a few of them.

Thin-tile vault, from a morphological standpoint, is made up of one or more leaf of thin-tile lay flat, and joined with plaster or lime or cement mortar. As a particularity of this arrangement, the load is applied parallel to the face of the thin-tile as opposed to the load-bearing masonry walls, where the load is applied perpendicularly to it.

From the perspective of structural behaviour, two main models have been used since the 19th century: the equilibrium-based approach and the elastic or cohesive-based approach. The first one conceives the vault as a series of voussoirs in equilibrium among them subjected to the effect of gravitational loads. In the second one, the vault is analyses as an element built with a single material with cohesive characteristics. These characteristics are obtained from the properties of its constituent materials (thin tiles and

mortar) and their homogenisation through the process of hydration of the binding material (gypsum, cement lime). Thus, the vault is subjected exclusively to compressive stresses in the equilibrium-based approach, whiles the existence of tensile stresses is to be considered in the cohesive-based approach.

Two different approaches have been used to analyse the compressive strength of the vault: a) at a complete structural system level. In this case the resource has been the load test. Load has been applied either in existing buildings or in complete specimens in laboratory conditions. b) at a structural component level. The compressive strength tests - and other type of tests - have been performed on sets of samples. There is little documented evidence of this kind in the literature.

To establish the compressive strength through experimental tests is a slow and expensive procedure. In masonry, simple equations involving the compressive strength of the constituent materials (brick and mortar) are often used to determine it. Thus, the main objective of this thesis is to ascertain whether the equations proposed in the standards and literature for different types of masonry can be useful for predicting the compressive strength of the thin-tile masonry. For this purpose, and based on the experimental results on one-leaf, two-leaf, and three-leaf thin-tile specimens, stress-strain law, failure modes, and mechanical properties have been analysed and compared with those corresponding to different masonries presented in the literature. After a thorough analysis, the main conclusions are drawn.

Resum

La volta catalana és un sistema estructural àmpliament utilitzat en l'àrea mediterrània, que de la mà de l'arquitecte Rafael Guastavino va saltar als Estats Units d'Amèrica. Tot i que hi ha evidències de l'ús de la volta ceràmica com a estructura principal des del segle XIV, potser el desplegament més espectacular es va produir al final del segle XIX, a través d'edificis d'estil modernista dissenyats per arquitectes com Antoni Gaudí, Lluís Domènech i Muntaner, i Lluís Muncunill, entre d'altres.

La volta catalana, des d'un vessant morfològica, està constituïda per una combinació d'una o diverses fulles de rajoles col·locades planes, i unides amb guix o morter de calç o ciment. Una particularitat d'aquesta disposició de les rajoles és que la càrrega és aplicada paral•lela a la cara de la rajola en contraposició a la fàbrica de rajol de les parets de càrrega on la càrrega és aplicada perpendicularment a aquesta.

Des de la perspectiva del comportament estructural, dos models, principalment, han estat utilitzats des del segle XIX: l'aproximació basada en l'equilibri i l'aproximació basada en l'elasticitat o cohesió. La primera concep la volta com una sèrie de dovelles, en equilibri entre elles, enfront de càrregues gravitatòries. La segona analitza la volta com un element format per un únic material cohesiu, obtingut a partir de les propietats dels seus materials constituents (rajoles i morter), homogeneïtzats a través del procés d'hidratació del material conglomerant (guix, cal o ciment). Així, la volta està subjecte exclusivament a tensions de compressió en l'aproximació basada en l'equilibri, mentre que l'existència de tensions a tracció, són considerades en l'aproximació basada en la cohesió.

Dues aproximacions diferents s'han utilitat per analitzar la resistència a compressió de la volta: a) a escala de sistema estructural complet. En aquest cas el recurs ha estat la prova de càrrega. La càrrega és aplicada tant a edificis existents com a voltes completes en condicions de laboratori. b) a escala de component estructural. Els assaigs de resistència a compressió, i altres tipus d'assaig, s'han realitzat en conjunts de provetes. Existeix poca evidència d'aquest tipus de proves en la literatura.

Determinar la resistència a compressió a través d'assaig sobre provetes és un procediment lent i car. En obra de fàbrica, normalment s'intenta establir aquesta resistència a partir dels materials constituents (peça i morter). Així, el principal objectiu de la tesi és comprovar si les equacions presents a les normes i la literatura per a diferents tipus de fàbrica, poden ser útils per predir la resistència a compressió de la fàbrica de rajola. Amb aquest objectiu, i a partir dels resultats experimentals obtinguts en provetes de fàbrica de rajola d'una, dues i tres fulles, el comportament tensió-deformació, el mode de falla i les propietats mecàniques s'analitzen i es comparen amb aquelles corresponents a diferents fàbriques presents en la literatura, Després d'una anàlisi minuciosa, s'extreuen les principals conclusions.

Resumen

La bóveda tabicada es un sistema estructural ampliamente utilizado en el área mediterránea que, de la mano del arquitecto Rafael Guastavino, dio el salto a los Estados Unidos de América. Aunque existen evidencias del uso de la bóveda tabicada como estructura principal desde el siglo XIV, quizás el despliegue más espectacular se produjo a finales del siglo XIX a través de edificios de estilo modernista diseñados por arquitectos como Antonio Gaudí, Luís Domènech y Muntaner y Luís Muncunill, entre otros.

La bóveda tabicada, desde una perspectiva morfológica, está constituida por una combinación de una o varias hojas de rasilla colocadas planas, y unidas con yeso o mortero de cal o cemento. Una particularidad de esta disposición de las rasillas es que la carga es aplicada paralelamente a la cara de la pieza en contraposición a la fábrica de ladrillo de las paredes de carga, que la carga es aplicada perpendicularmente a esta.

Desde la perspectiva del comportamiento estructural se han usado principalmente dos modelos a lo largo del siglo XIX: la aproximación basada en el equilibrio y la aproximación basada en la elasticidad o cohesión. La primera concibe la bóveda como una serie de dovelas en equilibrio entre ellas frente a cargas gravitatorias. La segunda analiza la bóveda como un elemento constituido por un único material cohesivo, obtenido a partir de las propiedades de sus materiales constituyentes (rasillas y mortero), homogeneizados a

través del proceso de hidratación del material conglomerante (yeso, cal o cemento). Así, la bóveda está sujeta exclusivamente a tensiones de compresión en la aproximación basada en el equilibrio, mientras que la existencia de tensiones de tracción, son consideradas en la aproximación basada en la cohesión.

Dos distintas aproximaciones se han usado para analizar la resistencia a compresión de la bóveda: a) a escala de sistema estructural completo. En este caso el recurso ha sido la prueba de carga. La carga se ha aplicado en edificios existentes así como en bóvedas completas en condiciones de laboratorio. b) a escala de componente estructural. Los ensayos de resistencia a compresión, y otros tipos de ensayos, se han realizado en conjunto de probetas. Existe poca evidencia de este tipo de ensayos en la literatura.

Determinar la resistencia a compresión a través de ensayos sobre probetas es un procedimiento lento y caro. En obra de fábrica, normalmente se intenta establecer dicha resistencia a partir de las propiedades de los materiales constituyentes (pieza y mortero). Así pues, el principal objetivo de esta tesis es comprobar si las ecuaciones presentes en las normas y en la literatura para distintos tipos de fábrica, pueden ser útiles para predecir la resistencia a compresión de la fábrica de baldosas. Con este objetivo, y a partir de los resultados experimentales sobre probetas de rasillas de una, dos y tres hojas, se analizan el comportamiento tensión-deformación, el modo de fallo y las propiedades mecánicas y se comparan con aquellas correspondientes a distintos tipos de obra de fábrica presentes en la literatura. Después de un análisis minucioso, se extraen las principales conclusiones.

1. Introduction

1.1. General introduction

Masonry is a traditional structural system, widely used throughout history until today, in buildings that are part of the Built Heritage, but also in those belonging to popular architecture. Well known its use for the construction of walls, it has also been used in other structural systems such as arches and vaults. From a morphological point of view, it is formed by pieces that can be made of different materials such as stone, ceramic or rammed earth. Normally the pieces are joined with a binder such as gypsum, lime or cement mortar, although can also be built without.

1.1.1. The thin-tile vault

A particular case of masonry as a structural system in the form of a vault, built with ceramic pieces, is the thin-tile vault. This kind of vault has been broadly used, along the last centuries, in the construction of buildings, and can be found in many countries of the Mediterranean area and more recently, in the United States of America. Its preservation as a Cultural Heritage is a challenge and one of the main objectives of governments and institutions.

It is characterized by the arrangement of one or more leaves of thin-tile bonded together with gypsum or lime or cement mortar. The most outstanding feature is its "in the air" construction, i.e. without the support of a centering, or with lightweight formworks. The technique consists of building a first leaf, usually with gypsum or fast-setting cement that provides a quick bond. This leaf works as a formwork, so that the following thin-tile and mortar leaves, can be built with a common binder such as cement or lime mortar. Other relevant characteristics are: reduced thickness, quick to build and the arrangement of the thin-tiles with respect to the application of the load, parallel to the face for thin-tile vault and perpendicular in masonry walls.

The origin of this structural system is unclear. Several authors (Choisy 1899; Bergós 1965) place it in the Roman era. At that time, the thin-tile vault would be used as a formwork for the concrete vaults.

Examples of thin-tile vault, also called Catalonian vault, Extremaduran vault, Roussillon vault, *volta in foglio*, *voûte, plate, timbrel vaults* or Saracen vault, dating from the beginning of the 12th century, with the vault used in the formation of the staircase vault can be found an Islamic house in Siyasa (Murcia). From the 14th century it began to be built in Catalonia, Valencia, Aragon and Extremadura. But it is in the 17th century, with its appearance in architectural treatises, when they are developed in a more extensive way (Redondo 2013). This spread continued until the 19th century through Castile (Spain), Roussillon (France), Italy, and later in Germany. The most important development in the use of thin-tile vault comes from Modernist Architecture with architects as representative as Antoni Gaudí, Lluís Domènech i Muntaner, and Lluís Muncunill, among others. It was also used by renowned architects belonging to the Modern Movement such as Le Corbusier. It is now that he makes the leap to United States of America with Rafael Guastavino (Collins 1968) (fig.1.1).

a) Steam Aymerich, Amat i Jover.

b) Hospital of the Holly Cross and Saint Paul.

Fig.1.1. Examples of Historical Building with thin-tile vault.

As indicated in (Suárez 2015) the approach to structural behaviour has evolved over time. Initially it was based on intuition. Rules based on geometric proportions were summarized in the construction treaties. Later, the focus was on reason, introducing new concepts such as equilibrium and material performance. Finally, the calculation tools arrived. From then on numerical expressions capable of objectively quantifying stress and efforts were available. Intuition, reason and calculation are complementary approaches that allow us to learn and characterize structural behaviour.

Until the 18th century, the structural behaviour of this type of vault was considered similar to voussoir vaults. The sizing was done from geometric rules, as appears explained in the architectural treatise of Fray Lorenzo de Sant Nicolás *Arte y Vso de Architectvra* (1639 y 1665), the most relevant text of construction and vault mechanics.

In 1754 the Count d'Espi wrote and published the book *Manière de rendre toutes sortes d'édifices incombustibles, ou Traité sur la Construction des Voutes, faites avec des briques et du plâtre, dites Voutes plates; et d'un Toit de brique, sans Charpente, appellé Comble Briquete*. The author differentiated the thin-tile vault from the voussoir vault (fig. 1.2) by indicating that the vault did not generate a thrust against the walls, attributing this particularity to its monolithic nature. Deepening in this idea of monolithism, in (Guastavino 1893) the author divides the masonry construction in two classes, the mechanical construction or by gravity referring to voussoir vault and the cohesive construction or by assimilation identified with the thin-tile vault.

The first one is based on the equilibrium of forces, under the gravitational action, between the different units (stone or ceramic) of the vault. The second one is based on the properties of cohesion and assimilation of several materials (thin-tile and mortar) that, due to a transformation (hydration), becomes a conglomerate material that thus acquires its monolithic nature (Gulli and Mochi 1995).

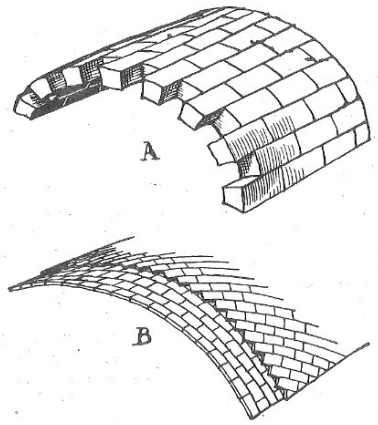

Fig.1.2. A) voussoir vault, B) thin-tile vault.

Rafael Guastavino was the first to attempt to formulate a rigorous scientific theory on the structural behaviour of the thin-tile vault (Huerta 2006; Gulli and Mochi 1995). The cohesive theory presents an elastic analysis of the thin-tile vault incorporating tensile stress and bending moment.

Therefore, in the 19th century, two different theoretical approaches to the thin-tile vault behaviour were formulated. On the one hand, the engineers of the époque applying the equilibrium based approach, which derives directly from the Safety Theorem of the Limit Analysis, and which is integrated into the geometric design rules of the architectural treatises of the ancient masters (Huerta 2001). On the other hand, the new hypothesis proposed by Guastavino, the so-called elastic approach, which defines the thin-tile vault as a homogeneous material subjected to elastic behaviour (Gulli and Mochi 1995). Today, both hypotheses still hold (Huerta 2003; Gonzalez 2004; Shin et al. 2016).

Equilibrium approach is raised and developed in (Heyman 1966). To include the structural theory of the masonry structures in the framework of the Limits Analysis, three fundamental hypotheses have to meet: a) the compressive strength of the material is infinite; b) the tensile strength of the masonry is null; c) the sliding between pieces never is reached. These conditions allow the application of the well-known plasticity limit theorems (Tralli, Alessandri, and Milani 2014).

There are many studies on different model strategies for the computational analysis of voussoir vaults (Tralli, Alessandri, and Milani 2014; Roca et al. 2010; D'Altri et al. 2019; Llopis et al. 2016). One of these strategies is the Thrust Network Analysis (TNA), developed in (Block and Ochsendorf 2007; Block, Ciblac, and Ochsendorf 2006) where the authors proposed a tool based on limit analysis for vaulted buildings. It uses the thrust lines to define the forces within masonry, and to predict possible equilibrium conditions. Collapse modes can also be obtained through the formation of a sufficient number of hinges. The application of TNA in voussoir vaults can be found in (Davis et al. 2012; Block and Lachauer 2014; Fantin and Ciblac 2016; Foti et al. 2016; Marmo et al. 2017; Fraddosio, Lepore, and Piccioni 2019; Ricci et al. 2019) among others. Concerning thin-tile vaults, several authors have also used the TNA application. For instance, in (Davis et al. 2012) authors have demonstrated the usefulness of generating new shapes of compression-only thin-tile vaults, which is a full three-dimensional equilibrium solution for the self-weight of the structure. Moreover, in (López et al. 2019) TNA was used to analyse single-curvature vaults consisting of thin-tile vaulting reinforced with concrete. Other authors (Fortea and Machado 2014) proposed the repair of vaults using an analytical model based on their own computer program. The reinforcement proposal is defined from the characteristics of a specific natural hydraulic lime (NHL) mortar formulated according to the mechanical and chemical characteristics of the existing mortar.

On the other hand, the elastic theory was developed at the beginning of the 20th century by several authors. Among others, in (Domenech 1900) the author emphasizes the need to consider the bending strength of the thin-tile vault. He argues this need on the basis

that, since the line of thrusts, generally, does not coincide with the geometry of the vault, it is necessary to count on the tensile strength of the piece and the strength of the mortar (bonding material).

In (Bayó 1910), and deepening into the need to consider bending strength, the author indicates that the thin-tile vault should be assimilated to a flexible sheets, but considering different coefficients of elasticity in tension and compression. The author indicates that, normally, the thrust line does not coincide with the geometry of the vault, being this difference the cause of the appearance of the bending stress. As indicated in (Huerta 2005), the thin-tile vault is assimilated to bi-articulated metal arches. To determine the thrust, it is necessary to define what Bayó calls the 'funicular of the static forces', so that the thrust line, in addition to being in equilibrium with the loads, should fulfil the conditions of elastic compatibility of deformation.

In (Cardellach 1910) the author associates the capacity of bending strength to two reasons: the fact of having a second leaf (duplicated leaf), and the structural quality of the constituent materials. This quality is associated with the good performance of the clay (increase in the tensile strength of the thin-tile) and to the use of Portland cement mortar. The author considers that with these two conditions (second leaf and quality of the materials) the leaves acquire the ability to transfer stresses in different directions. On the other hand, the author indicates that if the geometry and the materials allow it, a thin-tile vault could be built without thrusts. But, in the event that such thrusts exist, Cardellach considers the method of counteracting them to be a secondary issue.

As stated in (Rosell and Serrà 1987), Esteve Terradas Illa, engineer and mathematician, proposed in "llibreta de la volta" the theoretical and experimental elastic analysis of the thin-tile vault used as a base for a staircase. The author concludes that, due to the thickness of the thin-tile vault, that buckling phenomenon is the precursor to the collapse of this type of structures. The author highlighted the stiffening effect of the masonry ribs (fig. 1.3).

In (Moya 1947) the author emphasizes the importance of these ribs in enhancing the overall strength to dynamic or horizontal loads. It was also stated the influence of changes in temperature, in outdoor or exposed thin tile vaults.

In (Bosch 1949) the author defends that doubly curved thin-tile vault had a better performance in front of asymmetric and buckling loads; the non-need of second leaf of the vault. For the sake of lightness and ease in defining the constitutive model to be used in calculations, Bosch advised the use of a thin single-layered tile vault: a single-layer structure might be considered somehow as an isotropic material, what made the calculation cost far more affordable. On the other hand, in the thin tile vault, the ribs and the upper ceramic board (fig. 1.3) were considered as a unitary ensemble from a structural point of view. (Chamorro, Llorens, and Llorens 2012).

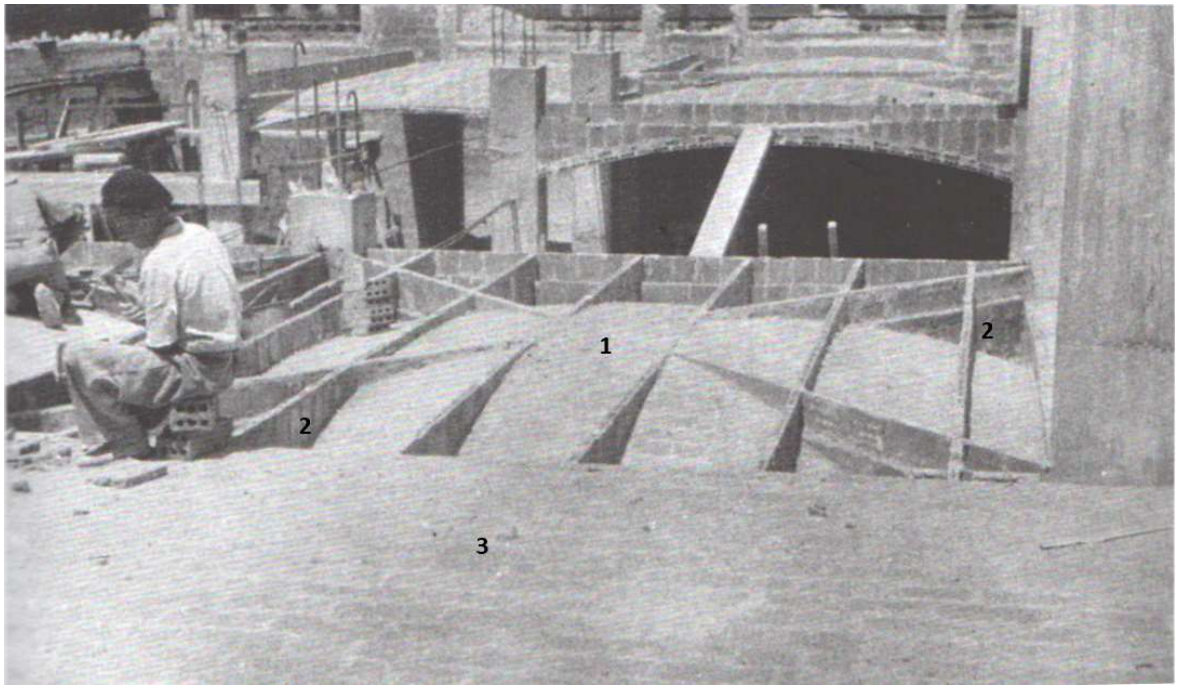

Fig.1.3. Structural unit assumed by Bosch i Reigth :Thin-tile vault (1), ribs (2) and upper slab (3) (Cabrera, Sala, and Jordi 2005).

As regards the elastic approach, in (Collins 1968) the cohesive theory was analysed defining the thin-tile vault from three fundamental perspectives: morphological, constructive and structural. From a structural point of view, the study presented by (Gulli and Mochi 1995) is particularly relevant in its two fundamental concepts: tensile strength

and absence of thrusts, based on analysis by several authors such as Guastavino himself, Antonio Gaudí, Jaume Bayó i Font or Josep Doménech i Estapá among others. The authors conclude that cohesive vault can be understood as homogeneous material structures that present two modes of structural behaviour: i) the line of thrust approximately coincide with the geometrical axis of the thin-tile vault. Therefore, it withstands compressive stresses and, due to its shape, the thrusts are clearly lower compared to those produced by a much heavier voussoir vault; ii) the thin-tile vault can absorb bending stresses through special measures in the construction phase that allow for the elastic settlement of the vault. In this second case, the vaults behave as simply supported beams, completely eliminating the thrust.

Analysing the elastic approach in great depth, in (Capozucca 1997) the author developed a method of analysis based on the Sandwich behaviour model proposed by (Flügge 1973). The proposed analytical model was a barrel vault where the outer leaves (made of thin-tile) support the maximum moment. This moment is defined as a function of the tensile strength of the lower thin-tile leaf in the central section of the vault. From comparison with experimental results on scale model tests under static loads, author concludes that the sandwich behaviour model allows the vault to be evaluated under static loading. Based on experimental values of portion of real structures in (Benfratello et al. 2010), the authors compared the experimental with analytical results from two behaviour models (homogeneous and stratified) and concluded that the results obtained encouraged in the use of the stratified model. The authors indicated the need for a deeper analysis of the thin-tile-mortar interface from the experimental and numerical point of view.

1.1.2. Experimental analysis of thin-tile masonry

The structural analysis of the thin-tile vault has been carried out at two different levels: global behaviour of the vault considered as a structural system; characterization of the masonry that builds the vault, which could be called as thin-tile masonry. In regard to the first level, the most common method has been to carry out static load tests. The reason

for performing these tests is usually to experimentally determine the suitability of the structure to withstand the imposed loads and evaluate the value of the thrust transferred to the supports. The first documented evidence of this type of test can be found in the 18th century in the south of France. Afterwards this practice spread out throughout the country because of the scientific interest of some people like the Duke of Belle Isle, the Count of Espie or later Patté i Rondelet (Redondo 2013).

This sort of static load test, with different variants, will be extended through the 19th and 20th centuries. Probably, the best documented static load tests were those carried out at the beginning of the 20th century by Rafael Guastavino. Aiming to introduce the thin-tile vault into the United States of America, and to validate the theoretical framework on which to support cohesive construction, Guastavino carried out various static load tests both on samples and on buildings already built. The first load test was performed in the Public Library of Boston (Mroszczzyk 2004) (fig. 1.4). Also, as it will be discussed below, author carried out tests to characterize the thin-tile masonry.

Fig.1.4. Static load test carried out by Rafael Guastavino (Guastavino/Collins archive. Columbia University).

At the end of the 20th century, and with the opportunity to measure displacements and deformations, the use of static load tests in vaults has spread. In (Gonzalez 2004) the author presents a static load test on a staircase thin-tile vault. The test was intended to lead to collapse, but due to the deformation of the walls, the test was halted. According to the author, the load applied at that moment was 2500 kg/m^2 and no deformation was observed in the vault. In (Atamturktur and Boothby 2007) the authors examine the spherical segmental domes built by the Guastavino Company in two buildings, the loggia domes of the City-County Building in Pittsburgh, Pennsylvania, and the reading room domes of the State Education Building in Albany, New York. The authors used experimental and analytical dynamic models to analyse if there was thrust and its magnitude. The authors concluded that significant horizontal thrust were in all elastic domes. On the other hand in (Endo et al. 2017) the authors presented studies on the static and dynamic behaviour of thin-tile vaults belonging to the so-called Administration Pavilion of the Hospital of the Holly Cross and Saint Paul (Barcelona). The authors performed one static load test and over 95 dynamic tests on thin-tile vault. Analytical simulations were then performed using finite element models (FEM). The authors conclude that the upper slab and ribs must necessarily be taken into account in both FEM models (dynamic and static).

In regard to the second level, namely, the characterisation of thin-tile masonry, the first documented evidence is described in (Guastavino 1893). In 1887, in the Department of Test and Experiments of the Fairbanks' Scale Company, together with the engineer A.V. Abbott, several tests on cement mortar and tile specimens were carried out. The tests were aimed at the characterization of compressive, tensile, shear, and bending strength. In (Redondo 2013) it is indicated that the same sort of specimen was supposed to be used for the both compressive and tensile strength test (fig 1.5).

Fig 1.5. specimen supposed to be used in compressive strength test by Guastavino (Guastavino 1893).

The author carried out a compressive strength test on 5 specimens. The first 4 were tested 5 days after manufacture. The average compressive strength value was 14.21 N/mm^2. The test on the fifth specimen was carried out after one year and presented a compressive strength of 22.68 N/mm^2.

On the other hand in (Redondo 2013) the author presents two experimental studies completed by Guastavino. The first study was carried out in 1927-1928 by Professor H.W. Hayward, was conducted at Massachusetts Institute of Technology (MIT). Compressive, tensile and shear-punch strength tests were carried out. The compressive strength tests were carried out on 12 specimens measuring 30.5x30.5 cm and two measuring 30.5x38.0 cm. According to the number of leaves (3, 4 or 5), the thicknesses were 10 cm, 14 cm and 18 cm. respectively (fig. 1.6). The curing time (i.e. time between the manufacturing of the specimen and the carrying out of the test), and in contrast to the previous tests carried out in 1887, were between 1 and 2 months. The results obtained in the compressive strength test published by the authors, can be seen in (fig.1.7).

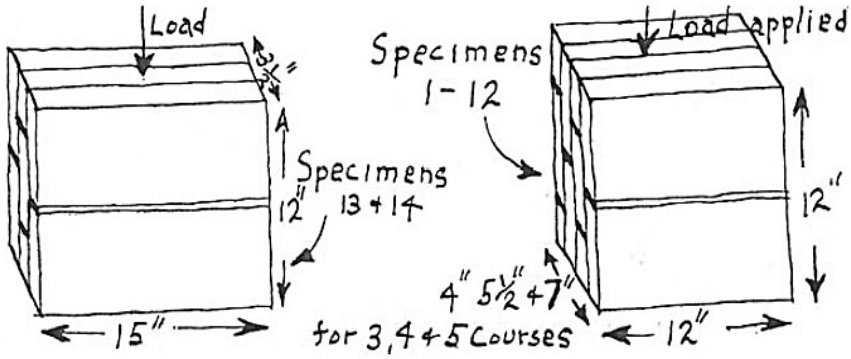

Fig. 1.6. Specimens used in test carried out at MIT in 1927 (Archive Guastavino/Collins. U. Columbia).

TEST FOR COMPRESSION.

ULTIMATE STRENGTH.

Test.	Courses.	Finish.	Backing Tile.	Date Made.	Date Tested.	Mortar.	Cross Section.	Total Load.	Load per sq. in.	Remarks.
#1	3	AKOUSTOLITH	National	3/8/27	5/5/27	Sand 2 Cement 1	48 sq. in.	118128 lbs.	2460 lbs.	Good fracture
#2	4	"	"	"	"	" " "	66 " "	193200 "	2927 "	Poor bond
#3	5	"	"	"	"	" " "	84 " "	239568 "	2852 "	Fair
	3	"	Ohio	3/14/27	"	" " "	48 " "	137890 "	2870 "	"
#5	4	"	"	"	"	" " "	66 " "	293664 "	4450 "	Good
#6	5	"	"	"	"	" " "	84 " "	337824 "	4022 "	Very good
#7	3	Hard burned reg. 6"x12"	"	3/23/27	"	" " "	48 " "	247296 "	5152 "	" "
#8	4	"	"	"	"	" " "	66 " "	218592 "	3312 "	Poor
#9	5	"	"	"	"	" " "	84 " "	370944 "	4416 "	Fair
#10	3	"	National	4/7/27	"	" " "	48 " "	160080 "	3335 "	"
#11	4	"	"	"	"	" " "	66 " "	205344 "	3111 "	"
#12	5	"	"	"	"	" " "	84 " "	314640 "	3745 "	"
13	3	Ohio Rough	Ohio	3/3/27	"	" 2½ "	54 " "	163392 "	3026 "	"
#14	3	National Rough	National	"	"	" " "	54 " "	135792 "	2515 "	Good

All tested specimens made at factory, R. Guastavino Company, Woburn, Mass.
and tested by Professor H. W. Hayward. M.I.T.

Fig.1.7. Compressive strength values from the test carried out by H.W. Hayward, in MIT in 1927 (Archive Guastavino/Collins. U. Columbia).

The maximum, minimum and average compressive strength values were 36.28, 17.32 and 24.24 N/mm^2 respectively. It can be seen that the average value is almost equal to that obtained after one year in the tests carried out in 1887. Therefore, the curing time of 5 days seems to be insufficient.

The second study was conducted by Professor A.F. Holmes, under the supervision of H.G. Protze, director of the testing laboratory at MIT in 1935. On this occasion the tests carried out attempted to determine the values of compressive, shear-puncture and bending strength. The compressive strength tests were performed on thin-tiles that had a corrugated surface (corrugations). These tests were performed on the thin-tile specimens and not on the complete thin-tile masonry arrangement (fig.1.8).

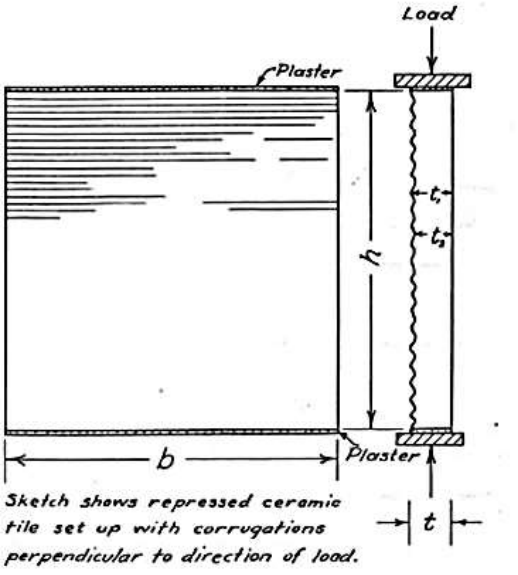

COMPRESSION TESTS.

Type of Tile	Method of Loading	Dimensions h	Dimensions Effective t	Dimensions b	Effective Area	Maximum Sustained Load	Apparent Unit Compr Stress lbs./sq.in.	Average lbs./sq.in.	Test No.	Sketches.
Hard-burned repressed ceramic tile; reg. thickness	Corrugations parallel to load direction	5 5/8"	3/4"	5 5/8"	4.22	36,600	8,680		1	
		5 5/8	3/4	5 5/8	4.22	42,200	10,000		2	
		5 1/2	3/4	5 5/8	4.22	41,900	9,930		3	
		5 1/2	3/4	5 7/16	4.18	43,600	10,430		4	
		5 7/16	3/4	5 5/8	4.22	33,900	8,040	9,420	5	
	Corrugations perpendic. to load direction	5 5/8	23/32	5 7/16	4.00	43,000	10,740		6	
		5 5/8	23/32	5 5/8	4.05	27,400	6,760		7	
		5 5/8	23/32	5 7/16	4.00	54,000	13,500		8	
		5 1/2	23/32	5 7/16	4.00	19,400	4,850		9	
		5 7/16	23/32	5 7/16	4.00	18,000	4,500	8,070	10	
Medium-burned repressed ceramic tile; reg. thickness.	Corrugations parallel to load direction	5 1/4	25/32	5 3/4	4.50	28,100	6,240		11	
		5 7/16	25/32	5 7/16	4.45	27,900	6,270		12	
		5 7/16	25/32	5 7/16	4.45	23,200	5,210		13	
		5 7/16	25/32	5 7/16	4.45	12,400	2,790		14	
		5 7/16	25/32	5 7/16	4.45	33,600	7,550	5,610	15	
	Corrugations perpendic. to load direction	5 1/4	3/4	5 3/4	4.31	17,400	4,040		16	
		5 7/16	3/4	5 7/16	4.26	14,400	3,380		17	
		5 7/16	3/4	5 7/16	4.26	19,200	4,500		18	
		5 7/16	3/4	5 7/16	4.26	20,900	4,900		19	
		5 7/16	3/4	5 7/16	4.26	9,600	2,260	3,820	20	
Akoustolith; reg. thick.	Large face parallel to load direction	5 7/8	7/8	6	5.25	5,200	990		21	
		5 7/8	7/8	6	5.25	5,840	1,110		22	
		5 7/8	7/8	6	5.25	5,730	1,090		23	
		5 7/8	7/8	6	5.25	5,840	1,110		24	
		5 7/8	7/8	6	5.25	5,020	960	1,050	25	

Fig.1.8. Geometry of specimen and compressive strength values of corrugated thin-tile rom the test carried up by A.F. Holmes in MIT in 1935 (Archive Guastavino/Collins. U. Columbia).

The test was performed on three different types of thin-tiles (hard- and medium-repressed and akoustolith) of approximately 14x14 cm. The load was applied in two directions (parallel and perpendicular) to the corrugations sense. The thickness of the specimen was

determined, as shown in (Fig. 1.7) as a relationship between the angle of the corrugations with respect to the application of the load. The authors defined two thicknesses: a) thin-tile thickness including the corrugation, b) thin-tile thickness excluding the corrugation. Thus, if the load was parallel to the corrugations, the thickness was the average of the two values, and in the opposite case, the considered thickness was the second value (b). The results obtained ranged from 66 N/mm^2 to 7.4 N/mm^2 according to the type of thin-tile and the direction of the applied load.

In (Bergós 1953) the author presents experimental values of most of the materials used in construction. The book has several chapters dedicated to masonry. Two chapters deal with the materials characterization and one is devoted to brick walls. In the chapter dedicated to bricks, different tests performed on bricks and tiles are described. Compressive, tensile, shear and flexural strength, and water absorption are determined. The properties of mortars made of different binders such as lime, natural cement or Portland cement, are described in the corresponding chapter. amount of water used for mixing, curing time, shrinkage and adhesion and compressive and tensile strength are the properties considered most important.

In the chapter where masonry walls are considered, compressive and shear strength tests were carried out on specimens manufactured using solid and hollow bricks with different mortars. Specimens used in the compressive strength tests had a dimension of 29.5 x 29.5 cm. The thickness varied depending on the type of brick used. From the results, the author analyses the incidence of some parameters such as: the type of mortar, thickness and number of bed joints of specimen or load application direction with regard to bed joints. The values obtained in specimens made of solid bricks and different kinds of mortar, with the load applied parallel (*tocho plano*) and perpendicular (*tocho de canto*) to the bed joints load are summarized below (Fig.1.9).

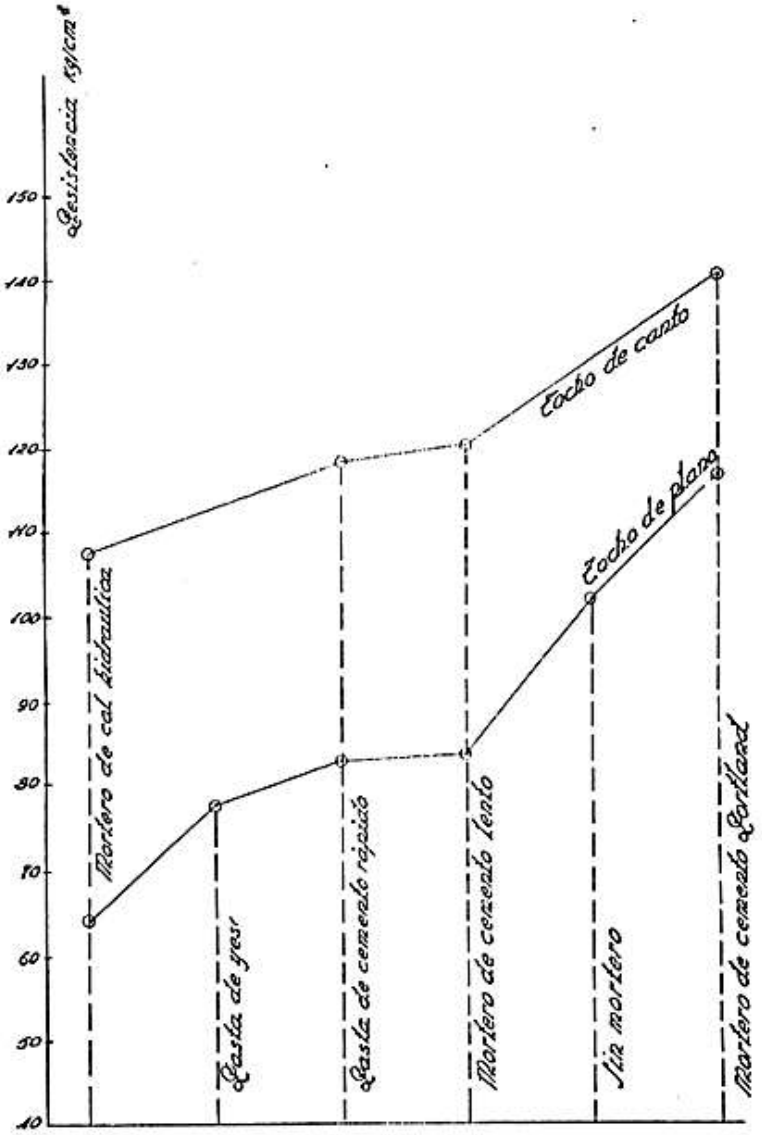

Fig. 131. — Influencia del conglomerante en la resistencia a compresión cúbica de las fábricas de ladrillo tocho.

Fig.1.9. Compressive strength values obtained by Bergós from specimens made with different mortars and with the application of the load parallel and perpendicular to the bed joints (Bergós 1953).

It can be seen that the specimens with the load applied parallel to the bed joints present higher values for compressive strength. The author indicates that the highest values are obtained when using Portland cement mortar. On the other hand the author concludes that for hollow brick masonry such a relationship remains unclear.

In (Bergós 1965) the author presents results on hollow brick walls and vaults. As in the previous work, the study covers materials, samples and construction elements such as partitions and vaults. With respect to the materials, the characterization of the brick was made for different pieces. Therefore, in (Fig. 1.9) the specimens used for the hollow brick and the simple hollow brick (hollow thin-tile) can be seen. In the first case the specimen is formed by half a piece, while in the second case different types of specimens formed by one or several pieces joined without mortar were used. In all the specimens, the tests were carried out by applying the load in the three axes (A, B and C in figure 1.10).

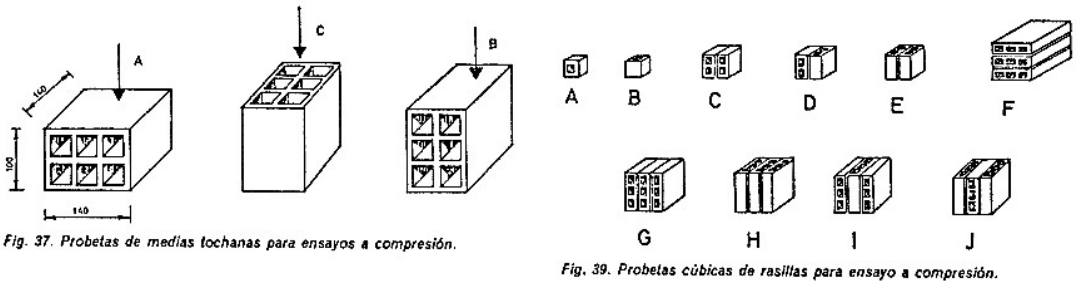

(a) (b)

Fig.1.10. Specimens of Hollow brick (a) and hollow thin-tile (b) used by Bergós in ceramic compressive strength test (Bergós 1965).

With regard to the thin-tiles, the author compared, among other parameters, the relationship between the axis of load application and compressive strength value (fig1.11.a), or the load applied up to the first crack and to failure (fig.1.11.b). In the first case, it is noted that the breaking loads increase with the increase in section, i.e. the section of the specimen minus the voids, although not proportionally. The load applied longitudinally to the voids has the highest compressive strength value. It should be mentioned that the author proposes two different values for the compressive strength: one at failure and another coinciding with the formation of the first crack.

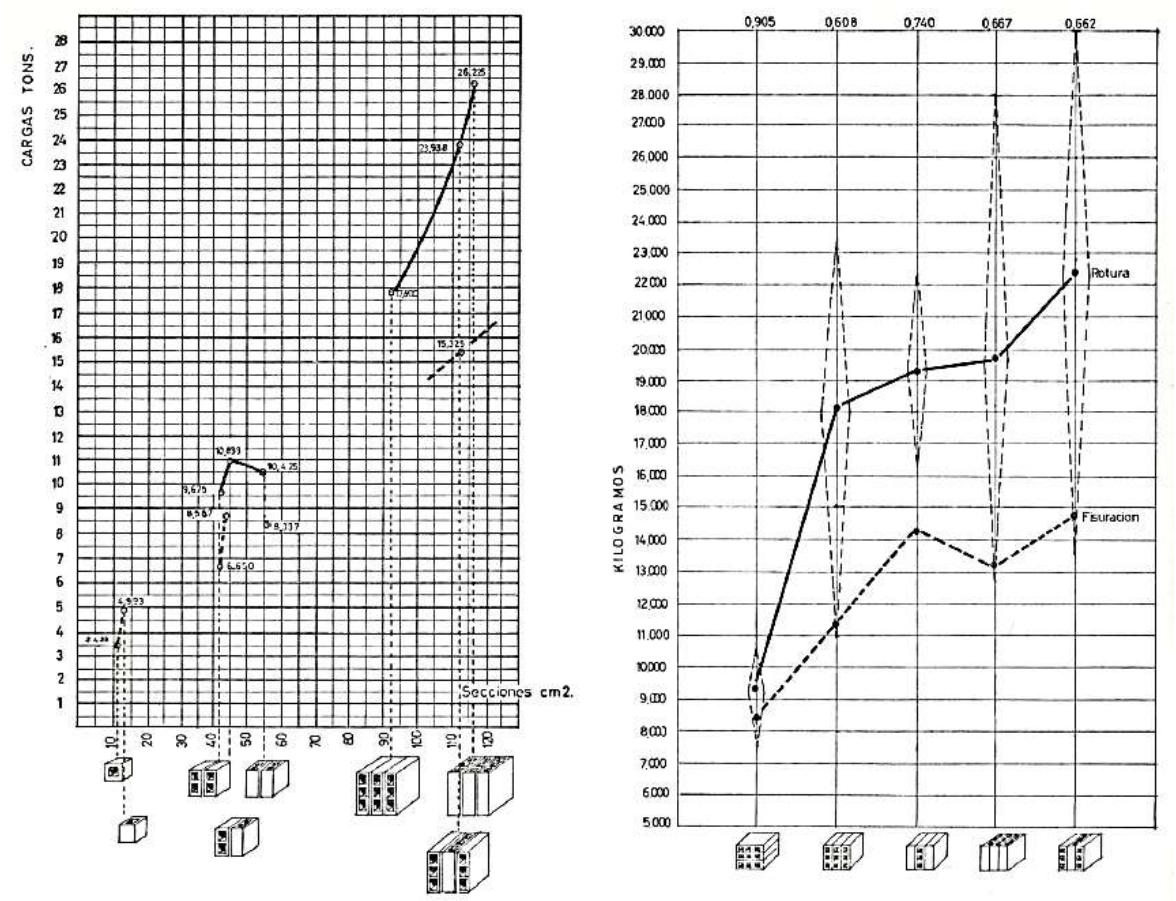

(a) (b)

Fig.1.11. Compressive strength Vs load application axis (a). Crack and failure load values (b) in hollow thin-tile specimens without mortar (Bergós 1965).

The (fig. 1.12) shows the specimens used in compressive strength test for hollow brick masonry (a) and thin hollow thin-tile masonry (b).

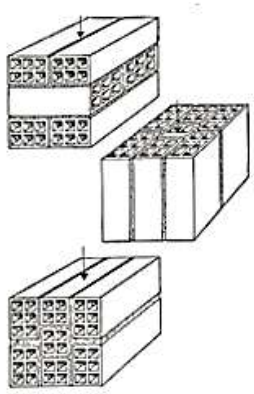

Fig. 38. Probetas cúbicas de lochana para ensayo a compresión.

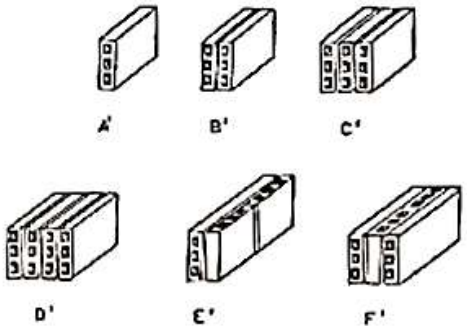

Fig. 40. Probetas prismáticas de rasillas para ensayo a compresión.

(a) (b)

Fig.1.12. Specimens of Hollow brick (a) and hollow thin-tile (b) used by Bergós in masonry compressive strength test (Bergós 1965).

Two of the results obtained by the author for hollow tile masonry are presented. The first one is about the incidence of the angle between the load and the bed joints, presenting values for crack and failure load (fig 1.13). When the load was applied perpendicularly to the bed joints, the crack and failure values corresponding to the compressive strength appeared very close to each other, while when the load was perpendicularly applied the difference between them was significant.

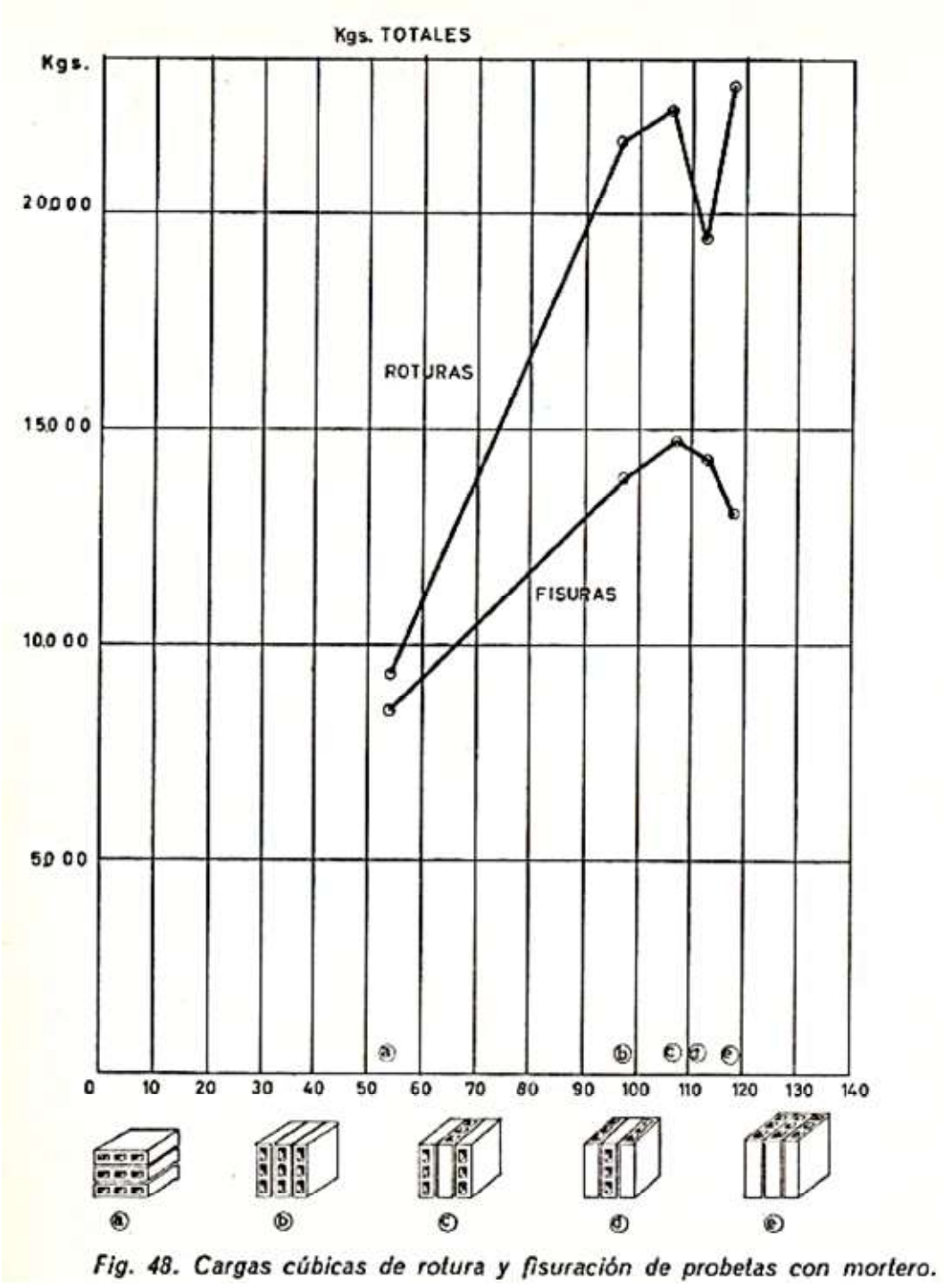

Fig.1.13. Load Vs bed joints orientation in masonry compressive strength test (Bergós 1965).

The second one, and even more relevant, was the relationship between the number of leaves and the stress level (fig1.14). In this case the results indicated that only from 4 leaves on, and for the case of hollow thin-tile masonry, the stress remained uniform.

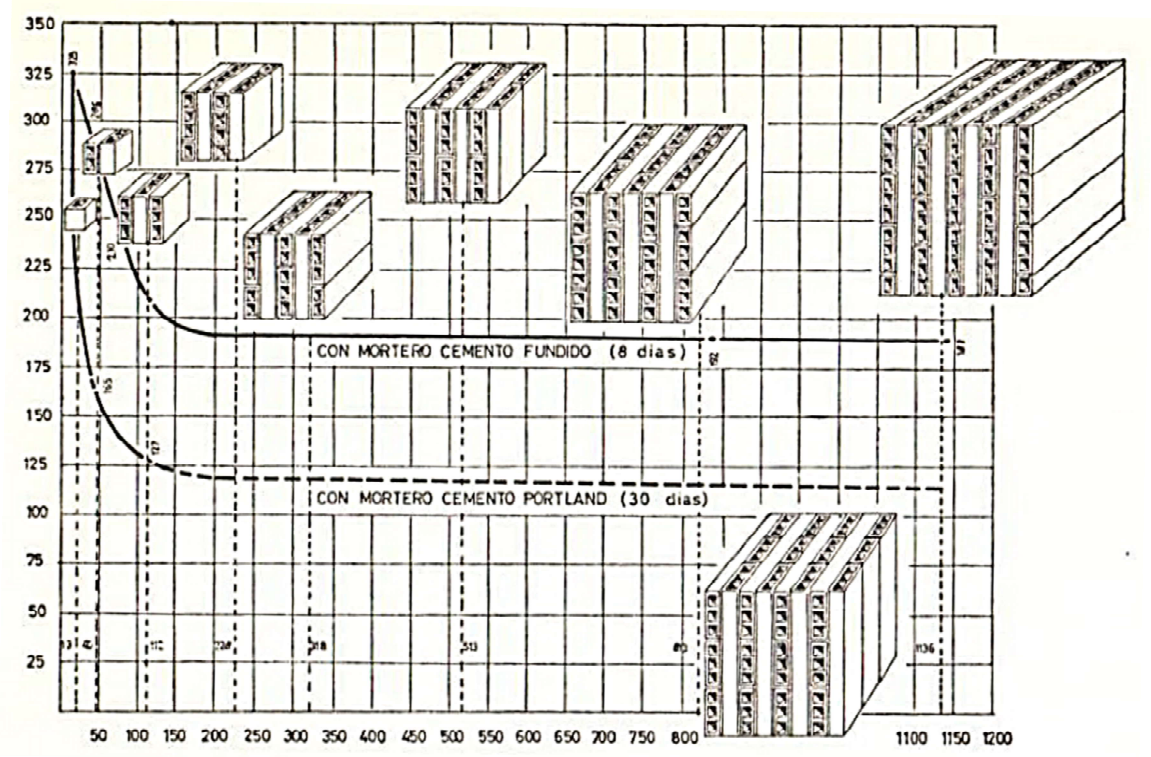

Fig.1.14. Stress Vs number of leaves in masonry compressive strength test (Bergós 1965).

The author also presents the stress-strain behaviour for a 7-leaf specimen (fig.1.15). The load was applied by steps of 10 kg/cm^2. In each step the load was kept constant for 30 seconds to allow the accommodation of the specimen. Afterwards, the shortening (total vertical deformation) was recorded. The specimen was then unloaded, and after 30 seconds the remaining or plastic deformation was recorded. Thus, the elastic deformation was obtained as the difference between both deformations. The author concluded that the results gave a clear idea of a semi-elastic behaviour of this type of masonry.

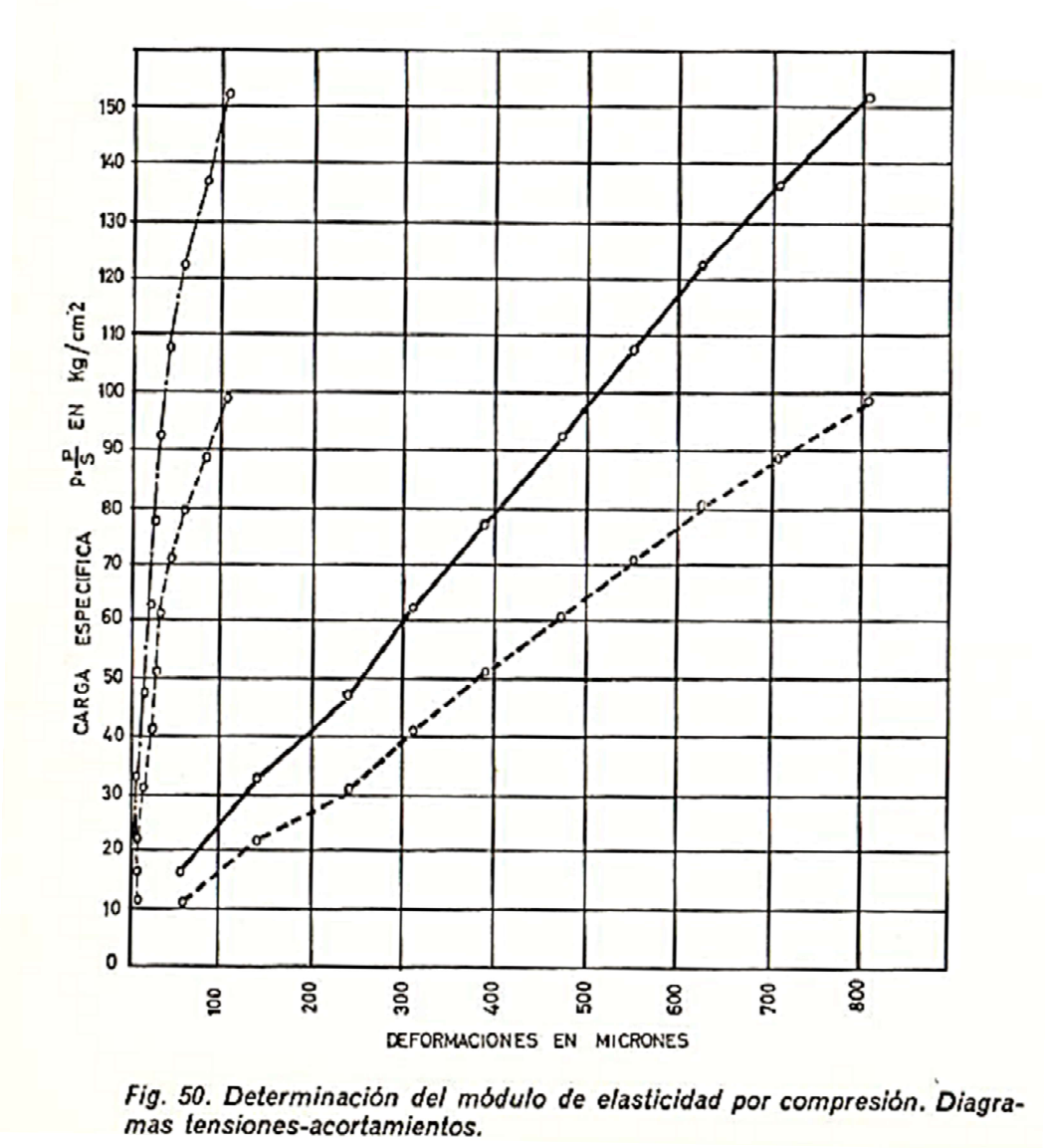

Fig. 50. Determinación del módulo de elasticidad por compresión. Diagramas tensiones-acortamientos.

Fig.1.15. Stress-strain behaviour for 7-leaf hollow thin-tile masonry. (Bergós 1965).

In the following chapters, the author presents tests on tensile and shear strength, axial flexo-pressure and eccentrically loaded partitions, finishing the experimental part with test performed in arches.

As explained before in (Atamturktur and Boothby 2007) examined spherical segmental domes built by the Guastavino Fireproof Construction Company. The authors presented the value for the Young's modulus of the thin-tile, mortar and thin-tile masonry. The first two were obtained experimentally, while the last was calculated through a homogenization procedure, incorporating the combined effect of both materials (thin-tile and mortar). The

compressive strength test of the thin-tiles was performed according to ASTM C67 (2000) on 13 samples measuring 15x15 cm. The values obtained were: thin-tile Young's modulus 13,200 N/mm^2 in the longitudinal direction and 15,400 N/mm^2 in the transverse direction. The mortar Young's modulus was 2,970 N/mm^2. Finally the Young's modulus for masonry was 7,600 N/mm^2.

In (Benfratello et al. 2010; 2012) the authors presented experimental values of thin-tiles and thin-tile masonry, obtained from parts of real structures. The thin-tile tensile strength value obtained after performing a three-point bending test was 6 N/mm^2. The thin-tile compressive strength obtained on three 2x2x2 cm samples was approximately 8 N/mm^2. The authors presented values of compressive strength on two-, three-, and four-leaf thin-tile masonry. All specimens had an average dimensions 320 x 320 mm. while the thickness took the value of 45, 75 and 105 mm. depending on the number of leaves. The maximum compressive strengths were 1.7, 2.5 and 2.9 N/mm^2 respectively. The stress-strain law presented an initial phase of adaptation of the specimen to the test bench, followed by an interval with a clearly elastic and linear behaviour that ended at approximately 80% of maximum stress. The calculated value for Young's modulus at the aforementioned interval was 330-500 N/mm^2. Afterwards, the stress-strain law exhibited a non-linear hardening behaviour until reaching the peak load. Finally, a strain softening behaviour was observed until arriving to the end of the test. The failure mode occurred in form of a detachment which thereafter led to the instability and failure of the tile-leaves. The crack, generally, began where the thickness of the mortar is reduced and at the thin-tile-mortar interface. The authors stressed the need for a thorough analysis of the tile-mortar interface both from an experimental and numerical point of view.

In order to characterize the materials (Endo et al. 2017), presented values of compressive strength and Young's modulus of thin-tiles and thin-tile masonry. The thin-tile specimens were obtained from demolished masonry vaults belonging to the Hospital of the Holly Cross and Saint Paul in Barcelona. The test were carried out according to the (UNE-EN 772-1 2016). The average compressive strength was 30.1 N/mm^2, and Young's modulus

8,000 N/mm^2. On the other hand authors presented results on two series of masonry specimens. The first series was built using thin-tiles recovered from the building and new mortar designed to reproduce the original one. The second series were obtained from some masonry vaults existing in the building itself. The compressive strength was 7.90 N/mm^2 (with standard deviation of 1.3 N/mm^2) and 7.28 N/mm^2 (1.49 N/mm^2) respectively. Authors presented also the values for compressive strength of detachment (i.e., separation of thin-tile leaf) of about 3.67 N/mm^2 (0.28 N/mm^2). The masonry average Young's Modulus was 2.500 N/mm^2.

In (López et al. 2019) the authors presented a construction system using the thin-tile vault as a formwork only during the curing process of a leaf of reinforced concrete. In such conditions, the structure became a composite system. Two full-scale prototypes were built and load-tested to failure. The thin-tile vault was built with thin-tiles of 277x134x13 mm. and Portland cement mortar. Two values of thin-tile compressive strength were obtained, 111 N/mm^2 in longitudinal direction and 87 N/mm^2 in the transversal direction. The mortar compressive strength for both vaults was 6.98 y 4.47 N/mm^2 respectively.

The authors indicated that this masonry was not clearly classified within (EC-6 1996) due to its multi-leaf condition and the presence of a mortar joint (mortar leaf) in the longitudinal direction. Thus, the authors proposed to determine the compressive strength of each leaf individually. Subsequently, the total compressive strength of the thin-tile vault was computed taking into account the thickness of each leaf. The compressive strength of the outer leaves (thin-tile leaves) was computed on the basis of the equation proposed in (EC-6 1996) that proposes calculate the compressive strength of the masonry from brick and mortar compressive strength values. Section 3.1.4 of this thesis explains that formula in detail. For the compressive strength of the central leaf (mortar leaf) authors proposed the value of 6.98 N/mm^2 obtained from the tests described above. Thus, the compressive strength of the thin-tile vault was 13.45 N/mm^2.

1.1.3. Compressive strength

From structural point of view, masonry is basically characterized by the compression forces applied to it. Thus the importance of determining its compressive strength, even in a simplified way, is evident.

Masonry may be considered to be a discontinuous material. The horizontal and vertical joints act as weak planes, inducing anisotropic behaviour both in the elastic and plastic domains. Therefore, the tolerance of the masonry is highly dependent on the orientation of the angle of incidence of the load relative to the bed joints. Two types of behaviour may be taken into consideration: uniaxial and biaxial. In the uniaxial case, the forces are only applied in one direction. Compressive strength depends mainly on the compressive strength of the bricks and the mortar, although brick is generally the component that most influences the global strength. Other additional parameters pertinent to strength are: stiffness and relative thickness of the two components, thickness and filling of the joint, or the joint between different layers of masonry.

In the biaxial case, the direction of application of the forces is at an angle with respect to the bed joints, or the material is subjected to forces in more than one direction. Hence, compressive strength and failure behaviour vary in this case depending on the angle. The applied state of stress may be explained by the main stress and the angle that they form with the bed joints or by the normal and tangential stresses on the plans of the mortar joints.

There are a large number of numerical and experimental studies aimed at understanding and explaining the behaviour of masonry. (Antoine 1992), (Lourenço 1998) present a view of the different aspects which affect masonry both in uniaxial and biaxial cases.

In the uniaxial case, this behaviour is explained by defining the stress-strain relationship, study of the failure mode and definition of mechanical properties, mainly compressive strength and Young's modulus.

1.1.4. Failure mode

Simple compression failure theories has been developed (Hilsdorf 1969) and generally accepted within the academic community. According to these theories, the difference between unit and mortar elastic properties is the precursor of failure. In general, when the mortar is softer than the brick, its deformation is restricted laterally. Therefore, a state of compression/biaxial stress occurs on the brick and triaxial compression on the mortar (fig.1.16).

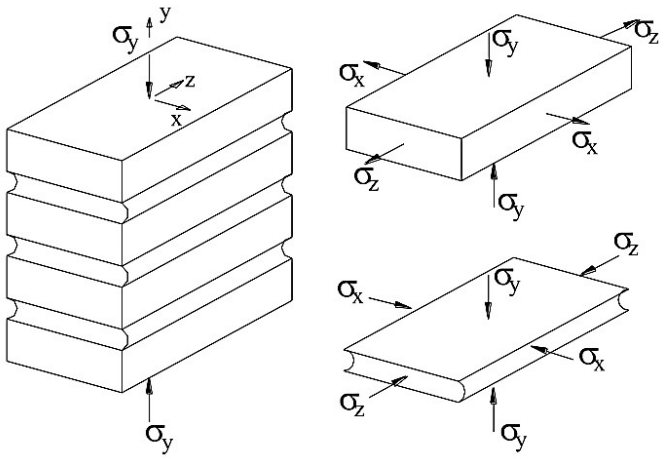

Fig.1.16. Triaxial state of stress in masonry specimens under vertical compression.

As a result, the failure of the brick in tension leads to masonry failure (Costigan, Pavía, and Kinnane 2015). In (Zucchini and Lourenço 2007) a previously homogenization approach developed by the authors is extended and validated with the theory and the comparison with experimental results extracted from the available literature. In this extension, the authors explain that in bricks with low compressive strength the masonry failure mode is caused by crushing of the brick by compression. They also indicate that with stiffer and stronger mortars the tensile strength of the brick does not play a significant role in the behaviour of the masonry, because the brick is subjected to a triaxial state of compression and failure is similarly caused by crushing of the brick.

The brick-mortar interface is the weakest link in masonry. Under certain load conditions, such as pure normal tensile stresses to the bed joint or pure shear stresses parallel to it,

the interface controls the mechanical behaviour. Tensile (mode I) and shear (mode II) modes are the failure mechanisms usually associated with the brick-mortar interface (Lourenço 1998), (Mosalam, Glascoe, and Bernier 2009).

The failure mode for the thin-tile vaults proposed in the equilibrium approach consisting, essentially, of the formation of a sufficient number of hinges. On the other hand, other modes of failure were presented in the literature. For example, in (López et al. 2019) The authors presented a single curvature vault consisting in a composite structure based on a thin-tile vault with a reinforced concrete. The authors concluded that in that vault sufficient tensile strength between the leaves it was necessary to be guaranteed. However, the precursor mechanism of collapse in thin-tile masonry is not clearly defined (Palizzolo et al. 2008).

Different studies have proposed the reinforcement of vaults with fiber-reinforced polymer (FRP). The objective of FRP reinforcement is to reduce or prevent the formation of hinges. This way, the strength of the vault can be controlled by local failure mechanisms such as masonry crushing, sliding of mortar joints o detachment of the leaves (De Lorenzis, Dimitri, and La Tegola 2007; De Santis, De Felice, and Roscini 2019), snap-through buckling and shear sliding (Castori, Borri, and Corradi 2016) or detachment of the FRP (Carozzi et al. 2018).

It can be observed that, in addition to the failure mode of the thin-tile vault consisting of the formation of a sufficient number of hinges, failure mechanisms (depending on the characteristics of the materials) can be: i) crushing of the material, or ii) loss of bond (detachment) of the thin-tile-mortar or thin-tile-FRP interfaces. In consequence, the analysis of the behaviour of the thin-tile-mortar interface becomes critical.

1.2. Motivation

The thin-tile masonry is widely known for its use in the construction of the thin-tile vault or Catalan Vault. It has also been used, although to a lesser extent, in the construction of

load-bearing walls. This structural system is part of the Cultural Heritage. Understanding its structural behaviour is indispensable in order to preserve it. Although there are some studies on the mechanical behaviour of the thin tile masonry, currently no consensus exists on which constitutive model is more appropriate to represent it.

Determining the compressive strength of masonry from experimental tests is a slow and expensive procedure. The usual way to determine this value is through phenomenological-based formulas, where the individual contribution of each one of the components (i.e. brick units and mortar) is statistically reflected. This is the most common approach both in literature and the standards. Nowadays, in the case of thin-tile masonry, there are very few experimental studies of compressive strength, which implies that we have hardly advanced since the preliminary studies presented by Bergós. Therefore, it is evident that there is still a great lack of knowledge about the general behaviour of this type of structure. This thesis aims to contribute to improving the understanding of the global behaviour of thin tile masonry structures, making special emphasis on its response to compression stresses.

1.3. Objectives

The main objective of this thesis is to deepen in the knowledge of the behaviour of thin-tile masonry in compressive stresses. In order to achieve this goal, the values of the compressive strength, the stress-strain relationship and the failure modes will be analysed experimentally. The results will be compared with the formulations obtained from the literature and the standards that are applied to similar types of masonry. Finally, it will be discussed to which extend these formulations can be applied to the description in terms of allowable stresses to the thin tile masonry.

In order to achieve this main objective, other specific objectives are proposed:

To verify if the single-layered thin-tile masonry and the usual arrangements of brick masonry used in the construction of load-bearing walls are comparable in terms of global

behaviour. For this purpose, the stress-strain laws and failure modes of both cases will be compared. Finally, it will be verified whether the expressions proposed by both the literature and the standards for brick masonry are applicable to thin-tile masonry.

To compare the mechanical behaviour of two-leaf and three-leaf thin-tile masonry with the case of the brick masonry loaded parallel to the bed joints. The degree of accuracy of the expressions from the literature and standards when used to predict the compressive strength of the thin-tile masonry will be analysed.

Determine if the equation used to compute the compressive strength of three-leaf masonry walls is appropriate to predict the compressive strength of the two-leaf thin-tile masonry.

Analyse the different failure modes, under compressive stress, of the thin-tile masonry. Attempt to establish whether the failure occurs in mode I (tensile failure) or mode II (shear failure).

1.4. Thesis structure

The document is structured as follows:

Chapter 1.

This chapter is divided in four sections. In the first one, a vision of the evolution along the history of the thin-tile vault and its structural performance is presented.

The second section deals with materials characterization techniques and structural analysis. The specificities regarding its application to the particular case of thin tile vaults are widely reviewed.

The last two sections are about the characteristic compressive strength of different types of masonry and the corresponding failure modes.

To conclude, the main objectives and the general organization of the Thesis are summarized.

Chapter 2.

The purpose of this chapter is to define and characterize the constituent materials used to build the samples for the tests. The methodology and objectives of each of the experimental tests carried out are presented.

Chapter 3.

The main results and its discussion are presented in this chapter.

Single-leaf and multi-leaf thin-tile masonries are clearly differentiated: characteristic compressive stress, failure modes, stress-strain laws and analytical models, derived from equations got from the literature, corresponding to these two models, are explained in detail.

Chapter 4.

The most relevant conclusions drawn from the research activities performed along the Thesis are to be presented in this chapter.

Finally, proposals for future lines of research, linked to some of the most relevant issues presented in the Thesis are suggested.

2. Materials and Methodology

In order to experimentally analyse the thin-tile masonry, this thesis presents three experimental tests. The first, and most extensive, aims to analyse the compressive strength, stress-strain behaviour, and failure mode of thin-tile masonry. At this propose, this experimental test presents three types of thin-tile masonry specimens: (a). single leaf specimen, (b). two leaves specimen: (two external leaves of masonry with a leaf of mortar in between), (c) Three leaves specimen: (three leaves of masonry alternated with intermediate mortar leaves). (fig.2.1). The values obtained for the one-leaf specimens will be compared with the load-bearing brick masonry, while the two- and three-leaf specimens will be compared with the brick masonry loaded parallel to bed joints, but also with multi-leaf wall masonry.

Fig.2.1. Specimens used in the first experimental test.

From the results of this first experimental campaign, it became necessary to carry out a second experimental test. The aim was discerning, whether the load descended only through the thin-tile leaves or part of this load descended through the mortar one. Although the second campaign did not shed light on the issue, the results are presented and used in the analytical model based on the multi-leaf wall masonry case.

The goal of the last experimental test was to analyse the development of failure mechanisms in multi-leaf thin-tile masonry. To achieve it, DIC technique has used during the compressive strength test of four specimens.

The same configuration and constituent materials (brick, thin-tile and mortar) have been used in all of them.

2.1. Materials

2.1.1. Thin-tiles and bricks

The two types of baked clay ceramic pieces used in the tests (brick and thin-tile) were respectively identified by C1 and C2. C1 manufactured according to traditional methodology throughout the process and baked in a wood-burning kiln. C2, corresponding to bricks and thin-tiles manufactured and baked using an industrial process. All the specimens have a size of 290 x 140 mm, with different thicknesses depending on the models available from the manufacturers. Each specimen was identified with four digits (CXYZ), where X corresponds to the type of ceramic piece and Y and Z correspond with its thickness. For example C145 corresponds to a specimen of C1 ceramic and with a thickness of 45 mm.

The compressive strength test was performed on 5 samples of each type of ceramic piece, accordingly to the standard (UNE-EN 772-1 2016). In order to guarantee the flatness of the surface, and consequently a perfect contact among the specimen and the plates of the press, the two sides have been cut. A universal press was used with a maximum load of 600 kN. The application of the load was carried out with displacement control at a speed of 0.01 mm/s. During the test, both the load and the displacement data were monitored. It was monitored using a linear variable displacement transducer (LVDT) on each side of the tested piece (Fig.2.2). To avoid the influence of the transversal restriction of the press plates, these were placed in the central third of the tested piece. The ceramic piece's compressive strength, (f_b) was calculated by dividing the load applied by the section resulting from the average of two readings in the middle part of each side, according to (UNE-EN 772-16 2011).

The standard defines the normalized compressive strength as the result obtained in the test corrected by two coefficients which take into account the conditioning method. In this study these conditions were the air drying of the tested piece, and its shape factor. With respect to this last factor, the standard establishes a minimum thickness of 50 mm for the test brick and proposes a correction factor depending on the width of the piece. That way it is possible to homogenize bricks with different sizes as is the case in this study. In those cases where the current thickness does not correspond to one of those indicated in the standard, a linear interpolation can be applied.

In some cases, the thin-tiles used in this study, are less than 50 mm thick. In order to measure the vertical strain, it was necessary to modify the test brick defined in the standard. It was decided that the specimen would be 260 mm high, 140 mm width and the thickness corresponding to each ceramic piece. It was verified that the compressive strength was not limited by the buckling phenomenon. After experimentally demonstrating that in pieces thicker than 10 mm, failure occurs when the maximum compression stress value was surpassed (see figure 2.2) the tests were carried out interpolating and applying the shape correction factor.

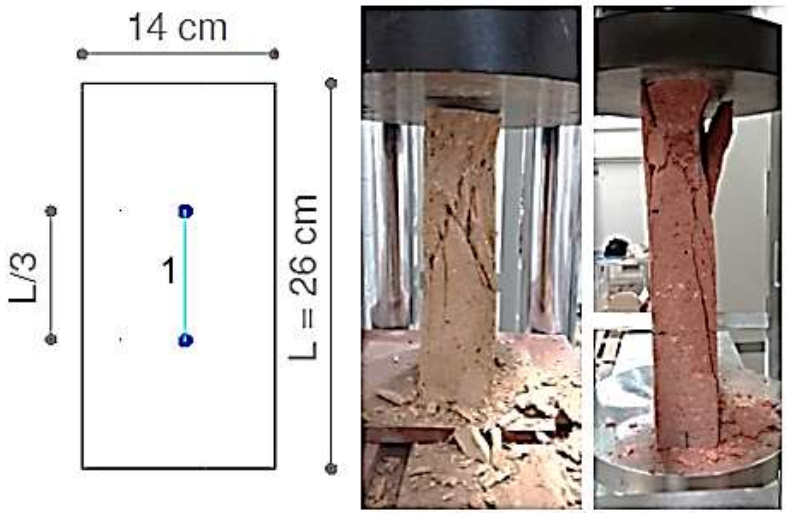

(a) (b)

Fig.2.2. Specimen used in compressive strength test of thin-tiles and bricks and LVDTs placement (a). Failure mode (b).

Young's modulus (E_b) was calculated as a drying modulus at 1/3 of f_b according to (UNE EN 1052-1 2014). In table 2.1 the mean value and the coefficient of variation (CoV) of the compressive strength (f'_b), normalized compressive strength (f_b) and Young's modulus (E_b) for each type of test clay brick may be observed.

Table 2.1. Mechanical properties of ceramic pieces in all experimental test.

Test	Type	Thickness (mm)	Identification	Number of specimens	Compressive strength (N/mm²) f'_b	Normalized compressive strength (N/mm²) f_b	Young's modulus (N/mm²) E_b
Compressive strength (UNE-EN 772-1 2016)	C1 thin-tile	18	C118	5	13.55 (0.22)	21.87 (0.22)	13,873 (0.38)
	thin-tile	32	C132	5	22.35 (0.32)	35.45 (0.32)	10,457 (0.17)
	brick	70	C170	5	23.57 (0.27)	35.60 (0.27)	13,595 (0.56)
	C2 thin-tile	18	C218	5	23.07 (0.15)	37.24 (0.15)	5,244 (0.08)
	thin-tile	28	C228	5	19.67 (0.21)	31.44 (0.21)	4,843 (0.25)
	brick	45	C245	5	11.68 (0.17)	18.22 (0.17)	4,003 (0.20)

Values in parentheses correspond to the coefficient of variation

It may be observed that the variation of E_b with f_b in C1 is highly significant, providing evidence of the difficulty of establishing values for samples manufactured manually. According to the methodology used in the manufacture of the manual bricks, they have been baked in a wood-burning kiln. That kind of kiln cannot assure a homogenous temperature distribution in all bricks. In ceramic pieces, there is a direct relationship

between baking temperature and porosity. In these conditions the open porosity could be a relevant factor when determining the compressive strength of piece. Although there is not a standard test described in the manuscripts proposed in the literature, the open porosity test could help to clarify such as relationship in future tests.

It can be seen that C1 thin-tiles present a much higher Young's modulus than C2, although they have very similar compressive strength. The collapse occurs due to failure of the material.

2.1.2. Mortar

Two types of predosed mortar were used: MP and MC. MP Stands for a mortar made of Portland cement and marble sand mortar, with a 28-days compressive strength of 7.5N/mm^2. This mortar is widely used in current construction. MC mortar was a natural hydraulic lime mortar (NHL) with marble sand and silica, with compressive strength at 28 days of 3.5 N/mm2. This is the typical mortar used in the traditional construction. For both types of mortar the binder-sand ratio was 1:6. The water content, according to the manufacturer's indications, was 4-4.5 l. and 4.5 l. for MP and MC mortars respectively.

The compressive strength of the mortar (f_m) was obtained according to the Standard (UNE EN 1015-11 2014). Each series of mortar was represented with 6 cubic specimens of 40mm. In total there were 72 MP and 72 MC mortar specimens corresponding to all experimental tests carried out in this thesis. The specimens were kept during the first five days in moulds inside a polyethylene bag to avoid the loss of humidity and then, until the test day, in a climate camera at a controlled temperature of 20 ± 1 ºC and relative humidity of 65 ± 5%. To correctly represent the characteristics of the mortar used in the construction of the masonry specimen, the test was performed at the same day as the masonry specimen. The mortar Young's modulus was determined from seven specimens of each type of mortar. It was calculated as the value of the slope within the linear interval of the stress–strain curve corresponding to the 30–50% of the ultimate stress. Vertical unitary deformation was recorded with strain gages.

In the table 2.2 the mean value and coefficient of variation (CoV) of the compressive strength (f_m) and Young's modulus ($E_{m\ 50\text{-}30}$) of the mortar specimens of all experimental test of this thesis is presented.

Table 2.2. Mechanical properties of mortar in all experimental test.

Test	Mortar	Experimental test	Identification	Number of specimens	Compressive strength (N/mm²) f_m	Young's modulus (N/mm²) $E_{m\ 50\text{-}30}$
Compressive strength (UNE EN 1015-11 2014)	Portland cement (MP)	1	MP01	6	5.95 (0.16)	
			MP02	6	10.97 (0.15)	
			MP03	6	21.27 (0.08)	
			MP04	6	9.96 (0.09)	
			MP05	6	7.76 (0.03)	7.976 (0.33)
			MP06	6	4.88 (0.11)	
			MP07	6	9.41 (0.05)	
			MP08	6	5.66 (0.06)	
			MP09	6	3.53 (0.04)	
			MP10	6	3.25 (0.15)	
		2	MP11	6	9.54 (0.06)	
		3	MP12	6	7.83 (0.13)	
	Natural hydraulic lime (MC)	1	MC01	6	7.11 (0.11)	
			MC02	6	8.60 (0.08)	
			MC03	6	7.54 (0.18)	
			MC04	6	6.07 (0.03)	
			MC05	6	7.20 (0.06)	
			MC06	6	7.15 (0.09)	5.102 (0.21)
			MC07	6	5.95 (0.06)	
			MC08	6	7.07 (0.08)	
			MC09	6	7.08 (0.03)	
			MC10	6	5.40 (0.06)	
		2	MC11	6	5.68 (0.06)	
		3	MC12	6	7.69 (0.11)	

Values in parentheses correspond to the coefficient of variation

It may be observed that there is a significant variation in the compressive strength of each series of test mortars, especially in the case of Portland cement mortar. Since it is a premixed mortar, the differences between masses can be attributed to the water content. Water excess is made for the sake of mortar workability.

2.2. Masonry specimens

The most common tests are those done using masonry triplets, prisms or wallettes according to different standards (UNE EN 1052-1 2014), (UNE-EN 772-1 2016), (UNE EN 1015-11 2014), (RILEM 1991).

The masonry compressive strength test was performed, in this thesis, in accordance with the standard (UNE EN 1052-1 2014). The thickness of this type of masonry prevented compliance with the geometrical limitations in the definition of the specimen. Therefore, specimens were built in accordance with (RILEM 1991), composed of three ceramic pieces and two horizontal 10 mm mortar joints for the upper and lower capping of the prism. This type of specimen (see Fig. 2.3) has been extensively used in the study of compression behaviour of masonry by different authors (Kaushik, Rai, and Jain 2007b), (Mohamad, Lourenço, and Roman 2007), (Domède et al. 2009), (Barbosa, Lourenço, and Hanai 2009), (Sousa and Sousa 2010).

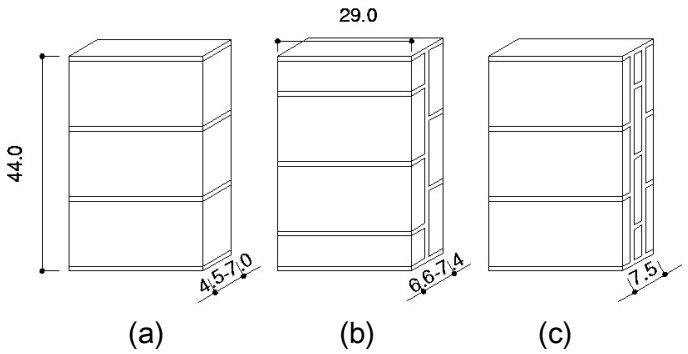

Fig. 2.3. Geometry and arrangement of the brick/thin-tiles in the one-leaf (a) two-leaf (b) and three-leaf (c) specimens.

It is known that the slenderness of a specimen influences the value obtained for compressive strength, as may be observed in (Fig. 2.4) (Sandoval et al. 2011). In order to determine the compressive strength of the masonry, it is necessary to achieve a slenderness which permits collapse of the specimen due to failure in the material and not due to effects of the second order, such as buckling.

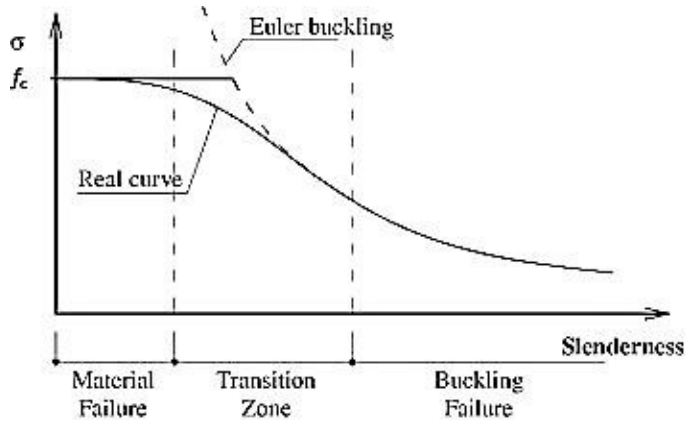

Fig. 2.4. Wall compressive stress (σ) against slenderness ratio (based on Morton) (Sandoval et al. 2011).

Therefore, to define the minimum and maximum slenderness of a specimen, it is necessary to take into account certain factors. On the one hand, the confinement caused by the press plates in specimens with small slenderness (h/b = 1) impeding lateral strain. This limitation means that the form of collapse is not produced purely by uniaxial compression, reaching increases of up to 50% in compressive strength. This effect is negligible in the central part of the specimens with a slenderness higher than h/b≥2.

On the other hand it may be observed in (Fig. 2.4) that when a certain degree of slenderness is achieved, the collapse of the specimen occurs at lower values of pure compression due to the effect of the buckling. In the standards (UNE EN 1052-1 2014) and (RILEM 1991) the slenderness is limited to maximum values of 15 and 12 respectively. (Freire 2011) according to (EC-6 1996), related the eccentricity of the load's application point and the slenderness of the sample with a reduction factor for walls of a single layer in compression. The former coefficient, gave for the particular case of null eccentricity and slenderness between 6 and 10, a value ranging from 0.94 and 0.98 (close to 1).

Other authors (Sandoval and Roca 2012) have analysed the influence of slenderness and stiffness on the behaviour of masonry walls. These studies indicate that the degree to which the load capacity of a wall decreases in relation to its slenderness is strongly linked to its degree of stiffness. The study suggests that both non dimensional parameters may be unified into just one equation [1]

$$\lambda = \frac{h}{t}\sqrt{\frac{f_c}{E}} \qquad [1]$$

Where h and t are the height and the thickness of the wall, f_c is the masonry compressive strength and E is Young's modulus. As is shown in (Fig. 2.5), for values of λ less than 1, the failure occurs for values lesser than the maximum compressive stress.

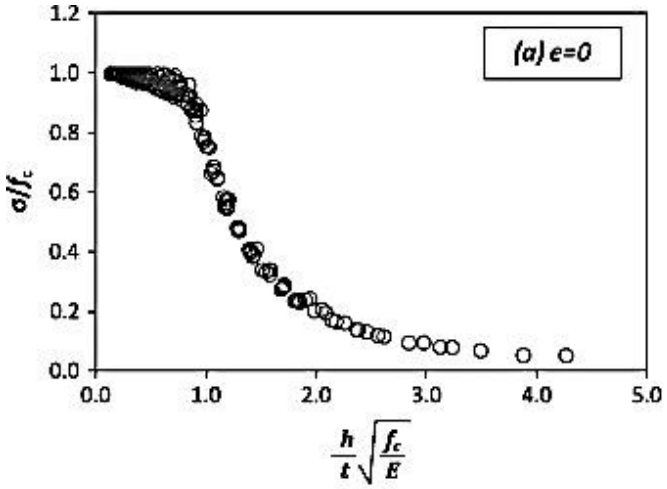

Fig. 2.5. Relationship between the last normalised resistance σ/f_c and the dimensionless parameter λ without load (Sandoval and Roca 2012).

All the specimens of this thesis measured 440x290 mm and its width ranged in the interval from 4.5 mm to 8.2 mm. The slenderness of specimens was higher than 2, and the values of λ from the equation [1] obtained in the current study varied between 0.17 and 0.42, confirming that the result of test was in the failure zone of the material (see the diagram in fig.2.4).

Based on these two points, and accepting that the two rules mentioned above allow greater slenderness, it is considered that the geometry of the specimen may be considered suitable for the characterisation of compressive strength.

2.2.1. First experimental test

A total of 24 specimens were manufactured and tested. Each specimen was identified with seven digits ($CUMW_XYZ$), where U corresponds to the type of ceramic used, W represents the kind of mortar, X the series of mortar, Y the number of leaves and Z

indicates the order in the series. For example C1MP$_2$21 stands for a specimen made using ceramic C1, mortar MP, series number 2, two leaves and first sample of the series. Two specimens were damaged during preparation tasks in the laboratory.

Before constructing the specimens, and in accordance with (UNE-EN 772-1 2016), the ceramic pieces were immersed in water for a minimum of 15 hours and allowed to drain for 15 minutes. Once the specimens were built, they were covered with a polyethylene sheet during the first three days. Afterwards, and until the day of the test, they were kept at a constant temperature (approximately 15ºC) and a relative humidity of approximately 65%. Half way through the curing period, and to balance the circulation of air on both sides of the specimen, they were turned. Hydraulic lime mortar has a longer hardening process time than Portland cement. Different authors indicate that this process, for lime mortars such as those used in this study, can be established at around 90 days (Lanas et al. 2004), (Fusade and Viles 2018). Hence, in order to guarantee an acceptable curing process of the lime mortar specimens, the test was carried out 84 days later.

For the compressive strength test, the procedure was similar to the one followed for the ceramic pieces, with displacement control at a speed of 0.002 mm/s. The displacement was recorded by two longitudinal linear variable displacement transducers (LVDT) (1, 2, 3 and 4) and a transverse LVDT (5 and 6) on each side of the specimen (Fig.2.6). The vertical LVDTs records the deformation of the central third of the specimen in accordance with the standard (UNE EN 1052-1 2014). The horizontal LVDTs allowed recording the deformation of the specimen cross section. For specimens of one leaf, the horizontals LVDTs were no reported.

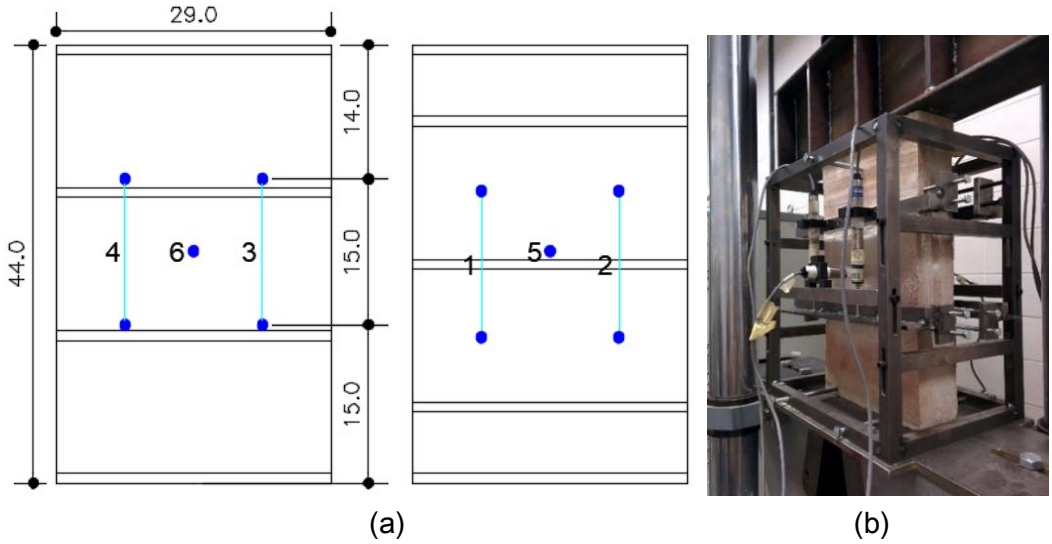

Fig. 2.6. Longitudinal and transverse LVDTs placement (a). Image of the specimen during test (b).

2.2.2. Second experimental test

A total of 8 two-leaf thin-tile specimens was manufactured and tested. The dimensions of the prisms were 450 mm in height, 280 mm in width and 82 mm in thickness. The specimens were made up of two leaves of thin-tile with a thickness of 28 mm and 45 mm respectively, and a 10 mm central leaf of mortar. Each specimen was identified with seven digits (C2MXYDZ), where X represent the mortar, and Y number of leaves and D indicated that the specimens are made up of different thin-tile leaves and Z indicate the order in the series. For example C2MC2D2 stand for a specimen made using natural hydraulic lime mortar two different leaves and second of the series. In order to test whether the stress was transmitted only though the thin-tile leaves, two strain gauges were placed on each ceramic leaf. Figure 2.7 shows the placement of the ceramic pieces, the dimension of the specimens and the location of the four strain gauges (numbers 1 to 4). LVDTs were also placed as the previous experimental test.

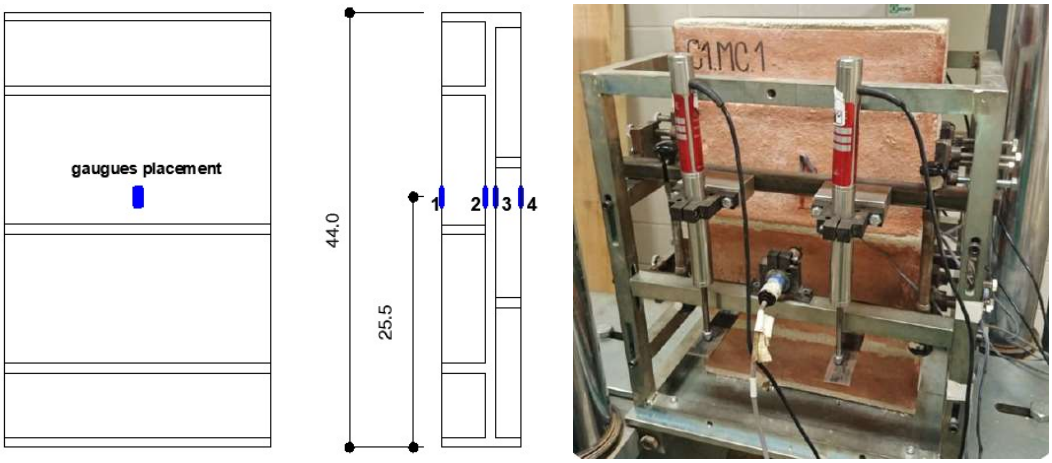

Fig.2.7. Specimen and placement of the strain gauges (1 to 4) (a). Specimen ready for testing (b).

To prevent the damage of the strain gauges while manufacturing the specimens, they were protected using SB-Tape waterproofing putty by Tokyo Sokki Kenkyujo Co., Ltd.

2.2.3. Third experimental test

A total of 4 specimens was manufactured and tested. One prism was built with each combination of thin-tile and mortar. Each specimen was identified with four digits (PXYZ), where X corresponds to the number of leaves and Y and Z indicate the type of mortar used (MP or MC). For example, P2MP stands for a specimen with two leaves made using Portland cement mortar for this experimental test.

2.3. Digital image correlation

Several experimental non-destructive techniques exist for the analysis of the stress-strain behaviour of materials. One of these techniques is Digital Image Correlation (DIC). This is an optical and contactless measurement technique based on the acquisition and treatment of pictures of a previously defined field of interest to obtain full-field displacements and deformations during the test. In the past decade, DIC has been introduced in the experimental measurement field of structural elements and has been proven to be a powerful tool for measuring full-field absolute and relative displacements (Barris et al. 2017).

In the field of masonry structures, DIC has already been implemented (Salmanpour and Mojsilović 2013) for example, to compare experimental results obtained with traditional hard-wired instrumentation with DIC results, concluding that this is a promising technique that measures displacements and deformations effectively. The DIC technique has also been used in the evaluation of brick masonry walls. For example, (Nghiem, Al Heib, and Emeriault 2015) assessed damage of masonry structures from the opening of the joints, whilst (Tung, Shih, and Sung 2008) used DIC to identify strain and crack variations, proving the possibility of observing crack formation in the early stages, even when they are not yet visually so. Finally, DIC has been used to analyses the damage evolution and compressive failure (Sassoni, Mazzotti, and Pagliai 2014; Ravula and Subramaniam 2017).

In this experimental programme, the Digital Image Correlation (DIC) technique was used to consistently acquire the field of displacements of the different specimens and better understand the behaviour of the thin-tile-mortar interface. In this case, a 3D configuration was used for all specimens (fig.2.8).

Prior to the beginning of the test, the surface of the specimens was prepared by the application of a surface coating of white paint followed by a black mist of paint applied with an airbrush. Once the specimen had been treated and placed into the testing frame, two high-resolution digital cameras with a recording resolution of 2452×2056 pixels, an image sensor format of 8.5×7.1mm and 8mm focal length lenses were placed with a relative angle between them of 16.5-16.6º to be acquired in the 3D configuration. Additional artificial light was used to provide constant illumination to the surface independently of ambient conditions.

Fig. 2.8. Placement of the cameras (a) and black mist of the specimen (b)

The cameras recorded pictures at a regular time intervals of one picture/second. A normalized squared differences correlation criterion was used in all cases. For the calculations, a subset size of 39pixels with a step size of 9pixels was used.

3. Results and discussion

3.1. Compressive strength of the one leaf specimens

In this section, the experimental results obtained for the single-leaf specimens will be compared to verify whether the behaviour of the single-leaf thin-tile masonry is comparable to that defined by the literature for the load-bearing wall brick masonry.

3.1.1. Stress-strain behaviour

The experimental stress-strain behaviour of one leaf specimens is presented in (Fig. 3.1). The compressive strength was determined as a ratio between the load applied and the least transverse section resulting from measuring the prism at the different cross sections: upper, lower, middle. The vertical strain, of each specimen, was calculated as the average of the four longitudinal LVDTs. The values corresponded to the average for the six specimens in each type of specimen.

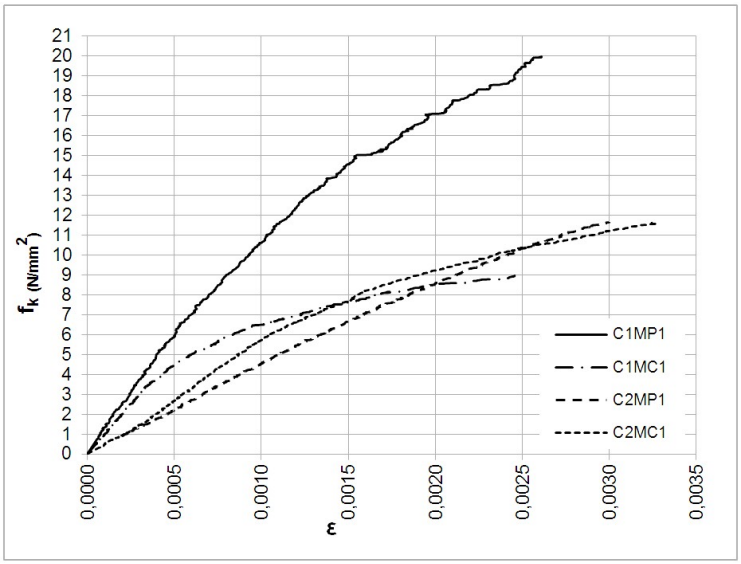

Fig. 3.1. Stress-strain behaviour of single-leaf masonry.

It is known that the behaviour of masonry is not linear. The different studies regarding stress-strain behaviour demonstrate that the behaviour continues to be linear up to a percentage of the compressive strength of the masonry, and then becomes non-linear. With the aim of just give a general context, table 3.1 shows the results obtained by several authors. According to them, the point where the non-linearity starts is located between 30 and 60% of f_k regardless of type mortar, brick or specimen. Non-linearity is associated, by some authors (Kaushik, Rai, and Jain 2007b), with the appearance of cracks in the specimens. Other authors like (Fonseca et al. 2015) indicate that an increase in the Poisson ratio could influence the onset of non-linearity. (Mohamad, Lourenço, and Roman 2007) concluded that the mortar governs the non-linear behaviour of concrete block masonry and (Domède et al. 2009) indicates the view that as long as the compressive strength of the mortar holds, the behaviour of the masonry is linear, beyond this point the behaviour of the mortar becomes plastic, leading to non-linearity in the behaviour of the masonry.

Table 3.1. The limit of linear behaviour according to various authors.

Author	Brick	Grades of mortar (cement:lime:sand)	Type specimens	f_k Percentage
(Kaushik, Rai, and Jain 2007b)	Clay bricks (four of different manufacturers)	Cement mortar and cement-lime mortar 1: 0 : 6 1 : 0 : 3 1 : 0.5 : 4.5	Prisms	33%
(Domède et al. 2009)	Clay brick masonry	NHL lime mortar 0 : 1 : 4.6	Prisms	40%-50%
(Nwofor 2012)	Clay brick masonry	Cement mortar and cement-lime mortar 1 : 0.25 : 3 1 : 0 : 4.5 1 : 0 : 6		40%
(Costigan, Pavía, and Kinnane 2015)	Clay brick masonry	Hydrated lime 0 : 1 : 3 NHL lime mortar 0 : 1 : 3	Walletes	30-60%

In (fig.3.2) may be observed the experimental results of this study. In order to better compare the performance of the different specimens, the stress-strain values were normalised to the peak values .The different curves showed firstly a linear stage that reached values between 30-60% of f_k. Non-linearity began without the appearance of cracks in the specimens.

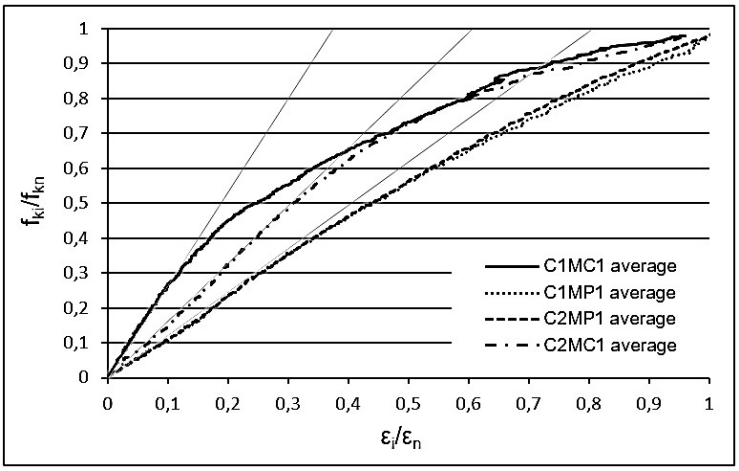

Fig.3.2. Normalized stress-strain relationship of average value of the experimental results of the different specimens.

Several authors propose formulas to describe the stress-strain curve of brick masonry. (Knutsson 1993), based on experimental values obtained by different combinations of

mortar and brick, concluded that this stress-strain relationship may be calculated by the following equations:

$$\varepsilon = -\frac{f_k}{E_o}\ln(1-\frac{\sigma}{f_k}), \qquad \text{if } \sigma/f_k \leq 0.75 \text{ Ritter curve} \qquad [2]$$

$$\varepsilon = -4\frac{f_k}{E_o}(0.403-\frac{\sigma}{f_k}) \qquad \text{if } \sigma / f_k > 0.75 \text{ Ritter curve correction} \qquad [3]$$

On the other hand (Kaushik, Rai, and Jain 2007a) propose that the ascending part of the stress-strain curve may be represented by a parabolic curve. This parabolic variation may be expressed in a non-dimensional way in terms of stress and strain ratios such as:

$$\frac{f_m}{f'_m} = 2\ \frac{\varepsilon_m}{\varepsilon'_m} - \left(\frac{\varepsilon_m}{\varepsilon'_m}\right)^2 \qquad [4]$$

In (fig. 3.3) the relationship between the models formulated by (Knutsson 1993) and (Kaushik, Rai, and Jain 2007a) may be observed in the experimental results of this study. These experimental values correspond to the average value of the specimens in each type of test. The experimental results demonstrate a closer conformity with the model proposed by (Kaushik, Rai, and Jain 2007a).

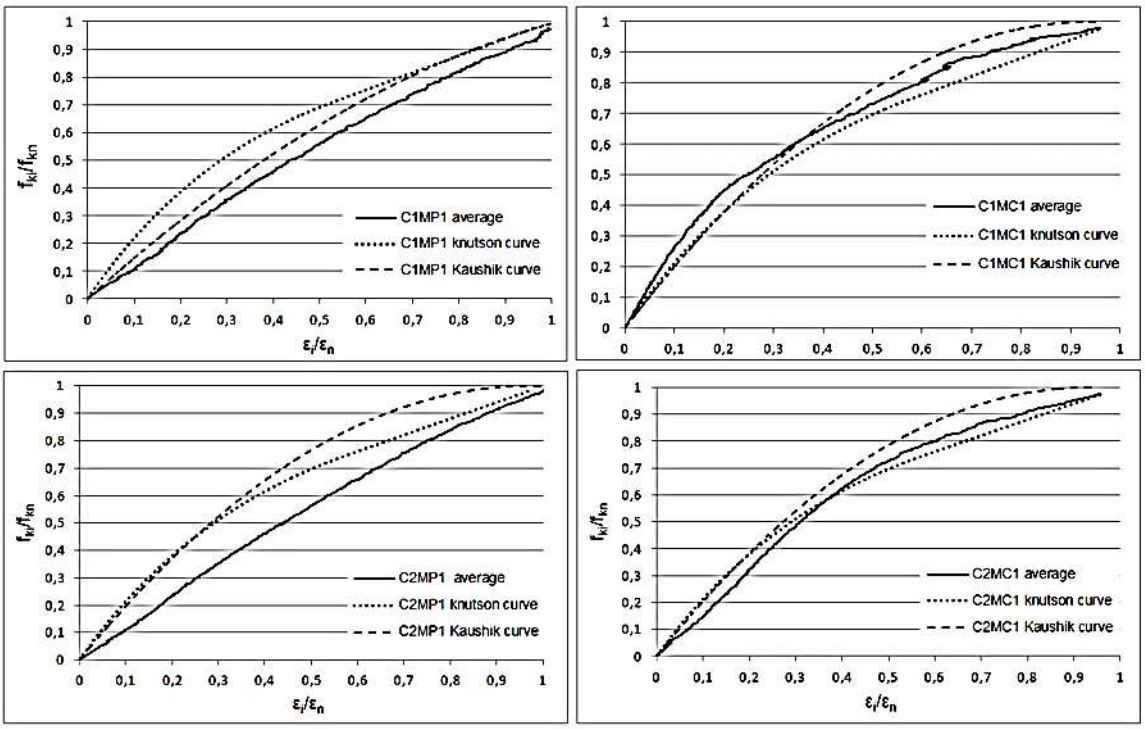

Fig. 3.3. Stress-strain relationship comparison proposed by (Knutsson 1993), (Kaushik, Rai, and Jain 2007a) and the average value of the experimental results of the different specimens.

In specimens C1MP1 and C2MC1 the brick and the mortar have similar Young's modulus. In C1MC1, the brick has a value superior to the mortar and in C2MP1 the mortar clearly demonstrates a higher value. In the first three cases there is a close approximation between experimental and numerical curves. In the case of C2MP1 specimens, the experimental result does not conform to the model. In (Kaushik, Rai, and Jain 2007a), the mortars have Young's modulus which are similar or lesser those of the brick. In the experimental test, the mortar is clearly harder than the brick. As can be demonstrate (Fig. 3.4) the specimens constructed with soft mortar (type O) have greater non-linearity than specimens manufactured with stronger mortars (Type M) which exhibit a more linear behaviour.

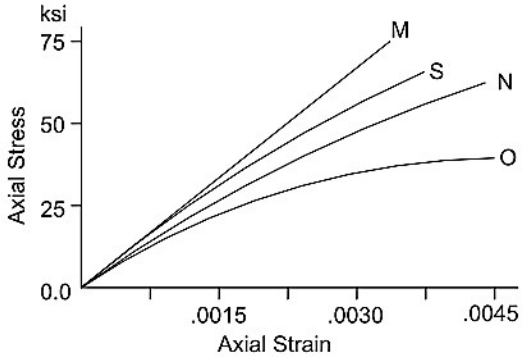

Fig.3.4. Stress-strain curves for specimens with different types of mortar (McNary and Abrams 1985).

In this matter, we could associate this lack of conformity, to the more linear behaviour caused by the stiffness of the mortar. Therefore, it could be observed that the stress-strain behaviour of the different groups of specimens is characteristic of brick masonry.

3.1.2. Failure mode

In the failure mode (Fig. 3.5) of the C1MP1 specimens, the first cracks appeared arbitrarily on one side or at an edge of all the bricks, taking any direction. As the load increased, more cracks surfaced up to the point of failure, which occurred by parts of the brick falling away. In the specimens C1MC1 the first vertical crack appeared on the face or at the edges of the brick. As the load increased, new vertical cracks were developed. Failure occurred either when a crack reaches both edges of the same brick or when this crack included several bricks. In specimens C2MP1 and C2MC1 the first cracks appeared in any direction anticipating what parts of the brick would break off right at the moment of maximum stress. Failure occurs when the brick reaches a sufficient level of degradation. The main difference between the two types of specimens was that in the first case the cracks usually appeared in the middle of the central part of the prism while in the second case they appeared in the contact interface between brick and mortar.

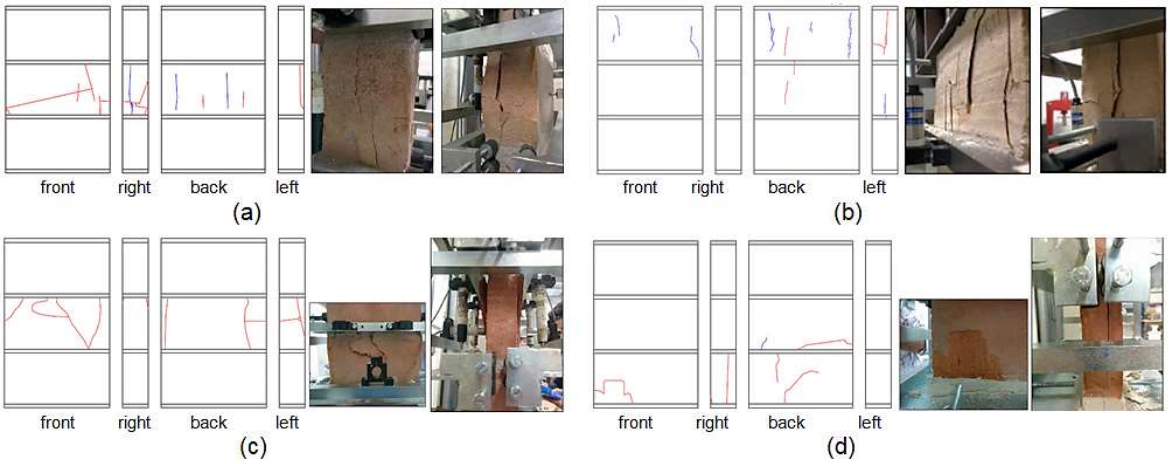

Fig.3.5. Failure mode for one-leaf specimens C1MP1 (a), C1MC1 (b) C2MP1 (c) C2MC1 (d).

The appearance of the first cracks mostly provided values ranging from 75 to 80% of f_k for C1, and 100% f_k for C2. In most cases, once maximum stress had been reached, the failure was brittle in Portland cement and ductile in lime mortar.

Thus, observing the failure mode and the mechanical properties, it could be observed that in the case of C1MP1 specimens, the mortar shows a similar stiffness to the brick and in specimens C2MP1 it shows greater stiffness. In these cases, failure occurs by crushing of the brick. In the cases of C1MC1 and C2MC1, where the mortar is soft with respect to the brick, failure occurs by tensile stress on the brick induced by the mortar. In the first case it occurs owing to the cracking phenomenon while in the second it can be attributed to spalling. It could be observed that, the failure mode of this type of masonry, conforms to criteria widely reported in scientific literature (Hilsdorf 1969), (Zucchini and Lourenço 2007).

3.1.3. Mechanical properties

Table 3.2 shows the compressive strength (f_k), the Young's modulus (E_k) calculated as a drying modulus at 1/3 of f_k as indicated in (UNE EN 1052-1 2014) and the relationship between the values of each of the specimens, as well as the average value and coefficient of variation for each group.

Table 3.2. Compressive strength (f_k), Young's modulus (E_k) and E_k / f_k relationship.

Code	f_k N/mm²	E_k N/mm²	E_k / f_k	Code	f_k N/mm²	E_k N/mm²	E_k / f_k
C1MP$_2$11	18.45	20,229	1,097	C2MP$_5$11			
C1MP$_2$12	15.26	13,497	884	C2MP$_5$12	18.26	4,317	236
C1MP$_3$13	23.24	12,420	534	C2MP$_6$13	15.20	6,920	455
C1MP$_3$14	24.71	21,248	860	C2MP$_6$14	15.30	4,558	298
C1MP$_7$15	20.30	7,840	386	C2MP$_8$15	11.58	5,507	476
C1MP$_8$16	20.40	15,045	738	C2MP$_9$16	11.86	8,906	751
$\bar{x}$	20.39 (0.18)	15,047 (0.33)	750 (0.34)	$\bar{x}$	14.44 (0.19)	6,042 (0.31)	443 (0.45)
C1MC$_1$11	13.55	8,834	652	C2MC$_6$11			
C1MC$_8$12	10.64	11,345	1,067	C2MC$_6$12	11.90	5,690	478
C1MC$_8$13	9.49	11,804	1,244	C2MC$_6$13	12.54	7,498	598
C1MC$_3$14	9.72	6,593	679	C2MC$_6$14	12.14	7,104	585
C1MC$_3$15	15.21	13,281	873	C2MC$_7$15	10.85	6,023	555
C1MC$_9$16	15.46	13,893	899	C2MC$_9$16	7.95	3,506	441
$\bar{x}$	12.34 (0.22)	10,958 (0.25)	902 (0.25)	$\bar{x}$	11.08 (0.17)	5,964 (0.26)	531 (0.13)

The values in brackets refer to the coefficient of variation

The values obtained for one-leaf thin-tile masonry with respect to those for load-bearing brick masonry, obtained from scientific literature, are compared.

From the values obtained for the mechanical properties, a large disparity may be observed in the calculated parameters, (values of f_k with CoV of 0.18-0.22), particularly in the parameters for strain (values of E_k with CoV 0.25-0.37). This is an expected and very common result, due to the heterogeneity of masonry resulting from the variability of the raw materials (brick and mortar) and the influence of workmanship.

The relationship between Young's modulus of the masonry and compressive strength is determined in (CTE. SE-F 2009) as E_k =1000 f_k, while (EC-6 1996) gives a value between 750 and 1000 f_k. This standard applies to modern mortars. On the other hand, different studies show that these values may vary significantly depending on the type of mortar used. Accordingly, (Kaushik, Rai, and Jain 2007b) indicate different standards and studies where this relationship (f_k / E_k) ranging from 210 to 1670. (Costigan, Pavía, and Kinnane 2015) report a value of 102 f_k. for NHL mortars, which is particularly low. In this Thesis (table 3.2) MP mortar values were 752 (CoV 0.38) and 902 (CoV 0.25) and MC mortar values were 443 (CoV 0.45) and 525 (CoV 0.15), which is in line with the literature.

3.1.4. Analytical model based on standards and recommendations

With respect to compressive strength, we may find several approximations in scientific literature, depending on the degree of sophistication of the model. (Ohler 1986), (Tassios 1988), (Binda, Fontana, and Frigerio 1988) propose equations based on the characteristics of the clay brick masonry and mortar. Most of the application standards (CTE. SE-F 2009; EC-6 1996) tend to give simplified equations as:

$$fk = K \cdot f_b^{\alpha} \cdot f_m^{\beta} \qquad [5]$$

Where f_k, f_b, f_m are the compressive strength of the masonry, the brick and the mortar respectively, and k, α, β are coefficients which are experimentally adjusted. The first corresponds to variations of the bonds of the masonry and the type of brick used, while the remaining two act as corrective coefficients. These empirical equations appear in the different standards; in this way (CTE. SE-F 2009) and (EC-6 1996) propose the characteristic compressive strength, f_k, in N/mm^2 of masonry made with ordinary mortar and normal joints, extended throughout the whole thickness of the brick, with a normal load on the bed joints, in stretcher or header masonry thickness of more than 10 cm. In these cases, the procedure to follow to obtain the different values is specifically regulated by the standards. Several authors, (Dayaratnam 1987), (Gumaste et al. 2007), (Nwofor 2012), propose specific values for k, α, β based on experimental results and (Knutsson 1993), (Kaushik, Rai, and Jain 2007a), (Costigan, Pavía, and Kinnane 2015), include formulas which relate the stress - strain relationship of masonry.

The study below will compare the results obtained from different simplified formulas, to determine the compressive strength of brick masonry loaded perpendicular to bed joints with those experimentally obtained in this study.

This equation proposed by (Ohler 1986) is based on the relationship between failure mode of the brick and of the mortar.

$$f_{\mathrm{k}} = f_{\mathrm{m}} + \frac{s f_{\mathrm{b}} - f_{\mathrm{m}}}{1 + \propto \frac{t f_{\mathrm{b}}}{m f_{\mathrm{tb}}}} \qquad [6]$$

where s and t define the failure mode of the brick and m is the slope of the envelope of the mortar. The values recorded by (Ohler 1986) forº these parameters are shown in tables 3.3 and 3.4 respectively. Parameter f_{tb} is the tensile strength of the clay brick. Calculations were made with a value of f_{tb} = 5% f_b as a generally accepted relationship. Parameter α relates the thickness of the horizontal mortar joint (t_m) and the thickness of the brick (t_b), this relationship being $\alpha = t_m / t_b$.

Table 3.3. Values for the parameters s and t suggested by (Ohler 1986).

	$0 < f_b/f_{bu}$	$0.33 < f_b/f_{bu} < 0.67$	$0.67 < f_b/f_{bu} < 1.0$
s	0.662	0.811	1.000
t	0.662	0.960	2.218

Table 3.4. Value for the parameters m suggested by (Ohler 1986).

f_{bu} (N/mm²)	31.6	21.4	15.4	6.4
m(-)	5.3	3.6	2.4	2.1

The next presented expression is an equation proposed by Engesser, and reviewed by (Huerta 2004), to find the compressive strength of stone masonry, and where it is recommended to apply a safety coefficient between 4 and 8 to the values obtained:

$$f_{\mathrm{k}} = \frac{1}{3} f_{\mathrm{b}} + \frac{2}{3} f_{\mathrm{m}} \qquad [7]$$

C.Rozza, as indicted by (García et al. 2012), proposed a method, which is very widespread in Italy, for calculating the loads on walls made with brick and stone masonry. The simplified equation for brick masonry is as follows:

$$f_{\mathrm{k}} = \frac{0.8\, V_{\mathrm{b}}\, f_{\mathrm{b}} + 1.2\, V_{\mathrm{m}}\, f_{\mathrm{m}}}{10} \qquad [8]$$

where V_b is the relative volume of the bricks and V_m of the mortar.

In (Tassios 2013) there is a further development regarding the uniaxial compressive strength of masonry of rectangular mortar blocks. This study, retrieves the simplified equation [9] proposed by the same author (Tassios 1988) for highly resistant, fully joined

brick masonry. It is also indicated that this simplified proposal for the equation might not be sufficiently accurate:

For $f_b > f_m$ $$f_k = [f_m + 0.4(f_b - f_m)] \cdot (1 - 0.8\sqrt[3]{\alpha})$$ [9]

As indicated previously, standards and scientific literature record a simple analytic equation [5] based on the resistance of the brick (f_b) and the mortar (f_m) and of the constants k, α and β.

(EC-6 1996) and (CTE. SE-F 2009) limit the use of this equation to masonry in which specimens where the load is applied to the face of the brick and both vertical and horizontal mortar joints are between 8 and 15 mm. The result obtained from the formulas proposed by these standards is the characteristic value. Both standards allow the compressive strength to be obtained based on the standard (UNE EN 1052-1 2014). This, establishes the characteristic compressive strength (f_k) based on the average value obtained experimentally (f) according to the formula (10).

$$f_k = \frac{f}{1.2}$$ [10]

In Table 3.5, and after determining the statistical dependence through a least-square regression of performed in the experimental results, several authors have estimated the values of k, α and β. (Kaushik, Rai, and Jain 2007a) obtained them based on the experimental results of prisms built with four different types of bricks and three types of mortar. The authors referred to the values proposed by (Dayaratnam 1987). (Gumaste et al. 2007), studied two types of traditional bricks in India: moulded bricks and wire cut baked bricks combined with different types of cement or lime mortar. With these materials, two types of prisms and two types of wallettes were built. Prisms were without vertical joints (Stack bonded) and with vertical joints (English bonded). (Nwofor 2012) studied a type of wire cut brick and different types of mortar of cement and cement and lime. The constructed prisms had vertical joints. (Costigan, Pavía, and Kinnane 2015), based on a

type of wire cut brick and various types of lime mortar, made wallettes. The authors propose different values depending on the type of mortar.

Table 3.5. Exponential equations for compressive strength proposed by several authors and standards.

Author	Equation
EC-6 (EC-6 1996)	$f_k = 0.55 f_b^{0.70} f_m^{0.30}$
CTE (CTE. SE-F 2009)	$f_k = 0.60 f_b^{0.65} f_m^{0.25}$
(Kaushik, Rai, and Jain 2007a)	$f_k = 0.63 f_b^{0.49} f_m^{0.32}$
(Dayaratnam 1987).	$f_k = 0.275 f_b^{0.50} f_m^{0.50}$
(Gumaste et al. 2007) (Stack bonded)	$f_k = 0.317 f_b^{0.866} f_m^{0.134}$
(Gumaste et al. 2007) (English bonded)	$f_k = 0.225 f_b^{0.855} f_m^{0.146}$
(Nwofor 2012)	$f_k = 0.61 f_b^{0.51} f_m^{0.36}$
(Costigan, Pavía, and Kinnane 2015) (MP)	$f_k = 0.46 f_b^{0.50} f_m^{0.50}$
(Costigan, Pavía, and Kinnane 2015) (MC)	$f_k = 0.69 f_b^{0.55} f_m^{0.37}$

In table 3.6 we find the experimental values obtained in this study and those obtained after applying the different formulas indicated above. For each one, the average value of the group (x), the coefficient of variation -in brackets- and the deviation of the average values with respect to the experimental results (Dev.) are presented. In order for the values obtained from (CTE. SE-F 2009) and (EC-6 1996) to be comparable, the values presented in the table are the average values obtained based on equation [10].

Table 3.6. Experimental values of compressive strength and comparison with different equations.

Equation	C1MP1		C1MC1		C2MP1		C2MC1	
	$\bar{x}$ (N_{mm^2})	Desv	$\bar{x}$ (N_{mm^2})	Desv	$\bar{x}$ (N_{mm^2})	Desv	$\bar{x}$ (N_{mm^2})	Desv
Experimental	20,39 (0,18)		12.34 (0.22)		14.44 (0.19)		11.13 (0.19)	
Ohler (6)	27,98 (0,08]	37%	24,07 (0,05)	96%	11.97 (0,06)	-15%	13,03 (0,04)	17%
Engesser (7)	21,29 (0,19)	5%	16,52 (0,01)	35%	9,53 (0,11)	-31%	10,65 (0,02)	-4%
Rozza (8)	2,77 (0,02)	-86%	2,71 (0,00)	-78%	1,40 (0,01)	-90%	1,41 (0,00)	-87%
Tassios (9)	17,24 (0,31)	-15%	10,97(0,02)	-10%	7,02 (0,20)	-47%	8,50 (0,04)	-24%
Exponencial (10)								
(EC-6 1996)	17.66 (0,13)	-13%	14.57 (0,01)	18%	8.26 (0,09)	-43%	9.04 (0,02)	-19%
(CTE. SE-F 2009)	14.12 (0,11)	-31%	12.04 (0,01)	-2%	7.17 (0,07)	-50%	7.73 (0,01)	-31%
(Kaushik, Rai, and Jain 2007a)	8,39 (0,14)	-59%	6,83 (0,07)	-44%	4,43 (0,41)	-68%	4,87 (0,08)	-56%
(Dayaratnam 1987)	6,13 (1,32)	-70%	4,41 (0,07)	-64%	2,69 (0,39)	-80%	3,11 (0,08)	-72%
(Gumaste et al. 2007) (Stack bonded)	9,92 (0,56)	-51%	9,12 (0,04)	-26%	4,88 (0,19)	-66%	5,08 (0,04)	-54%
(Gumaste et al. 2007) (English bonded)	6,98 (0,43)	-66%	6,37 (0,07)	-48%	3,42 (0,14)	-76%	3,58 (0,03)	-68%
(Nwofor 2012)	9,70 (1,50)	-52%	7,69 (0,09)	-37%	4,86 (0,51)	-65%	5,41 (0,10)	-51%
(Costigan, Pavía, and Kinnane 2015) (MP)	10,25 (2,21)	-49%	7,38 (0,12)	-40%	4,49 (0,66)	-67%	5,21 (0,14)	-53%
(Costigan, Pavía, and Kinnane 2015) (MC)	13,00 (2,06)	-36%	10,24 (0,12)	-17%	6,27 (0,67)	-54%	7,01 (0,14)	-37%

The values in brackets refer to the coefficient of variation.

After comparing the results above, we could firstly conclude that, the proposal of (Ohler 1986) overestimates f_k, providing variations increased by up to 96% for C1MC1. The proposal of Rozza (García et al. 2012) underestimates, to a very significant extent, the experimental values. Regarding the equation proposed by Engesser (Huerta 2004) it may be observed that it does not conform to the values in a homogeneous manner, giving overestimates or underestimates, depending on the type of clay brick masonry and mortar. The equation proposed by (Tassios 2013) is the one which most closely conforms to the results of C1 (underestimated values of 10-15%), while for C2 the difference is more significant. Regarding exponential formulas, it may be observed that all significantly underestimate the experimental values, by between 30 -70%.

Table 3.7 shows the average adjustment value. This corresponds to the average of the variations of the exponential formulas given by different authors, with respect to the experimental values for each type of prism.

Table 3.7. Proposed exponential equations and adjustment to experimental values.

Author	Average
EC-6 (EC-6 1996)	-14% (-1.77)
CTE (CTE. SE-F 2009)	-28% (-0.69)
(Kaushik, Rai, and Jain 2007a)	-57% (-0.18)
(Dayaratnam 1987).	-72% (-0.10)
(Gumaste et al. 2007) (Stack bonded)	-50% (-0.34)
(Gumaste et al. 2007) (English bonded)	-65% (-0.18)
(Nwofor 2012)	-52% (-0.23)
(Costigan, Pavía, and Kinnane 2015) (MP)	-53% (-0.22)
(Costigan, Pavía, and Kinnane 2015) (MC)	-37% (-0.44)

The values in brackets refer to the coefficient of variation.

As could be observed, there are values of k, α and β where the variation is similar for all combinations of masonry and mortar, especially those proposed by (Dayaratnam 1987) with a decreased estimate of -72%, but with a coefficient of variation of 0.10. It may be verified that several authors (Kaushik, Rai, and Jain 2007a), (Nwofor 2012), (Gumaste et al. 2007) or (Costigan, Pavía, and Kinnane 2015) presented their results with reduced estimates of around 55%.

(Martinez 2003), based on the elastic development proposed by (Francis, Horman, and Jerrens 1971), defines the parameters α and β. The first as the relationship between the thicknesses of the brick and the mortar ($\alpha = h_m/h_b$). The second as the relationship between the Young's modulus ($\beta = E_b/E_m$). The author analyses the influence of these two parameters on the transversal stress of the brick and the mortar. In (fig.3.6) it is possible to observe, for different values of α, the relationship between compressive vertical stress and the transversal stress in the brick–mortar interface, when β varies. It could be concluded that, as the value of α becomes smaller, induced tensile stresses in the brick

due to the mortar behaviour, will also decrease. The effect of the restriction of the brick on the mortar it does not have much influence either.

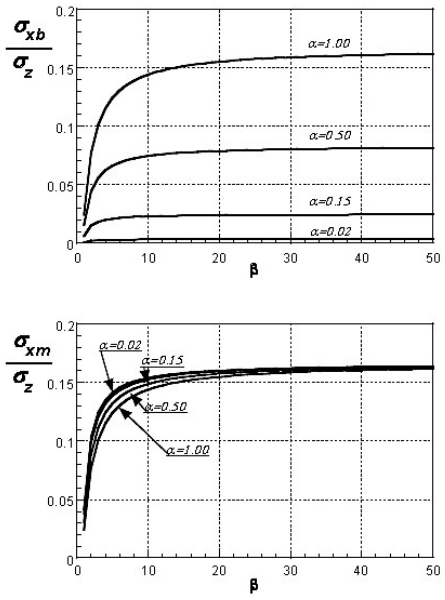

Fig.3.6. Transversal stress of the brick and mortar relative to the vertical compression stress, in relation to α and β. (Martinez 2003)

In the current thesis, by placing the brick with the load parallel its face, the value of α will be less than in the case of conventional masonry arrangements and, therefore, the stress induced by the mortar on the brick will diminish.

The experimental tests in this thesis are too limited to serve to establish an exponential formula which explains its. To verify, whether the exponential type of equation would be applicable to a masonry type such as, that which is the subject of this study, and using regression analysis based on the least square adjustment method for the experimental values, the equation [11] can be formulated.

The values of k, α, and β have been obtained with a determining coefficient (R^2) of 0.74 and a standard estimation error (σ) 1.85 N/mm^2.

$$f_{\mathrm{k}} = 0.10 f_{\mathrm{b}}^{0.34} f_{\mathrm{m}}^{1.93} \qquad [11]$$

It has been observed previously that as a result of the position of the brick there is a reduction of the tensile stress induced by the mortar. If coefficients k, α and β were observed, It can be seen that they bear no resemblance to the usual values. Thus, we see that the k, α and β values proposed by the standards and its recommendations may not be applicable to one-leaf thin-tile masonry. Thus, a new k, α and β values will be needed. It is clear that this is a very limited study and that it will be necessary to extend the experimental characteristics by increasing the number of tests, as well as the types of masonry and mortar. Adjusting these results is beyond the scope of the thesis.

As could be seen in the results from the equations proposed by (Gumaste et al. 2007), the fact of whether the specimens are manufactured with or without vertical joints, modifies the compressive strength values. The values obtained (see table 3.5) from the equation proposed for specimens without vertical joints are 30% higher than those obtained from the equation for specimens with joints. In (Fonseca et al. 2015) the test was performed on concrete blocks. The test was based on prisms of three blocks and wallettes. Two types of prisms were manufactured, with vertical joints in the middle and without vertical joints. The authors indicate that triplets with vertical joints and wallettes had similar values for compressive strength. These values were lower than the triplets without joints, to the order of 42-66%, depending on the type of mortar. In the same study it was concluded that specimens with vertical joints better represent, in terms of compressive strength, the masonry behaviour.

3.2. Compressive strength of multi-leaf specimens

The behaviour of brick masonry under uniaxial compression is closely tied to the orientation of the effort in regard to the bed joints. In preliminary research, (Samarasinghe 1980), (Hodgkinson and Davies 1982), (Dhanasekar, Kleeman, and Page 1985), (Naraine and Sinha 1989), (Drysdale and Hamid 1982), (Antoine 1992), (Capozucca 2004), (Singh and Shina 2004), (Hamid et al. 2005), (Badarloo, Tasnimi, and Mohammadi 2009), (Capozucca 2017), analysed this behaviour with different orientations.

A peculiar aspect of the thin-tile masonry is the vertical thin-tile-mortar interface, in other words the interface between the thin-tile- and mortar-leaf. Two singular cases of brick masonry with vertical mortar-piece interface are, brick masonry loaded parallel to bed joints and multi-leaf wall masonry.

In this section, the experimental results obtained for the two- and three-leaf specimens will be compared to verify whether or not their behaviour is comparable to that defined in the literature for brick masonry loaded parallel to bed joints or multi-leaf wall masonry.

3.2.1. Stress-strain behaviour

Fig. 3.7 shows the stress-strain behaviour from the compressive strength test of the two-leaf (a) and three-leaf (b) specimens from the first experimental test. In order to better compare the performance of the different specimens, the stress-strain values were normalised to the peak values. However, in the case of the three-leaf specimens the vertical deformation was normalised to the deformation at the moment of detachment ε_{vd}. To preserve the integrity of the equipment, the LVDTs were removed when the maximum stress was exceeded. As a result, the diagrams do not show performance in the descending branch.

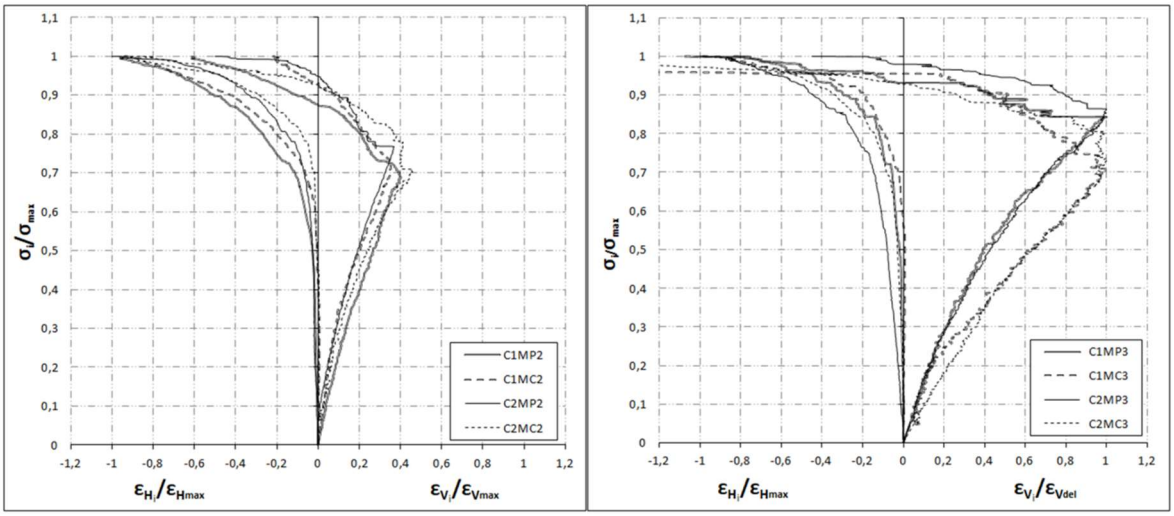

(a) (b)

Fig. 3.7. Normalised stress-strain behaviour of two-leaf (a) and three-leaf (b) masonry from first experimental test.

In the experimental results, the usual behaviour in brick masonry can be seen up to values of 70-85% of the maximum stress. This point coincides with the detachment stress. From this point, there is an increase in the usual horizontal deformation, but an unusual elongation in the vertical one. The vertical LVDTs were attached to the exterior thin-tile leaves. Individually, these leaves are very slim. Due to increase of the horizontal deformation, a rotation of the outer leaves might be possible. Hence, the vertical LVDTs, after detachment, record the vertical shortening of the leaf produced by the load, but also the extension of the latter because of the rotation.

Up to the detachment stress, and with respect to the vertical deformation, can be drawn: for three-leaf specimens a clear relationship between the vertical deformation and the type of mortar; for two-leaf specimens no clear influence of either the mortar or the thin-tile. The horizontal deformation was influenced by both components of the specimens. Thus: the specimens with the MP mortar were softer than those with the MC mortar; the specimens with the C1 thin-tile were softer than the C2 in the case of two-leaf specimens, but backwards for three-leaf specimens.

From the stress-strain experimental behaviour can be drawn: for thin-tile masonry the behaviour up to the detachment, is that expected for brick masonry loaded parallel to bed joint; with regard to three-leaf specimens, the vertical deformation is mainly influenced by the mortar; the horizontal deformation of the specimens observed can be attributed to the transverse deformation of each leaf or, due to their individual slenderness, to the separation between the thin-tile leaves.

From second experimental test, figure 3.8 shows the stress-strain behaviour of the average of the four specimens of each type. Now, all values have been normalized to the peak values. The vertical displacement corresponds to the average value of the four strain gauges. Therefore, the experimental strain-stress behaviour presents the deformation experienced by the thin-tile piece and not by the ceramic leaf as a whole. The horizontal displacement is the average of the two horizontal LVDTs. These record the transversal

opening of the prism, including the two thin-tile and mortar leaves. During the test, the vertical LVDTs values were kept around zero until the detachment. This unreal behaviour can be associated with the rotation of the ceramic leaves as a result of the horizontal deformation of the specimen. This opening, magnified by the 9 cm horizontal separation between the prism and the LVDTs due to the setup of the test, led to those unreal values. In consequence, in this thesis the results obtained by the vertical LVDTs, in the second test, were not presented.

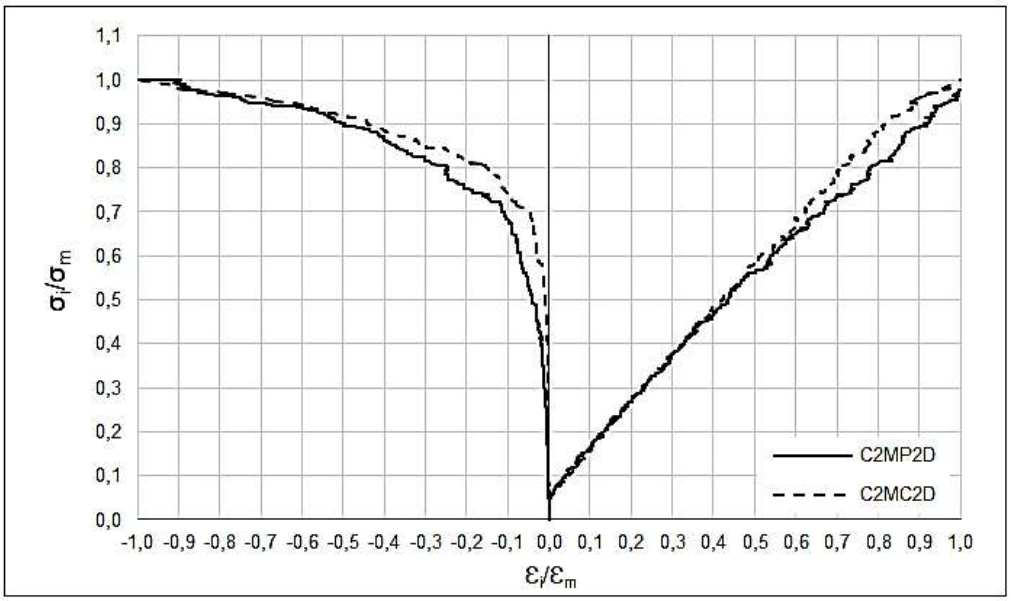

Fig. 3.8. Normalized stress-strain behaviour of specimens from second experimental test.

For both groups of specimens, it can clearly notice a difference in behaviour from 60-70% of the peak stress, when detachment occurs. Vertical deformation for C2MC2D specimens remains almost linear until reaching values of 90% of maximum stress, while the C2MP2D specimens show slight inflection starting at this point. Hence, the hypothesis that the deformation recorded by the vertical LVDTs beyond the detachment stress registers also the extension due to the rotation of the leaf was confirmed. The horizontal deformation for both types of specimens behaves similarly, while C2MP2D specimens have greater horizontal deformation before detachment.

3.2.2. Failure mode

The development of failure mode in two- and three-leaf specimens is presented in (Fig. 3.9). A red line represents the new crack, while the blue line was used for the existing one. The failure mode began with the appearance of a crack in one or two vertical thin-tile-mortar interfaces. The splitting was initiated around the horizontal edge mortar joint and gradually was propagated towards the centre of specimen. As the load was increased, the crack was lengthened along the interface up to the detachment of one of the leaves. After, in most cases, a new crack appeared in another thin-tile-mortar interface. The collapse was widely reached by buckling of the leaves, but in some cases on two-leaf specimens, due to the crushing of one of the leaves.

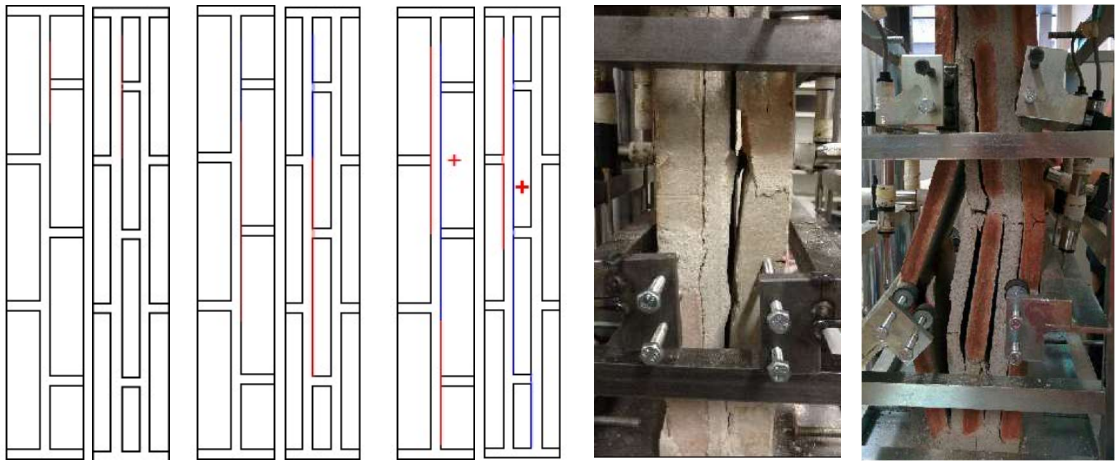

Fig. 3.9. General pattern of failure of the two- and three-leaf specimens. (a) Start of the crack, (b) propagation of the crack along the interface, (c) completion of the propagation and appearance of a new crack (detachment), (d) collapse of the specimen.

Similar failure mode has been explained by several authors for masonry with loads parallel to the bed joints (Page 1981), (Hoffmann and Schubert 1994), (Augenti and Parisi 2010), (Galman 2016) but also this mode of failure coincides with what is described in the literature for three-leaf walls with a softer inner leaf (Egermann, Frick, and Neuwald-Burg 1993; Binda et al. 2006; Vintzileou 2011)

3.2.3. Mechanical properties

From the results of the all experimental test carried out in this thesis, table 3.8 shows, the average value and the coefficient of variation for peak compressive strength (f_{kt}), detachment compressive strength (f_{ktd}) and the Young's modulus (E_{kt}) calculated as a secant modulus at 1/3 f_{kt} of thin-tile masonry. Detachment compressive strength was computed as the stress at moment of detachment of one of the leaves described in the failure mode.

Table 3.8. Mechanical properties of the thin-tile masonry specimens.

Experimental test	leaves	Materials		identification	Number of specimens	Peak compressive strenght	Detachment compressive strenght	Young modulus
		thin-tile	mortar			f_{kt} (N/mm²)	f_{ktd} (N/mm²)	E_{kt} (N/mm²)
1	2	C132	MP	C1MP2	6	12.43 0.34)	7.74 (0.40)	16.270 (0.21)
			MC	C1MC2	6	8.62 (0.10)	4.99 (0.24)	18.269 (0.47)
		C228	MP	C2MP2	6	10.36 0.15)	7.18 (0.11)	11.839 (0.34)
			MC	C2MC2	6	8.37 (0.06)	6.70 (0.09)	14.122 (0.18)
	3	C118	MP	C1MP3	6	7.64 (0.43)	6.54 (0.43)	14.305 (0.44)
			MC	C1MC3	6	5.30 (0.15)	4.17 (0.28)	9.247 (0.54)
		C218	MP	C2MP3	6	7.86 (0.27)	6.76 (0.30)	11.536 (0.39)
			MC	C2MC3	6	7.07 (0.05)	5.94 (0.14)	10.823 (0.20)
2	2	C228 +	MP	C2MPD	4	11,49 (0,12)	7,26 (0,25)	10.769 (0,11)*
		C245	MC	C2MCD	4	8,99 (0,08)	6,50 (0,12)	10.001 (0,14)*
3	2	C228	MP	P2MP	1	12.71	6.54	
			MC	P2MC	1	8.61	3.53	
	3	C218	MP	P3MP	1	8.50	6.79	
			MC	P3MP	1	6.63	5.04	

*Values obtained from average value of strain gauges

Values in parentheses correspond to the coefficient of variation.

Based on the result of the first experimental test, the compressive strength of specimens built with MC mortar was lower than those built with the MP mortar. This loss can be quantified as approximately 15% for C2 and 31% for C1 thin-tiles. Nevertheless, detachment compressive strength was 9% and 36% respectively. In turn, the compressive strength of specimens built with C1 thin-tiles was higher than those built with the C2 thin-tile; being most noticeable in the specimens of two-leaf. This effect can be related to the different compressive strength of the thin-tile.

The detachment compressive strength of two-leaf specimens noted an increase of 19% over three-leaf specimens for C1 thin-tile, and 9.5% for C2. This difference seems to indicate that the stress was not distributed similarly in the thin-tile and the mortar leaves.

From the comparison of first and second experimental test can be drawn that the prisms with different leaves (C2MPD and C2MCD) presented higher maximum compressive strength, but very similar detachment compressive strength. This difference can be associated to the greater thickness of one of the leaves.

The values obtained in the last experimental test, with regard to the first, in general, were in good agreement, except for the detachment compressive strength of the P2MC prism which presented values 52% lower than the precedent ones.

3.2.4. Analytical model based on brick masonry loaded parallel to bed joint

In brick masonry loaded parallel to the bed joints, the most common mode of failure is the detachment into multiple leaves. This detachment affects its load-bearing capacity, mainly due to the more significant influence of the slenderness of each of the leaves. This is especially relevant in thin-tile masonry due to the reduced number and thickness of the leaves. In consequence, the value of detachment compressive strength (f_{ktd}) is especially relevant.

According to existing studies, when the angle between the bed joints and the load is equal to 90° (normal stress) or 0° (parallel stress), the stress-strain behaviour of both masonry is similar (Samarasinghe, Page, and Hendry 1982), (Senthivel, Sinha, and Madan 2000). On the other hand, when the load is parallel to the bed joints the standards (CTE. SE-F 2009) and (EC-6 1996) suggest the use of the same equation [5], but with the value f_b as the compressive strength of the brick with regard to the orientation of the load. Thus, due to the arrangement of several thin-tile and mortar leaves, the thin-tile masonry could be considered a singular case of brick masonry loaded parallel to the bed joints.

To check whether the equation [5] is suitable to thin-tile masonry, Table 3.9 shows the values for K, α, β and the coefficient of determination (R^2) obtained through the regression analysis based on the adjustment least minimum squares method of the first experimental test values.

Table 3.9. Coefficients K, α, β for adapting the exponential equation and the coefficient of determination (R^2).

Thin-tile masonry	*Compressive strength*	*K*	*α*	*β*	R2
Two-leaf	peak	1,498.00	-1.68	0.03	0.21
	detachment	3.19	0.14	0.04	0.46
Three-leaf	peak	0.16	0.57	0.84	0.60
	detachment	0.38	0.47	0.67	0.65

From the comparison of the K, α, β values of this thesis with those obtained from the literature it can be drawn: for two-leaf masonry, the values showed an excessive difference and a low coefficient of determination. Therefore, it becomes clear that equation [5] does not accurately predict the compressive strength. On the other hand, for three-leaf masonry, values were found usual for brick masonry, but with higher influence of the mortar compressive strength. Similar influence was appreciated in the stress-strain behaviour. Consequently, equation [5] seems adequate to compute the compressive strength only in three-leaf thin-tile masonry.

As mentioned in Section 3.2.2, the failure mode of the thin-tile masonry agreed with that described for masonry loaded parallel to the bed joints. In this regard, (Hoffmann and Schubert 1994) indicated that, for the compressive strength of masonry loaded parallel to bed joints, the adhesive shear strength (cohesion) between the brick and the bed joint mortar becomes decisive. In this instance, premature separation of the masonry leaves is conceivable if there is a significant difference in stiffness between them.

The results presented in chapter 2 showed that the thin-tile leaves were significantly stiffer than the mortar ones. Table 3.10 shows the detachment compressive strength,

considering that the load is carried solely by the thin-tile leaves (f_{ktdc}). This value was calculated as the total load applied to the specimen, divided by its cross-section discounting the area of the mortar leaf.

Table 3.10. Compressive strength at detachment, considering the thin-tile leaves only.

Two-leaf		Three-leaf	
	f_{ktd} (N/mm²)		f_{ktd} (N/mm²)
C1MP2	10.00 (0.44)	C1MP3	10.04 (0.40)
C1MC2	5.89 (0.23)	C1MC3	6.07 (0.25)
C2MP2	9.44 (0.14)	C2MP3	9.98 (0.31)
C2MC2	8.77 (0.09)	C2MC3	8.76 (0.17)

Values in parentheses correspond to the coefficient of variation.

No substantial differences of compressive strength at detachment were observed between two- and three-leaf. Thus, the mortar-leaf seemed do not bear the load, or those load was very small. This phenomenon could be associated with different stiffness of the thin-tile and mortar leaves. Similar results were obtained by other authors (Page 1981).

3.2.5. Analytical model based on multi-leaf masonry walls

The other case of brick masonry with vertical mortar-piece interface is multi-leaf wall masonry. It is usually made up of two outer leaves of brickwork or stonework, with an inner leaf or core, generally of lower quality, filled with soft material, such as small pieces of stone and/or brick and mortar (Vintzileou and Tassios 1995).

In order to determine the compressive strength of three-leaf masonry, (Egermann 1993) proposes the following equation [12]:

$$f_{\mathrm{wc,0}} = \frac{V_{\mathrm{e}}}{V_{\mathrm{w}}}\,\theta_{\mathrm{e}} f_{\mathrm{c,e}} + \frac{V_{\mathrm{i}}}{V_{\mathrm{w}}} \cdot \theta_{\mathrm{i}} \cdot f_{\mathrm{c,i}} \qquad [12]$$

Where $f_{c,e}$, $f_{c,i}$ and $f_{wc,0}$, represent the compressive strength of the outer leaves, inner leaf, and wall. V_e, V_i i V_w represent the volume of the outer, the inner and total of the wall, while θ_e < 1 and θ_i >1 are experimentally determinant factors that take into account the interaction between outer and inner leaves.

Other studies that analyse multi-leaf walls using ceramics and mortar are (Drougkas et al. 2015), which analyse a cylindrical, solid clay brick pillar filled with ceramics and Portland cement. The authors state that the compressive strength of the pillar is lower than that of any of its macroscopic constituent materials in the outer and inner leaves. A simple analytical model, based on compressive strength and Young's modulus of the macroscopic components, was able to emphasize the principal structural characteristics that affect its response to compression better than an analytical model based on the maximum stress of the components. (Badarloo, Tasnimi, and Mohammadi 2009) Analyses panels with solid brick/cement/perforated brick subjected to parallel and perpendicular loads to bed joints and different degrees of pre-compression. In all cases, the fundamental mode of failure involved the separation of the central leaf from the outer leaves.

The mode of failure described in section 3.2.2 of this thesis, indicates the appearance of a crack separating the outer leaves from the inner one. This mode of failure is in compliance with what is described in the literature for three-leaf walls with a softer inner leaf.

In this section, and to ascertain whether the equation [12] proposed to determine the compressive strength of multi-leaf masonry (Egermann 1993) is useful for predicting the compressive strength of two-leaf masonry, the experimental values were compared with the analytical values obtained by using equation [12]. Table 3.11 presents the experimental values of the three experimental tests, in terms of compressive strength of thin-tiles, mortar, and the two-leaf thin-tile specimens.

One of the important values in computing the compressive strength of multi-leaf wall masonry is the uniaxial compressive strength of each leaf. In general, this value is obtained experimentally. In this thesis the compressive strength of the external (thin-tile) leaf ($f_{c,o}$) could not be obtained experimentally due to its slenderness. Instead, equation [11] proposed in section 3.1.4 was used to determine the values of ($f_{c,o}$):

$$fc, o = 0.10 f_b^{0.34} f_m^{1.93} \qquad [11]$$

where f_b *and* f_m were the compressive strength of the thin-tile and mortar respectively.

The modulus of elasticity (E_{co}) was obtained from the E_{co}/f_{co} relationship proposed in the mentioned section. The values of the compressive strength ($f_{c,i}$) and modulus of elasticity (E_{ci}) of the inner (mortar) leaf, and being the same material, coincide with the values f_m and $E_{m50\text{-}30}$ of the mortar. Table 3.11 also presents the thickness of the thin-tile leaves (t_{c1} and t_{c2}), mortar leaf (t_m) and the total thickness of the specimen (t_t).

Table 3.11. Computed compressive strength ($f_{c,o}$ and $f_{c,i}$) and Young modulus ($E_{c,o}$ and $E_{c,i}$) of external and internal leaves

specimen	experimental test	Experimental compressive strength (N/mm²) Thin-tile (f_b)	Mortar (f_m)	specimens Peak (f_{kt})	Detachment (f_{kto})	tick of leaves (mm) tc1	tm	tc2	tt	Mechanical properties of leaves (N/mm²) Outer $f_{c,o}$	$E_{c,o}$	inner $f_{c,i}$	$E_{c,i}$
C1MP1 21	1	35.45	6.32	13.12	7.03	29.5	17.0	28.0	74.5	11.82	8.889	6.32	6.421
C1MP1 22		35.45	6.32	10.08	4.60	31.0	12.0	32.5	75.5	11.82	8,889	6.32	6,421
C1MP2 23		35.45	10.46	13.00	9.10	30.0	16.5	29.5	76.0	31.23	23,485	10.46	10,627
C1MP3 24		35.45	10.00	19.97	13.22	27.5	19.5	28.0	75.0	28.63	21,530	10.00	10,160
C1MP7 25		35.45	9.41	10.71	7.23	29.0	16.5	30.0	75.5	25.46	19,146	9.41	9,561
C1MP8 26		35.45	5.82	7.72	5.25	30.0	16.5	30.0	76.5	10.07	7,573	5.82	5,913
C1MC1 21		35.45	7.11	7.95	4.39	30.0	9.5	31.5	71.0	14.84	13,386	7.11	4,749
C1MC2 22		35.45	8.60	9.70	2.88	29.5	12.5	27.0	69.0	21.41	19,312	8.60	5,745
C1MC3 23		35.45	7.54	9.57	5.62	29.0	15.5	29.0	73.5	16.62	14,991	7.54	5,037
C1MC7 24		35.45	5.95	8.76	6.12	31.0	14.0	30.0	75.0	10.51	9,480	5.95	3,975
C1MC7 25		35.45	5.95	7.42	5.52	30.0	14.5	28.5	73.0	10.51	9,480	5.95	3,975
C1MC9 26		35.45	7.08	8.32	5.38	29.0	13.5	29.5	72.0	14.69	13,250	7.08	4,729
C2MP4 21		31.44	9.96	11.45	8.48	26.0	18.0	26.0	70.0	27.27	12,081	9.96	10,119
C2MP4 22		31.44	9.96	11.91	7.50	26.5	16.5	26.0	69.0	27.27	12,081	9.96	10,119
C2MP5 23		31.44	7.68	11.88	6.18	28.0	13.5	26.5	68.0	16.54	7,327	7.69	7,813
C2MP6 24		31.44	4.88	9.08	6.47	26.5	16.0	26.5	69.0	6.89	3,052	4.88	4,958
C2MP8 25		31.44	5.51	9.49	7.26	26.0	18.5	25.0	69.5	8.71	3,859	5.51	5,598
C2MP9 26		31.44	3.53	8.34	7.20	28.5	16.5	26.5	71.5	3.68	1,630	3.53	3,586
C2MC4 21		31.44	6.08	8.02	6.43	27.5	15.0	26.0	68.5	10.51	5,518	6.08	4,061
C2MC4 22		31.44	6.08	7.63	6.35	27.0	15.0	24.5	66.5	10.51	5,518	6.08	4,061
C2MC5 23		31.44	7.20	8.89	6.04	27.0	22.5	26.0	75.5	14.57	7,649	7.20	4,810
C2MC5 24		31.44	7.20	8.70	7.80	26.5	17.0	26.5	70.0	14.57	7,649	7.20	4,810
C2MC8 25		31.44	7.07	8.91	6.73	26.5	17.0	26.0	69.5	14.09	7,397	7.07	4,723
C2MC1 26		31.44	5.40	8.04	6.82	26.5	12.0	26.0	64.5	8.37	4,394	5.40	3,607
C2MP2D1	2	18.22 / 31.44	9.54	11.00	4.95	44.4	9.7	26.7	80.8	14.4 / 19.3	6,042 / 8,539	9.54	9,693
C2MP2D2		18.22 / 31.44	9.54	12.30	8.89	45.6	9.8	25.9	81.4	14.4 / 19.3	6,042 / 8,539	9.54	9,693
C2MP2D3		18.22 / 31.44	9.54	9.82	6.74	44.9	10.0	27.3	82.1	14.4 / 19.3	6,042 / 8,539	9.54	9,693
C2MP2D4		18.22 / 31.44	9.54	12.80	8.46	44.6	10.0	26.4	81.0	14.4 / 19.3	6,042 / 8,539	9.54	9,693
C2MC2D1		18.22 / 31.44	5.68	8.05	5.69	45.2	10.5	25.7	81.3	11.08 / 13.13	5,964 / 6,973	5.69	3,801
C2MC2D2		18.22 / 31.44	5.68	9.41	6.65	44.5	9.4	26.0	79.8	11.08 / 13.13	5,964 / 6,973	6.65	4,442
C2MC2D3		18.22 / 31.44	5.68	9.70	7.50	45.0	10.3	24.8	80.0	11.08 / 13.13	5,964 / 6,973	7.50	5,010
C2MC2D4		18.22 / 31.44	5.680	8.80	6.16	45.0	10.1	26.4	81.5	11.08 / 13.13	5,964 / 6,973	6.16	4,115
P2MP	3	31.44	7.83	12.70	6.54	26.5	17.0	26.0	69.5	17.14	7,593	7.83	5,230
P2MC		31.44	7.69	8.61	3.53	26.7	17.3	26.2	70.2	16.56	7,336	7.69	5,137

Table 3.12 shows the experimentally adjusted values of experimentally determined factors θ_e, θ_i and the determination coefficient (R^2) obtained through the regression analysis based on the adjustment least minimum squares method of the experimental values of the 34 specimens from table 3.11.

Table 3.12. Experimental values obtained of θe, θi and the determination coefficient (R^2).

	θ_e	θ_i	R^2
Peak stress	0,38	3,45	0.94
Detachment stress	0.15	2.95	0.90

The value obtained for coefficient θe appears reasonable for the peak strength, but low for detachment strength, if it is compared with values proposed in the literature (Egermann and Neuwald-Burg 1994; Binda et al. 2006; Drougkas, Roca, and Molins 2015; Demir and Ilki 2014; Tassios 2004). While coefficient θi is higher in both cases. This seems to indicate that in thin-tile masonry compressive strength, the mortar leaf plays a more influential role than the thin-tile leaves. From the values of this thesis it can be drawn: the mortar leaf is much thinner than the thin-tile leaves; mortar and thin-tile leaves had similar stress as was confirmed by DIC images. Therefore, the mortar leaf role seems more related to keep the leaves bonded, than with load-bearing strength.

As for rigidity, in (Stavroulaki and Papalou 2014) and as a result of the Young's modulus relationship between the inner (E_{ci}) and the outer leaves (E_{co}) E_{ci}/E_{co} = 0.2, can be observed that the inner leaf experiences greater stress than the outer ones in the upper part of the specimen. This stress is mostly transferred to the outer leaves, with residual stress remaining in the inner one. As the E_{ci}/E_{co} ratio approaches 1, the stress becomes more uniform. In the numerical model proposed by authors, a perfect union between all leaves is supposed, and as a result, the appearance of the crack was not considered.

In this thesis, the outer leaves had a higher Young's modulus value than the inner ones ($E_{c,o} > E_{\mathrm{c,i}}$). As can be noted in (Fig. 3.8) (section 3.2.1), the thin-tiles show a linear

vertical deformation with no visible change at detachment. The specimens presented a low horizontal deformation at this point. As can be seen in (Fig. 3.9 a), after the collapse of the specimens the mortar leaf is separated from the two ceramic leaves, which would confirm that a certain amount of stress is transferred through this leaf. Thus, these specimens behave as described by (Stavroulaki and Papalou 2014).

The appearance of the crack observed in the specimens, could be associated with a loss of contact in the outer-inner leaf interface, as a result of the tensile stress induced by the inner leaf. This behaviour coincides with the observations of the authors (Egermann 1993), (Vintzileou and Tassios 1995), (Valluzzi, Da Porto, and Modena 2004), (Oliveira et al. 2012), (Pappas 2012).

In thin-tile masonry the weak point is the thin-tile-mortar interface in the plane parallel to the application of the load. In section 3.2.4, this detachment was attributed to shear failure, coinciding with the mode II failure. This section seems to indicate that the detachment is caused by the normal tensile force applied to the interface, coinciding with mode I failure. Therefore, a more in-depth analysis of the failure mode of thin-tile masonry is required.

3.3. Development of failure mode

The failure mode of brick masonry loaded parallel to the bed joints is characterized by the development of cracks between brick and bed joints (mode II). Consequently, the adhesive shear strength between brick and mortar becomes decisive for determining the compressive strength of this brick masonry (Hoffmann and Schubert 1994).

The loss of bond between the leaves is a common problem in multi-leaf wall masonry (Vintzileou and Tassios 1995; Vintzileou 2007; Drougkas et al. 2015). The deformation of walls can be divided into two phases, an initial phase where there is full union between outer and inner leaves, and where no damage can be observed. The second phase begins with the appearance of a bond failure between the outer and the inner leaves. The

behaviour during collapse depends on the ratio between the rigidity of the different leaves. If the inner leaf is more rigid than the outer, the collapse of the system is the result of compression failure. Meanwhile, if the inner leaf is softer, under a certain load, it begins to yield. As a result of this compression, the stress is practically constant in the inner leaf, while the increased load is distributed to the outer leaves. Thus the outer leaves are subjected to compressive stress due to the vertical load, and a horizontal force when the inner one, softer, yields. This stress state leads to an out-of-plane rotation of the outer leaves (Egermann, Frick, and Neuwald-Burg 1993; Valluzzi, Da Porto, and Modena 2004; Vintzileou and Tassios 1995). Therefore, the loss of bond between the leaves is due to tensile stresses perpendicular to the wall (mode I) (Pappas 2012). It is considered that as long as the vertical cracks in the interface between the leaves have not formed in all its extension, there is no detachment (Oliveira et al. 2012).

From the hypothesis that: *i*) the load is all borne by the thin-tile leaves, *ii*) the influence of the mortar in the behaviour of the specimen seems related to its bond ability. It does not clear that the failure mode is related to the shear stress in the vertical mortar-thin-tile interface, but with a tensile stress on the interface. This tensile stress could be due to the lateral movement of the thin-tile leaf, due to its slenderness. In this section analyse the deformation field of the leaves along of the compressive strength test.

As previously stated, the failure mode of this type of masonry structures consists on the appearance of a crack in a vertical thin-tile-mortar interface that propagates through this interface leading to failure. To analyse the results, three different cross sections were established and analysed in the prism. At each section, one point was defined on each leaf (thin-tile and mortar) (fig.3.10). Each point was identified with two numbers, corresponding to the cross section and the leaf, respectively. For example, point 2.4 stands for a point located at the second cross section and fourth leaf. For each point, the displacement during the test in the X (horizontal) and Y (vertical) axes was acquired with LVDTs and the DIC technique, and was analysed.

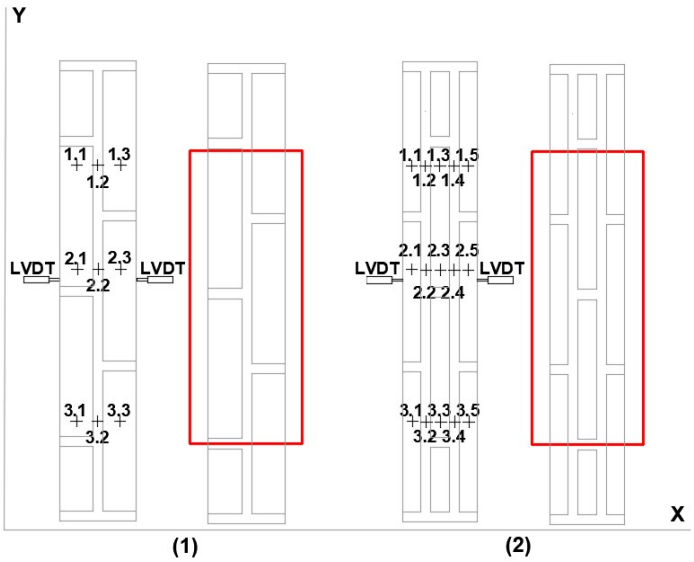

Figure 3.10. Control points, LVDTs placement and DIC-analysed area on two-leaf (1) and three-leaf (2) specimens.

Figure 3.11 shows the displacement of the points in both axes (X and Y) with respect to the stress of the two-leaf prism P2MP. The black lines represent the displacement of the thin-tile leaves (*i*.1 and *i*.3, *i* being the number of the section analysed) and the orange line that of the mortar leaf (*i*.2). The figure also shows, with grey line, the average value of the two horizontal LVDTs located at the mid height of the specimen (*H*), indicated in Figure 3.11.

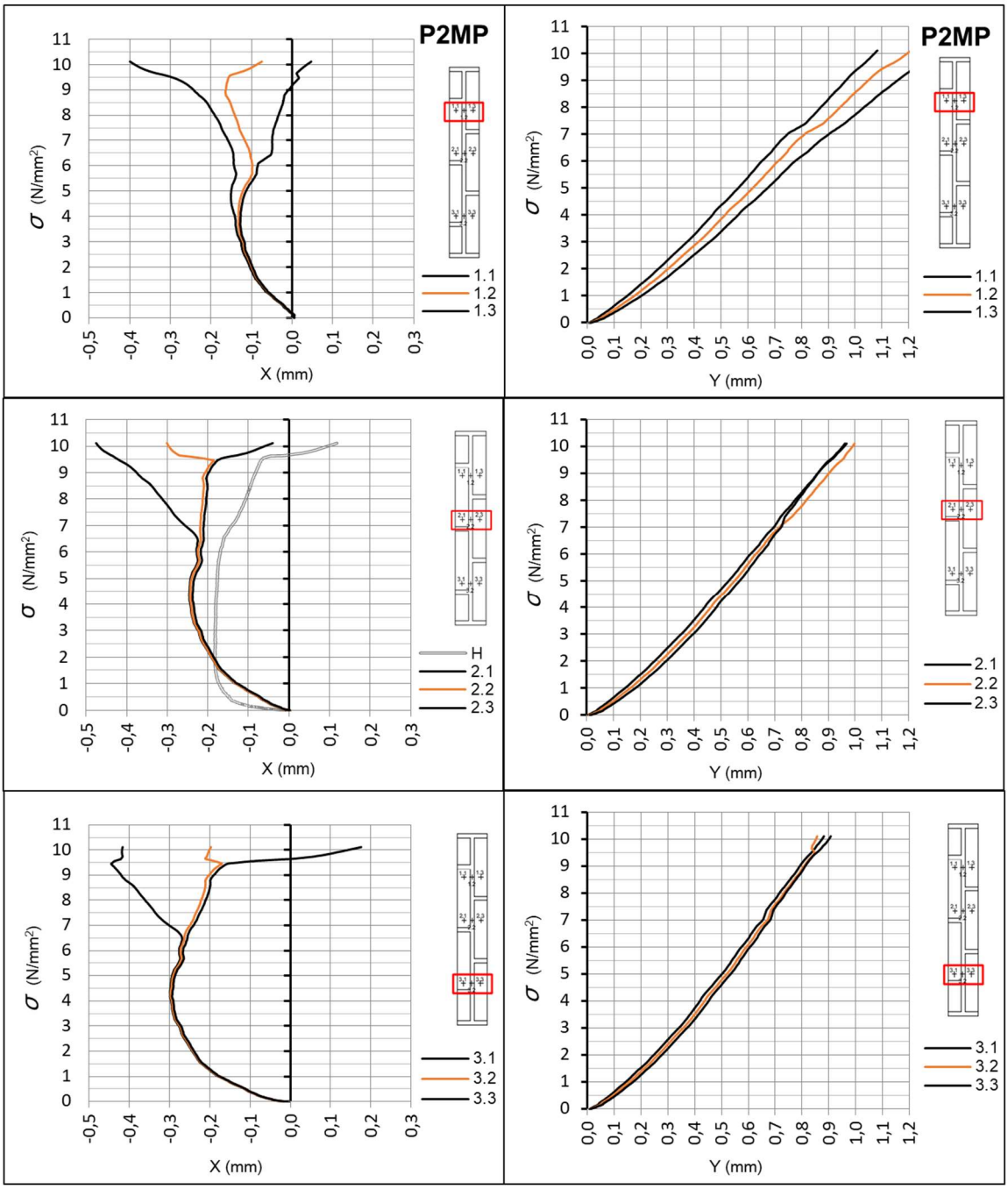

Fig.3.11. Stress-displacement experimental pattern in the X axis (a) and Y axis (b) of the selected points in the P2MP prism.

The experimental results of the LVDTs (*H*) present, until the stress = 0.5 N/mm² (σ *=0.5 N/mm²*), a horizontal displacement of the prism that can be associated with a movement of instability of the prism at the beginning of the test. A progressive change of the slope continues until σ *=1.5 N/mm²*. Between σ *=6.0-6.5 N/mm²* another progressive change of slope, coincides with the propagation of the crack through the height of the

prism. Subsequent detachment of one of the leaves (*1*), as observed in cross sections *2* and *3* (points *2.1* and *3.1*). From this point onwards, the displacement continues in a slightly linear manner until, approximately, σ *=9.5 N/mm²* where the separation of the leaf *2* is also observed in points *2.3* and *3.3*. At this instance, buckling of each of the leaves is observed on the prism and collapse is attained.

From DIC results, in the upper cross section (*1*) of the X axis, the beginning of the separation of the different leaves is observed, being more significant from σ *=3.5 N/mm²*. This tendency is maintained until σ *=6.0 N/mm²*, when the leaf *3* presents a different behaviour with respect to the other leaves. Leaves *1* and *2* are detached at σ *=9.0 N/mm²* with no signs of separation so far. In the cross sections *2* and *3* the detachment of leaf *1* takes place at σ *=6.5 N/mm²* and the detachment of leaves *2* and *3* in σ *=9.5 N/mm²*.

Regarding the Y-axis displacement, all the points present a similar displacement without any indication of the separation between the different leaves nor during the formation of the crack. All the specimens in this study show the same behaviour on the Y axis.

Figure 3.12 shows the vertical and horizontal deformation during the test of the prism P2MP acquired with the 3-DIC system. The images of the DIC correspond to the specific stress level identified at the foot of each image. The lilac colour indicates maximum compressive strains, whereas the red colour indicates maximum tensile strains.

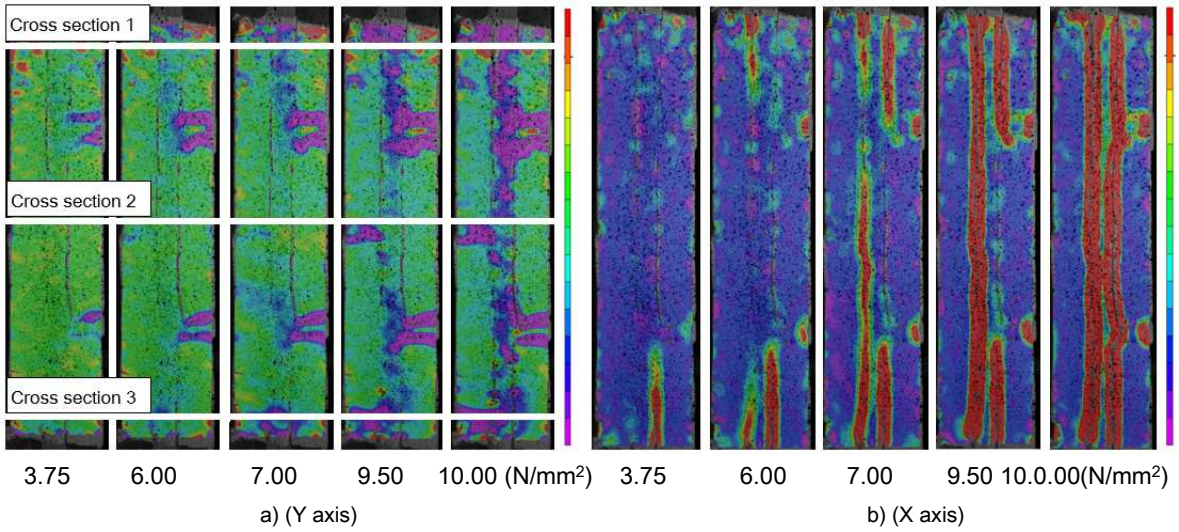

Fig.3.12. Field of deformations of vertical (a) and horizontal (b) of the prism P2MP acquired with DIC system at stress = 3.75, 6.00, 7.00, 9.50 and 10.00 N/mm^2.

In the vertical deformation field (Figure 3.12.a), it can be observed that, initially, the horizontal mortar joints are the areas that present greater deformation. On the other hand, the mortar leaf can be observed to present the same deformation as the thin-tile leaves and until the crack appears in the two vertical interfaces.

In the horizontal deformation field (figure 3.12.b), the propagation of the crack in the vertical thin-tile-mortar interface can be observed as the load increases (red colour). Thus, it appears that the appearance of the crack is not caused by the difference in vertical deformation between the leaves of the thin-tile and those of the mortar, but by a tensile stress perpendicular to this interface (failure mode I).

Figure 3.13.a shows the X-axis time-displacement relationship, whilst Figure 3.13.b and 3.13.c show the DIC vertical and horizontal deformation field of the P2MC specimen.

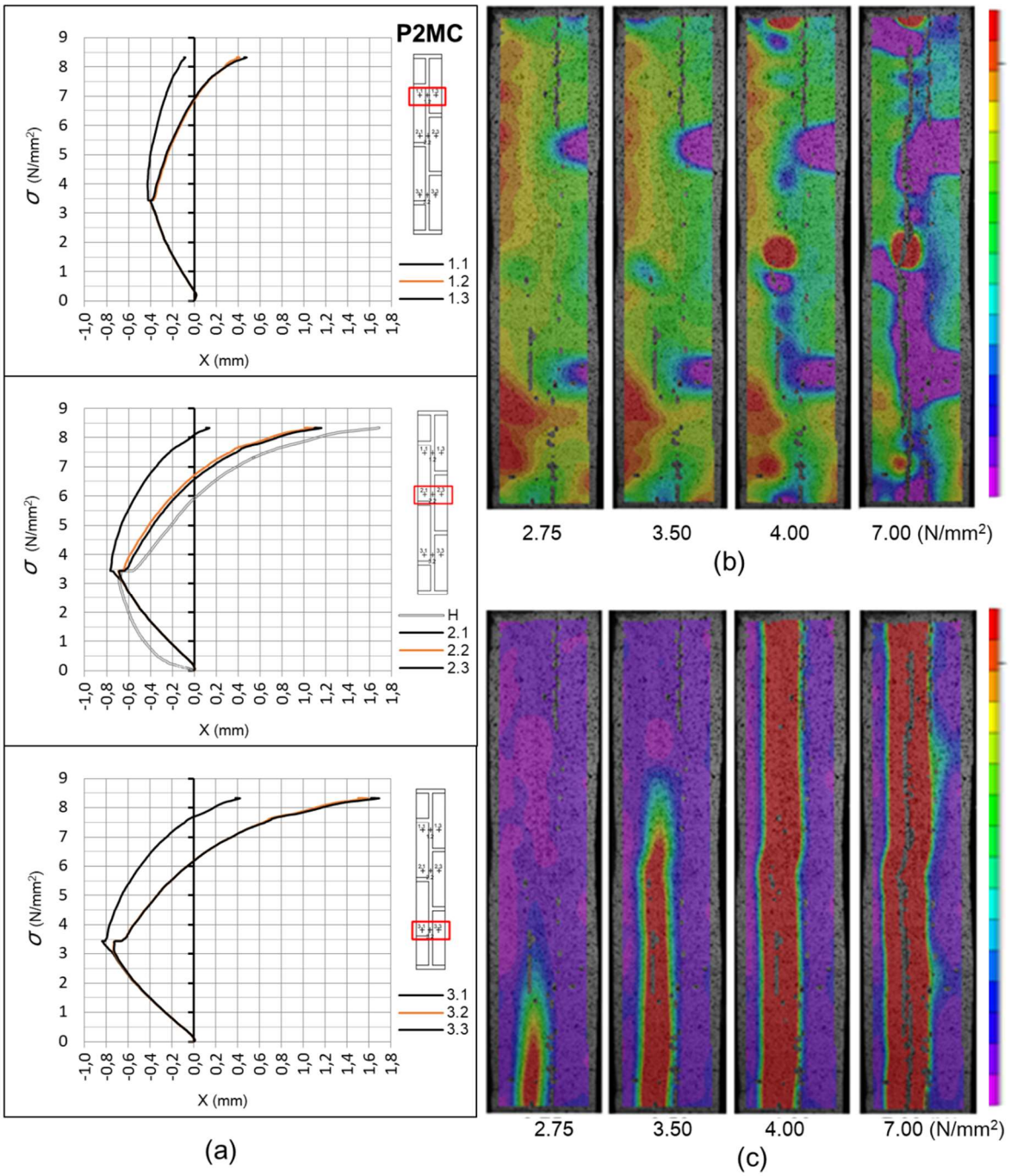

Fig.3.13. Stress-X displacement (a) and the DIC images of the vertical (b) and horizontal (c) deformation field at f_k = 2.75, 3.50,4.00 and 7.00 N/mm² of P2MC prism.

In this specimen the crack appears in the cross section *i*=3 at around σ=*3.0 N/mm²*. The separation of thin-tile leaf *1* quickly takes place (σ=*3.5 N/mm²*), but mortar leaf *2* continues bonded to thin-tile leaf *3* until the end of the test. The DIC images of the vertical deformation (Y axis) show that the application of the load was not symmetrical in the different leaves, with thin-tile leaf *3* presenting higher deformation values. Due to the non-

symmetrical loading of the leaves, a sudden detachment occurs due to the buckling of the specimen. Despite this quick detachment, the crack is produced by tensile stress perpendicular to the thin-tile-mortar interface. In this case, the out-of-plane rotation of the prism could be associated with the precursor of the crack.

Figures 3.14 and 3.15 show three-leaf specimens P3MP and P3MC, respectively. In X-axis displacement (Figure 3.14.a and 3.15.a), the outer thin-tile leaves are represented in black, the mortar leaves in orange and the central thin-tile leaf in green lines. Figures 3.14.b and 3.15.b show the DIC images of the vertical field of deformation, whilst Figures 3.14.c and 3.15.c present the DIC images of the horizontal field of deformation of the specimens.

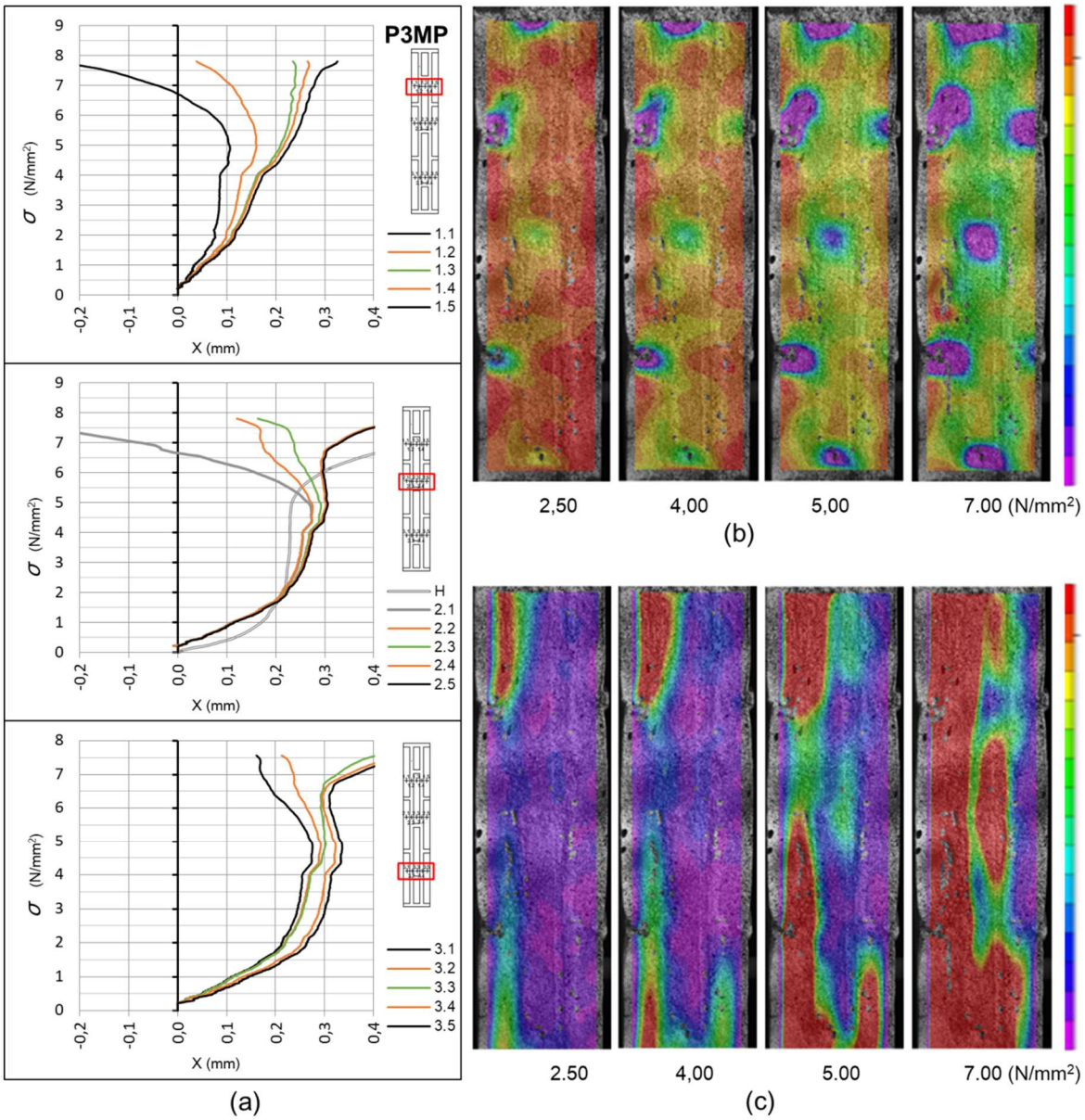

Fig.3.14. Stress-X displacement (a) and the DIC images of the vertical (b) and horizontal (c) deformation field at f_k = 2.50, 4.00, 5.00 and 7.00 N/mm² of P3MP prism.

In the P3MP prism, the separation of the outer leaves begins at a σ, ranging between *0.50 N/mm²* (cross section *1*) and *1.5 N/mm²* (cross section *2*) (Figure 6a), whilst the crack appears between σ =*5.00-6.00 N/mm²* (cross section *1*, *3* and *2* respectively). Regarding the movement described by the transverse LVDTs (H, grey line in Figure 6a), a first progressive change of slope is observed up to σ =*2.50 N/mm²*, which could be associated with the transverse deformation of the prism. From this point on until σ =*5.00 N/mm²*, the experimental pattern shows almost no displacement. Coincident with the formation and

propagation of the crack (σ =*5.00-7.00 N/mm²*) H presents again the progressive change of slope described in the P2MP prism.

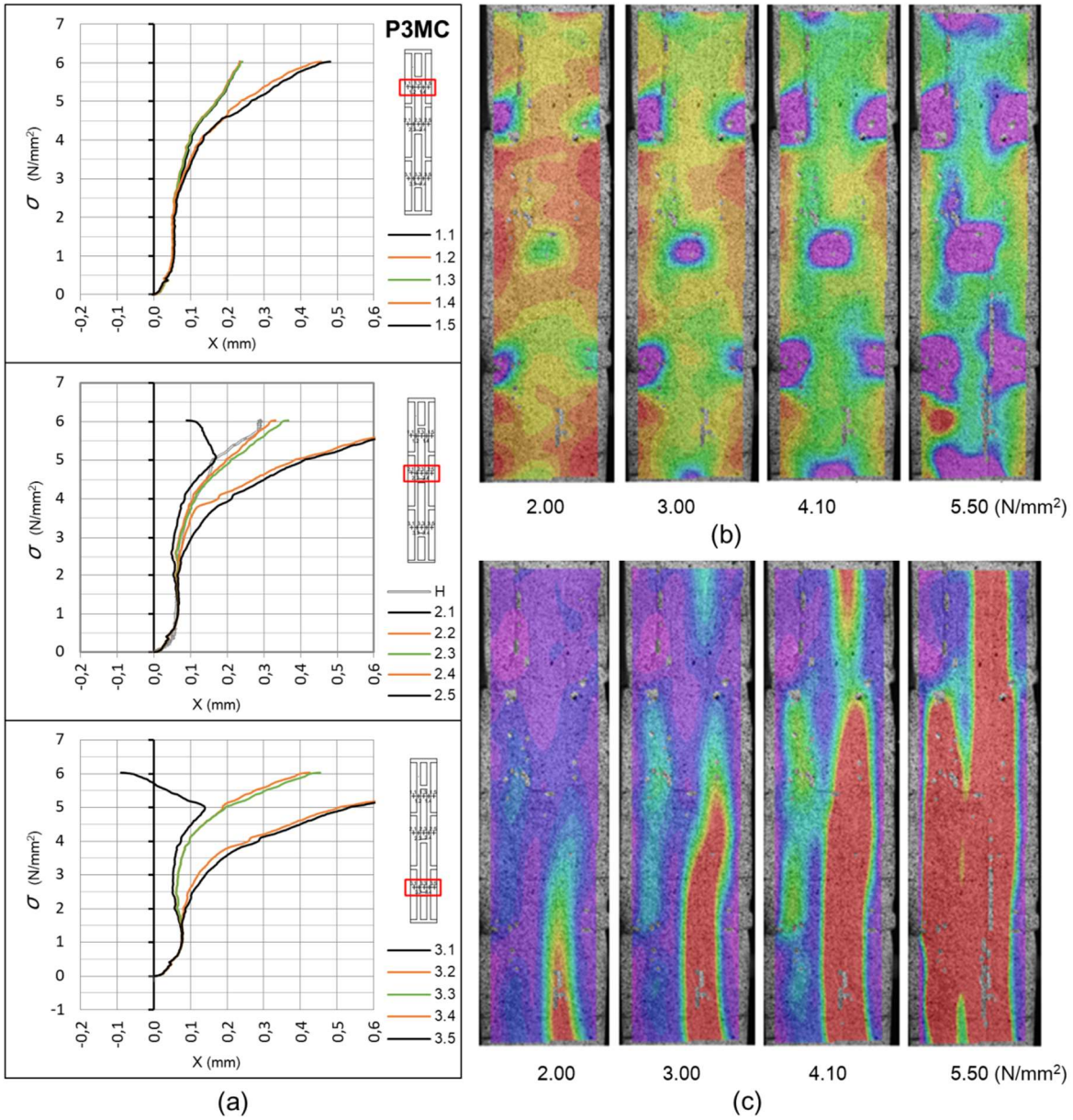

Fig.3.15. Stress-X displacement (a) and the DIC images of the vertical (b) and horizontal (c) deformation field at f_k = 2.50, 4.00, 5.00 and 7.00 N/mm² of P3MC prism.

On the P3MC prism, and for cross sections *2* and *3*, the separation between leaves *3* and *4* is observed (Figure 7a) from σ =*1.50 N/mm²* .The splitting occurs at *f* σ =*3.75 N/mm²*. The second crack appears at σ =*5.00 N/mm²*, this time between leaves *1* and *2* (cross

section *2* and *3*). Again, a progressive change of slope is observed in the graph of the LVDTs, now between $\sigma = 2.50–5.00\ N/mm^2$.

Several authors (Oliveira et al. 2012) have indicated that the moment of detachment is coincident with the complete development of the crack across the entire interface. Thus, the detachment point is considered here to be the end of the progressive change of slope recorded by transverse LVDTs. Hence, the values of detachment compressive strength presented in Table 3.8 (Section 3.2.3) were obtained from the load at this time.

The DIC images of the three-leaf specimens (Figures 3.14.b and 3.15.b) show the initial cracks around the horizontal-edged mortar joint and their subsequent propagation as was observed in the two-leaf specimens. Cracks also formed in the central part of the prism (cross section *2*). In this cross section, an increase in vertical deformation (Figures 3.14.c and 3.15.c) is observed in the horizontal mortar joint corresponding to the central thin-tile-leaf. This increase leads to the appearance of normal tensile stresses at the vertical mortar-thin-tile interface (X-axis) and, finally, to the development of cracks.

4. Concluding remarks

4.1. Conclusions

This thesis deals with the experimental analysis of behaviour thin-tile masonry under compressive stress. The analysis was focused on the stress-strain behaviour, the failure mode and the mechanical properties for masonry build with one- two- and three-leaf. The conclusions derived from this analysis are presented below.

Concerning the type of test and testing procedure.

It has been confirmed that the sizes of the specimens allow the test to be performed in the material failure zone.

The work of (Fonseca et al. 2015) and (Gumaste et al. 2007) indicate that prisms with vertical joints or walletes better represent, in terms of compressive strength, the behaviour of masonry with the load applied parallel to the face of the brick. These same authors indicate that prisms without vertical joints give higher values for compressive strength.

This thesis was undertaken on prisms without vertical joints. The values of compressive strength based on the exponential formulas proposed by the standards and scientific literature give lower values than those the results obtained in this thesis. The study of the influence of the vertical joints on the prisms for this type of masonry should be undertaken in future research.

From the detachment stress the vertical LVDTs record two movements: deformation of the leaf due to the load; and elongation of the leaf due to the rotation. Therefore, the stress-strain behaviour after the detachment stress cannot be properly recorded.

Concerning one-leaf thin-tile masonry

The stress-strain behaviour of one-leaf thin-tile masonry can be described using the equations proposed in literature to depict the stress-strain relationship of brick masonry usual in bearing wall. In most cases, it was found that the experimental results of this thesis were in accordance with the equation proposed by (Kaushik, Rai, and Jain 2007a). Hence, the one-leaf thin tile masonry loaded parallel to face brick, behaves similarly to brick masonry loaded perpendicular to the face brick.

Scientific literature indicates that the stress-strain behaviour of the load-bearing wall brick masonry, in the case of loads applied perpendicular to the face, continues to be substantially linear up to values between 30 and 60% of f_k, then, it becomes non-linear. According to the results of this thesis, the linearity remains at 45- 60% for f_k. Afterwards, and in the non-linearity zone, the specimen does not crack. Thus, such the non-linearity is governed by the mortar.

The standards establish a relationship of the Young's modulus (E_k) of about 750-1,000 times the compressive strength (f_k). However, in the examples presented in the specialized literature, a greater variability is observed (E_k=210-1.670 f_k). In this study, and for one-leaf specimens, the values obtained for specimens manufactured with MP mortar

were 752 f_k (CoV 0.38) and 902 f_k (CoV 0.25) and with MC mortar 443 f_k CoV 0.45) and 525 f_k (CoV 0.15), which are in accordance with the scientific literature.

The mortar-brick thickness ratio is a key issue when addressing the analysis of the mortar-induced tensile stress on the brick. In one leaf thin-tile masonry this ratio is lower than load-bearing brick masonry. The values of k, α and β proposed in the formula [11], from the experimental values of this study, present significant variations with respect to the scientific literature. Although the number of experimental test is limited, the achieved results, together with the reduction of tensile stress on the brick, appear to indicate that the values for k, α and β proposed in the scientific literature are not appropriate to determine the compressive strength of this type of masonry. Therefore, it is necessary to particularize the specific values for k, α and β for this type of masonry. To do this, it is imperative to perform a large number of tests, which is beyond the scope of the thesis.

Concerning multi-leaf thin-tile masonry

The stress-strain behaviour, until attaining the compressive strength corresponding to the onset of the detachment, is similar to the brick masonry loaded parallel to the bed joints. From this point until collapse, the vertical LVDTs exhibit unusual deformation that can be associated to potential rotation of the outer leaves.

For three-leaf thin-tile masonry, mortar has a clear influence of vertical deformation, until arriving to the detachment stress. On the other hand, it has no clear influence on the two-leaf masonry.

Horizontal deformation is influenced for both constitutive materials (mortar and thin-tile) in multi-leaf thin-tile masonry. In the detachment stress, specimens made of Portland cement mortar, present higher horizontal deformation than those build with hydraulic lime mortar.

The uniaxial detachment compressive strength in multi-leaf thin-tile masonry is of particular importance. Once this value is exceeded, and depending on the geometry and

compressive strength of the individual leaves, detachment phenomenon occurs. Thereafter, each leaf transfers the load individually, which does not prevent that may exist increases in stress at an assembly level.

The exponential formulation proposed by the standards for a brick masonry loaded parallel to the bed joints, seems to be only applicable to the case of a three-leaf thin-tile specimen. For this specific masonry arrangement the values for K, α, β are similar to those found in the literature, but with a more significant impact of the mortar on the overall strength of the thin-tile masonry.

The equation used to determine the compressive strength of the multi-leaf wall masonry appears to be applicable to the two-leaf thin-tile masonry. The value obtained for coefficient θi is high compared to the literature, while θe appears low when considering the detachment stress but reasonable for peak stress. In all cases the mortar leaf plays a key role. It seems more related to its ability to hold the different leaves together than to a possible contribution to compressive strength.

Concerning failure mode

The failure of the specimens of one-leaf, was caused either by the cracking, in those cases in which the failure was due to the tensile stress induced by the mortar, or by crushing, depending on the mechanical properties of the constituent materials. According to the literature, the observed behaviour follows the same patterns as brick masonry.

The failure mode of the multi-leaf thin-tile masonry is characterized by the appearance of a crack in the interface between brick and mortar that, in the long run, frees and separate the different leaves. At this point, the leaves transfer the load individually.

From the analysis of the deformation in both axes it could be established that the leaves of the masonry are detached due to the horizontal deformation (X axis) of the specimen.

Horizontal mortar joints present more deformation than mortar leaves, so it can be considered that the load is transmitted mainly through the thin-tile leaves.

The failure mode observed in all specimens (two- and three-leaf) show that the stress-displacement curves of cross sections have the same Y-displacement along the test, even during the formation of the crack, but it does not apply for the X-displacement. Due to the deformation of the horizontal mortar joints under vertical compression stresses, tensile stresses appear on the vertical interface between mortar and thin-tile adjacent to these areas. The tensile stress, in turn, causes cracks to appear which eventually lead to separation of the different leaves (mode I).

The final collapse of the assembly is linked to the buckling phenomenon, occurring once the leaves behave independently. The origin of the observed phenomenon is the transverse deformation of the horizontal mortar joints. When deformed, they exert a force perpendicular to the outermost vertical leaves, causing their rotation. The loss of verticality together with the effect of the vertical load they transfer, initiate a process without convergence that causes first instability and finally the failure.

According to the literature, detachment stress coincides with the full development of the crack in a thin-tile mortar interface. In this thesis, this point coincided with the end of the change of slope recorded by the horizontal LVDTs.

4.2. Perspectives and future work

The contribution of this thesis represents a step forward for the analysis of the behaviour under compressive stress parallel to bed joints of thin-tile masonry. Nevertheless, this approach requires further research. In this section, lines of extension and future works are suggested.

Unified theory.

In the thesis, there is not an analytical procedure capable of coping with the assessment of thin-tile masonry under compression, in a global way. The different configurations, one-leaf, two-leaf and the three-leaf assemblies, have been treated as independent issues. The analytical models analysed are mainly related on the compressive strength of the masonry components. For the one- and three -leaf masonry, the equation is focused on the thin-tile and mortar compressive strength, while for two-leaf it is based on the strength of the leaves. Develop a more unified theory would be of great interest.

Numerical modelling.

From the failure mode, it has been shown that collapse is achieved when the tensile stress in the vertical thin-tile-mortar interface exceeds the adhesive stress in that interface. Thus, a possible extension of this thesis could be to define a procedure to numerically model the complex behaviour happening around the zone of the onset of cracking.

Influence of number of leaves

In the tests carried out by Bergós, different stresses were already present, depending on the number of leaves. Hence, analysing the influence of the number of the leaves and their thickness, in the peak and detachment compressive strength, could be also, an issue of interest.

Bending behaviour and buckling phenomenon characterization

The Catalan vault, and from the elastic approach, is subject to bending stress. Although to a lesser extent, this type of masonry has been used to build of load-bearing walls. As well as compressive strength, a common problem in very thin walls is buckling. Consequently, a proper characterization on thin-tile elements in bending, would allow a deeper knowledge on this type of masonry. The same happen with buckling phenomenon. There is a huge field of application in repairing if the scientists and technicians could have at disposal such kind of tools.

5. References

Antoine, A. 1992. *In-Plane Behaviour of Masonry:A Literature Review*. Luxembourg: Comission of European Communities: Industrial processes.

Atamturktur, S., and T.E. Boothby. 2007. "Finite Element Modeling of Guastavino Domes." *Bulletin of the Association for Preservation Technology* 28: 21–29.

Augenti, N., and F. Parisi. 2010. "Constitutive Models for Tuff Masonry under Uniaxial Compression." *Journal of Materials in Civil Engineering* 22 (11): 1102–11. https://doi.org/10.1061/(ASCE)MT.1943-5533.0000119.

Badarloo, B., A.A. Tasnimi, and M.S. Mohammadi. 2009. "Failure Criteria of Unreinforced Grouted Brick Masonry Based on a Biaxial Compression Test." *Scientia Iranica Transaction A-Civil Engineering* 16 (6): 502–11.

Barbosa, C.S., P.B. Lourenço, and J.B. Hanai. 2009. "On the Compressive Strength Prediction for Concrete Masonry Prisms." *Materials and Structures* 43 (3): 331–44. https://doi.org/10.1617/s11527-009-9492-0.

Barris, C., L. Torres, I. Vilanova, C. Miàs, and M. Llorens. 2017. "Experimental Study on Crack Width and Crack Spacing for Glass-FRP Reinforced Concrete Beams." *Engineering Structures* 131 (January): 231–42. https://doi.org/10.1016/j.engstruct.2016.11.007.

Bayó, J. 1910. "La Bóveda Tabicada." In *Anuario Asociación de Arquitectos de Catalunya.*, 157–84.

Benfratello, S., G. Caiozzo, M. D'Avenia, and L. Palizzolo. 2012. "Tradition and Modernity of Catalan Vaults: Historical and Structural Analysis." *Meccanica Dei Materiali e Delle Strutture , University of Palermo* 3 (5): 44–54.

Benfratello, S., L. Palizzolo, F. Giambanco, and M. D'Avenia. 2010. "On the Analysis of Catalan Thin Vaults." Edited by Estonia W.P. De WILDE, Free University of Brussels, Belgium, C.A. Brebbia, Wessex Institute of Technology, UK and U. MANDER, University of Tartu. *WIT Transactions on the Built Environment*

112: 453–64. http://library.witpress.com/viewpaper.asp?pcode=HPSM10-042-1.

Bergós, J. 1953. *Materiales y Elementos de Construcción.Estudio Experimental*. Barcelona.

———. 1965. *Tabicados Huecos.* Edited by Col·legi Oficial d'Arquitectes de Catalunya i Balears. Barcelone.

Binda, L., A. Fontana, and G. Frigerio. 1988. "Mechanical Behaviour of Brick Masonries Derived from Unit and Mortar Characteristics." In *8th International Brick and Block Masonry Conference*, 205–16. Dublin. https://doi.org/10.1017/CBO9781107415324.004.

Binda, L., J. Pina-Henriques, A. Anzani, A. Fontana, and P.B. Lourenço. 2006. "A Contribution for the Understanding of Load-Transfer Mechanisms in Multi-Leaf Masonry Walls: Testing and Modelling." *Engineering Structures* 28 (8): 1132–48. https://doi.org/10.1016/j.engstruct.2005.12.004.

Block, P., T. Ciblac, and J. Ochsendorf. 2006. "Real-Time Limit Analysis of Vaulted Masonry Buildings." *Computers and Structures* 84 (29–30): 1841–52. https://doi.org/10.1016/j.compstruc.2006.08.002.

Block, P., and L. Lachauer. 2014. "Three-Dimensional Funicular Analysis of Masonry Vaults." *Mechanics Research Communications* 56: 53–60. https://doi.org/10.1016/j.mechrescom.2013.11.010.

Block, P., and J. Ochsendorf. 2007. "Thrust Network Analysis: A New Methodology for Three-Dimensional Equilibrium." In *Journal of the International Association for Shell and Spatial Structures*, 48:167–73.

Bosch, I. 1949. "La Boveda Vaida Tabicada." *Revista Nacional de Arquitectura*, 1949.

Cabrera, A., M. Sala, and C. Jordi. 2005. *Les Voltes de Quatre Punts. Estudi Constructiu i Estructural de Les Cases Barates.* Girona: University of Girona. Department of Architecture and Construction Engineering.

Capozucca, R. 1997. "Analysis of Thin Composite Masonry Vaults." *Masonry International Journal Papers* 11: 19–25.

———. 2004. "Masonry Panels with Different Mortar Joints under Compression." In *13th International Brick and Block Masonry Conference*, edited by 2004 Eindhoven University of Technology, 27–34. Amsterdam.

———. 2017. "Experimental Response of Historic Brick Masonry under Biaxial Loading." *Construction and Building Materials* 154: 539–56. https://doi.org/10.1016/j.conbuildmat.2017.07.186.

Cardellach, F. 1910. *Filosofía de Las Estructuras. Filiación Racional de Las Formas Resistentes Empleadas En La Ingeniería y En La Arquitectura Histórica y Moderna.* Barcelona: Libreria de Agustin Bosch.

Carozzi, F.G., C. Poggi, E. Bertolesi, and G. Milani. 2018. "Ancient Masonry Arches and Vaults Strengthened with TRM, SRG and FRP Composites: Experimental Evaluation." *Composite Structures* 187: 466–80. https://doi.org/10.1016/j.compstruct.2017.12.075.

Castori, G., A. Borri, and M. Corradi. 2016. "Behavior of Thin Masonry Arches Repaired Using Composite

Materials." *Composites Part B: Engineering* 87: 311–21. https://doi.org/10.1016/j.compositesb.2015.09.008.

Chamorro, M.A., J. Llorens, and M. Llorens. 2012. "Ignasi Bosch i Reitg (1910-1985): Una Patente Para Construir Bóvedas Tabicadas." In *Construyendo Bóvedas Tabicadas. Actas Del Simposio Internacional Sobre Bóvedas Tabicadas (2011)*, edited by Universidad Politécnica de València, 238–47. Valencia: Arturo Zaragozá;Rafael Soler;Rafael Marin.

Choisy, A. 1899. *Historie de l'architecture.Tome 1*. Edited by Gauthier-Villars. Paris. https://gallica.bnf.fr/ark:/12148/bpt6k6417116t/f537.item.texteImage.

Collins, G. R. 1968. "The Transfer of Thin Masonry Vaulting from Spain to America." *Journal of the Society of Architectural Historians* 27 (nº3): 176–201.

Costigan, A., S. Pavía, and O. Kinnane. 2015. "An Experimental Evaluation of Prediction Models for the Mechanical Behavior of Unreinforced, Lime-Mortar Masonry under Compression." *Journal of Building Engineering* 4: 283–94. https://doi.org/10.1016/j.jobe.2015.10.001.

CTE. SE-F. 2009. "Codigo Técnico de La Edificación. Documento Básico SE-F Seguridad Estructural: Fábrica." Madrid: Ministerio de Vivienda.

D'Altri, A.M., V. Sarhosis, G. Milani, J. Rots, S. Cattari, S. Lagomarsino, E. Sacco, A. Tralli, G. Castellazzi, and S. De Miranda. 2019. "Modeling Strategies for the Computational Analysis of Unreinforced Masonry Structures: Review and Classification." *Archives of Computational Methods in Engineering*. https://doi.org/10.1007/s11831-019-09351-x.

Davis, L., M. Rippmann, T. Pawlofsky, and P. Block. 2012. "Innovative Funicular Tile Vaulting: A Prototype Vault in Switzerland." *Structural Engineer* 90 (11): 46–56.

Dayaratnam, P. 1987. *Brick and Reinforced Brick Structures*. New Delhi: M. Primlani for Oxford & IBH Pub. Co.

Demir, C., and A. Ilki. 2014. "Characterization of the Materials Used in the Multi-Leaf Masonry Walls of Monumental Structures in Istanbul, Turkey." *Construction and Building Materials* 64: 398–413. https://doi.org/10.1016/j.conbuildmat.2014.04.099.

Dhanasekar, M., P.W. Kleeman, and A.W. Page. 1985. "Biaxial Stress-Strain Relations for Brick Masonry." *Journal of Structural Engineering* 111 (5): 1085–1100. https://doi.org/10.1061/(ASCE)0733-9445(1985)111:5(1085).

Domède, N, G Pons, A Sellier, and Y Fritih. 2009. "Mechanical Behaviour of Ancient Masonry." *Mater Struct* 42 (1): 123–33. https://doi.org/10.1617/s11527-008-9372-z.

Domenech, J. 1900. "La Fábrica de Ladrillo En La Construcción Catalana." In *Anuario de La Asociación de Arquitectios de Catalunya*, 37–48.

Drougkas, A., P. Roca, and C. Molins. 2015. “Numerical Prediction of the Behavior, Strength and Elasticity of Masonry in Compression.” *Engineering Structures* 90 (May): 15–28. https://doi.org/10.1016/j.engstruct.2015.02.011.

Drougkas, A., P. Roca, C. Molins, and V. Alegre. 2015. “Compressive Testing of an Early 20th Century Brick Masonry Pillar.” *Materials and Structures/Materiaux et Constructions* 49 (6): 2367–81. https://doi.org/10.1617/s11527-015-0654-y.

Drysdale, R.G., and A.A. Hamid. 1982. “Anisotropic Tensile Strength Characteristics of Brick Masonry.” In *Sixth International Brick Masonry Conference*, 143–53. Rome.

EC-6. 1996. “Eurocode 6 - Design of Masonry Structures.”

Egermann, R. 1993. “Investigation on the Load Bearing Behaviour of Multiple Leaf Masonry.” *IABSE Reports = Rapports AIPC = IVBH Berichte* 70. https://doi.org/http://dx.doi.org/10.5169/seals-53311 Detailed information.

Egermann, R., B. Frick, and C. Neuwald-Burg. 1993. “Analytical and Experimental Approach to the Load Bearing Behaviour of Multiple Leaf Masonry.” *Transactions on the Built Environment Vol 4, © 1993 WIT Press, Www.Witpress.Com, ISSN 1743-3509* 4. http://www.ncbi.nlm.nih.gov/entrez/query.fcgi?cmd=Retrieve&db=PubMed&dopt=Citation&list_uids=17363372.

Egermann, R., and C. Neuwald-Burg. 1994. “Assessment of the Load Bearing Capacity of Historic Multiple Leaf Masonry Walls.” In *10th International Brick and Block Masonary Conference*, 1603–12.

Endo, Y., M. Llorens, P. Roca, and L. Pelà. 2017. “Dynamic Identification and Static Loading Tests of Timbrel Vaults: Application to a Modernist 20th Century Heritage Structure.” *International Journal of Architectural Heritage* 11 (4): 607–20. https://doi.org/10.1080/15583058.2016.1277566.

Fantin, M., and T. Ciblac. 2016. “Extension of Thrust Network Analysis with Joints Consideration and New Equilibrium States.” *International Journal of Space Structures* 31 (2–4): 190–202. https://doi.org/10.1177/0266351116661814.

Flügge, W. 1973. *Stresses in Shells*. 2on ed. New York: Springer Berlin Heidelberg. https://doi.org/10.1007/978-3-642-88291-3.

Fonseca, F.S., G. Mohamad, P.B. Lourenço, H.R. Roman, and A.T. Vermeltfoort. 2015. “Deformation and Failure Mode of Masonry.” In *12th North American Masonry Conference Masonry: Science • Craft • Art Denver, Colorado*.

Fortea, M., and R. Machado. 2014. “Diagnose and Repair of Domed Elements of Masonry.” In *Construction and Building Research*. https://doi.org/10.1007/978-94-007-7790-3_49.

Foti, P., A. Fraddosio, N. Lepore, and M.D. Piccioni. 2016. “Three-Dimensional Lower-Bound Analysis of

Masonry Structures." In *Structures and Architecture - Proceedings of the 3rd International Conference on Structures and Architecture, ICSA 2016*, 558–66.

Fraddosio, A., N. Lepore, and M.D. Piccioni. 2019. "Lower Bound Limit Analysis of Masonry Vaults Under General Load Conditions." In *RILEM Bookseries*, 18:1090–98. Springer Netherlands. https://doi.org/10.1007/978-3-319-99441-3_118.

Francis, J., C.B. Horman, and L.E. Jerrens. 1971. "The Effect of Joint Thickness and Other Factors on the Compressive Strength of Brickwork." In *Proc. Of the 2nd International Brick Masonry Conference*, 31–37. Stoke on Kent.

Freire, M.J. 2011. "Modelizaciones Elásticas y Plásticas e Inestabilidad de Elementos Estructurales Verticales de Fábrica." Escuela Técnica Superior de Arquitectura de a Coruña.

Fusade, L., and H. Viles. 2018. "A Comparison of Standard and Realistic Curing Conditions of Natural Hydraulic Lime Repointing Mortar for Damp Masonry: Impact on Laboratory Evaluation." *Journal of Cultural Heritage*, December. https://doi.org/10.1016/j.culher.2018.11.011.

Galman, I. 2016. "Influence of Load Direction on Behaviour and Mechanical Parameters of Clay-Brick Masonry Walls under Cyclic Compression." *Architecture Civil Engineering Environment*.

García, D., J.T. San-Jose, L. Garmendia, and R. San-Mateos. 2012. "Experimental Study of Traditional Stone Masonry under Compressive Load and Comparison of Results with Design Codes." *MATERIALS AND STRUCTURES* 45 (7): 995–1006. https://doi.org/10.1617/s11527-011-9812-z.

Gonzalez, J.L. 2004. "La Bóveda Tabicada: Pasado y Futuro de Un Elemento de Gran Valor Patrimonial." In *In Prologue of Truño, A. Construcción de Bóvedas Tabicadas*, 11–60. Madrid: INSTITUTO JUAN DE HERRERA.

Guastavino, R. 1893. *Essay on the Theory and History of Cohesive Construction, Applied Especially to the Timbrel Vaults*. Edited by TICKNOR AND COMPANY. Boston.

Gulli, R., and G. Mochi. 1995. *Bóvedas Tabicadas : Architettura e Costruzione*. Rome: CDP Editrice. http://ccuc.cbuc.cat/record=b1911979~S23*cat.

Gumaste, K. S., K. S. Nanjunda Rao, B. V. Venkatarama Reddy, and K. S. Jagadish. 2007. "Strength and Elasticity of Brick Masonry Prisms and Wallettes under Compression." *Materials and Structures* 40 (2): 241–53. https://doi.org/10.1617/s11527-006-9141-9.

Hamid, A.A., W.W. El-Dakhakhni, Z.H.R. Hakam, and M. Elgaaly. 2005. "Behavior of Composite Unreinforced Masonry-Fiber-Reinforced Polymer Wall Assemblages under in-Plane Loading." *Journal of Composites for Construction* 9 (1): 73–83. https://doi.org/10.1061/(ASCE)1090-0268(2005)9:1(73).

Heyman, J. 1966. "The Stone Skeleton." *International Journal of Solids and Structures* 2 (2): 249–79. https://doi.org/10.1016/0020-7683(66)90018-7.

Hilsdorf, H.K. 1969. “Investigation into the Failure Mechanism of Brick Masonry Loaded in Axial Compression.” In *Designing, Engineering, and Constructing with Masonry Products*, edited by F.B. Johnson, 34–41. Huston, Texas: Gulf Publishing Company. https://doi.org/10.1016/B978-0-12-530990-5.50005-5.

Hodgkinson, H.R., and S. Davies. 1982. “The Stress Strain Relationships of Brickwork When Stressed in Oirections Other than Normal to the Bed Face.” In *6th IBMAC*, 290–99. Rome.

Hoffmann, G., and P. Schubert. 1994. “Compressive Strength of Masonry Parallel to the Bed Joints.” In *Proceedings of 10th International Brick and Block Conference*, 1453–62.

Huerta, S. 2001. “Mechanics of Masonry Vaults: The Equilibrium Approach.” *3rd International Seminar in Historical Constructions, Guimarães, Portugal*, 47–70.

———. 2003. “The Mechanics of Timbrel Vaults: A Historical Outline.” In *Essays on the History of Mechanics*, 89–134. Birkhäuser, Basel. https://doi.org/10.1007/978-3-0348-8091-6_5.

———. 2004. *Arcos, Bóvedas y Cúpulas. Geometría y Equilibrio En El Cálculo Tradicional de Estructuras de Fábrica*. Madrid: INSTITUTO JUAN DE HERRERA. http://oa.upm.es/1136/1/Huerta_2004_Arcos_bovedas_y_cupulas.pdf.

———. 2005. “Mecánica de Las Bóvedas Tabicadas.” *Arquitectura COAM* 339: 102–11.

———. 2006. “La Construcción Tabicada y La Teoría Cohesiva de Rafael Guastavino.” In *Escritos Sobre La Construcción Cohesiva y Su Función En La Arquitectura*.

Kaushik, H.B., D.C. Rai, and S.K. Jain. 2007a. “Stress-Strain Characteristics of Clay Brick Masonry under Uniaxial Compression.” *Journal of Materials in Civil Engineering* 19 (9): 728–39. https://doi.org/10.1061/(ASCE)0899-1561(2007)19:9(728).

———. 2007b. “Uniaxial Compressive Stress-Strain Model for Clay Brick Masonry.” *Current Science* 92 (4): 497–501. http://www.iisc.ernet.in/currsci/feb252007/497.pdf.

Knutsson, H.H. 1993. “The Stress-Strain Relationship for Masonry.” *Masonry International* 07. http://www.masonry.org.uk/index.php/masonry/publications/masonry_international/masonry_international_papers/volume_07/the_stress_strain_relationship_for_masonry.

Lanas, J., J.L. Pérez, M.A. Bello, and J.I. Alvarez. 2004. “Mechanical Properties of Natural Hydraulic Lime-Based Mortars.” *Cement and Concrete Research* 34 (12): 2191–2201. https://doi.org/10.1016/j.cemconres.2004.02.005.

Llopis, V., A. Alonso, E. Fenollosa, and A. Martínez. 2016. “Análisis Constructivo y Estructural de La Catedral de Valencia.” *Informes de La Construcción*. https://doi.org/10.3989/ic.15.102.

López, D., P. Roca, A. Liew, T. Van Mele, and P. Block. 2019. “Tile Vaults as Integrated Formwork for Reinforced Concrete: Construction, Experimental Testing and a Method for the Design and Analysis of

Two-Dimensional Structures." *Engineering Structures*. https://doi.org/10.1016/j.engstruct.2019.03.034.

Lorenzis, L. De, R. Dimitri, and A. La Tegola. 2007. "Reduction of the Lateral Thrust of Masonry Arches and Vaults with FRP Composites." *Construction and Building Materials*. https://doi.org/10.1016/j.conbuildmat.2006.07.009.

Lourenço, P.B. 1998. "Experimental and Numerical Issues in the Modelling of the Mechanical Behaviour of Masonry." In *Structural Analysis of Historical Constructions II*, edited by P Roca, J L González, E Oñate, and P B Lourenço, 57–91. Barcelona: Cimne.

Marmo, Francesco, Daniele Masi, Salvatore Sessa, Ferdinando Toraldo, and Luciano Rosati. 2017. "Thrust Network Analysis of Masonry Vaults Subject to Vertical and Horizontal Loads." In *COMPDYN 2017 - Proceedings of the 6th International Conference on Computational Methods in Structural Dynamics and Earthquake Engineering*, 1:2227–38. https://doi.org/10.7712/120117.5562.17018.

Martinez, J.L. 2003. "Determinación Teórica y Experimental de Diagramas de Interacción de Esfuerzos En Estructuras de Fábrica y Aplicación Al Análisis de Construcciones Históricas." Universidad Politécnica de Madrid.

McNary, W. S., and D.P. Abrams. 1985. "Mechanics of Masonry in Compression." *Journal of Structural Engineering* 111 (4): 857–70. https://doi.org/10.1061/(ASCE)0733-9445(1985)111:4(857).

Mohamad, G., P.B. Lourenço, and H.R. Roman. 2007. "Mechanics of Hollow Concrete Block Masonry Prisms under Compression: Review and Prospects." *Cement and Concrete Composites* 29 (3): 181–92. https://doi.org/10.1016/j.cemconcomp.2006.11.003.

Mosalam, K., L. Glascoe, and J. Bernier. 2009. "Mechanical Properties of Unreinforced Brick Masonry , Section1." https://doi.org/10.2172/966219.

Moya, L. 1947. *Bóvedas Tabicadas*. Dirección General de Arquitectura. http://oa.upm.es/38027/.

Mroszczzyk, L. 2004. "Rafael Guastavino and the Boston Public Library."

Naraine, K., and S. Sinha. 1989. "Behavior of Brick Masonry Under Cyclic Compressive Loading." *J. Struct. Eng.* 115 (6): 1432–45. https://doi.org/10.1061/(ASCE)0733-9445(1989)115:6(1432).

Nghiem, H.L., M. Al Heib, and F. Emeriault. 2015. "Method Based on Digital Image Correlation for Damage Assessment in Masonry Structures." *Engineering Structures* 86 (March): 1–15. https://doi.org/10.1016/j.engstruct.2014.12.021.

Nwofor, T.C. 2012. "Experimental Determination of the Mechanical Properties of Clay Brick Masonry." *Canadian Journal on Environmental, Construction and Civil Engineering* 3 (3): 127–45.

Ohler, A. 1986. "Calculation of Masonry Compressive Strength Considering the Multi-Axle States of Stress in Units and Mortar." *Bautechnik 5*.

Oliveira, D.V., R.A. Silva, E. Garbin, and P.B. Lourenço. 2012. “Strengthening of Three-Leaf Stone Masonry Walls: An Experimental Research.” *Materials and Structures* 45 (8): 1259–76. https://doi.org/10.1617/s11527-012-9832-3.

Page, A.W. 1981. “The Biaxial Compressive Strength of Brick Masonry.” *ICE Proceedings* 71 (3): 893–906. https://doi.org/10.1680/iicep.1981.1825.

Palizzolo, L., S. Benfratello, A. Caffarelli, F. Giambanco, and R. Urso. 2008. “Bovedas Tabicadas: Experimental and Numerical Analysis.” *WIT Transactions on the Built Environment* 97: 503–12. https://doi.org/10.2495/HPSM080511.

Pappas, A. 2012. “Calibration of the Numerical Material Behaviour of Multi-Leaf Stone Masonry Walls Based on Experimental Results.”

Ravula, M.B., and K.V.L. Subramaniam. 2017. “Experimental Investigation of Compressive Failure in Masonry Brick Assemblages Made with Soft Brick.” *Materials and Structures* 50 (1): 19. https://doi.org/10.1617/s11527-016-0926-1.

Redondo, E. 2013. “La Bóveda Tabicada En España En El Siglo XIX: La Transformación de Un Sistema Constructivo.” E.T.S. Arquitectura (UPM). http://oa.upm.es/22064/.

Ricci, E., A. Fraddosio, M.D. Piccioni, and E. Sacco. 2019. “A New Numerical Approach for Determining Optimal Thrust Curves of Masonry Arches.” *European Journal of Mechanics, A/Solids* 75 (May): 426–42. https://doi.org/10.1016/j.euromechsol.2019.02.003.

RILEM. 1991. “LUM B1.Compressive Strength of Small Walls and Prisms.”

Roca, P., M. Cervera, G. Gariup, and L. Pelà. 2010. “Structural Analysis of Masonry Historical Constructions. Classical and Advanced Approaches.” *Archives of Computational Methods in Engineering*. https://doi.org/10.1007/s11831-010-9046-1.

Rosell, J., and I. Serrà. 1987. “Estudis d’Esteve Terrades Sobre La Volta de Maó de Pla.” In *Cinquanta Anys de Ciència i Tècnica a Catalunya : Entorn l’activitat Científica d’E. Terrades (1883-1950) : (27 i 28 de Setembre Del 1984)*, edited by Institut d’Estudis Catalans (IEC), 13–22. http://hdl.handle.net/2117/9370.

Salmanpour, A.H., and N. Mojsilović. 2013. “Application of Digital Image Correlation for Strain Measurements of Large Masonry Walls.” *In: Proceedings of the 5th Asia Pacific Congress on Computational Mechanics*.

Samarasinghe, W. 1980. “The In-Plane Failure of Brickwork.” The University of Edinburgh. http://hdl.handle.net/1842/8315.

Samarasinghe, W., A.W. Page, and A.W. Hendry. 1982. “A Finite Element Model for the In-Plane Behaviour of Brickwork.” In *Proceedings of the Institution of Civil Engineers*, 171–78. https://doi.org/https://doi.org/10.1680/iicep.1982.1878.

Sandoval, C., and P. Roca. 2012. “Study of the Influence of Different Parameters on the Buckling Behaviour of Masonry Walls.” *Construction and Building Materials* 35: 888–99. https://doi.org/10.1016/j.conbuildmat.2012.04.053.

Sandoval, C., P. Roca, E. Bernat, and L. Gil. 2011. “Testing and Numerical Modelling of Buckling Failure of Masonry Walls.” *Construction and Building Materials* 25 (12): 4394–4402. https://doi.org/10.1016/j.conbuildmat.2011.01.007.

Santis, S. De, G. De Felice, and F. Roscini. 2019. “Retrofitting of Masonry Vaults by Basalt Textile-Reinforced Mortar Overlays.” *International Journal of Architectural Heritage*. https://doi.org/10.1080/15583058.2019.1597947.

Sassoni, E., C. Mazzotti, and G. Pagliai. 2014. “Comparison between Experimental Methods for Evaluating the Compressive Strength of Existing Masonry Buildings.” *Construction and Building Materials* 68 (October): 206–19. https://doi.org/10.1016/j.conbuildmat.2014.06.070.

Senthivel, R., S.N. Sinha, and A. Madan. 2000. “Influence of Bed Joint Orientation on the Stress-Strain Characteristics of Sand Plast Brick Masonry under Uniaxial Compression and Tension.” In *12th International Brick/Block Masonry Conference*, edited by Construction and Architectonic Technology Department of the Polytechnic Unversity of Madrid, 1655–66. Madrid.

Shin, H.V., C.F. Porst, E. Vouga, J. Ochsendorf, and F. Durand. 2016. “Reconciling Elastic and Equilibrium Methods: For Static Analysis.” *ACM Transactions on Graphics* 35 (2). https://doi.org/10.1145/2835173.

Singh, B.K., and S.N. Shina. 2004. “Energy Dissipation in Interlocking Grouted Stabilised Mud Block Masonry under Cyclic Uniaxial Compressive Loading.” In *13th International Brick and Block Masonry Conference*, 201–8. Amsterdam: Eindhoven University of Technology, 2004.

Sousa, R., and H. Sousa. 2010. “Experimental Evaluation of Some Mechanical Properties of Large Lightweight Concrete and Clay Masonry and Comparison with EC6 Expressions.” In *Eighth International Masonry Conference*, 545–54. Dresden.

Stavroulaki, M., and A. Papalou. 2014. “Parametric Analysis of Old Multi-Leaf Masonry Walls.” *International Journal of Conservation Science* 5 (4).

Suárez, F. 2015. “Intuition, Reason and Calculation on the Structural Analysis of a Ribbed Vault.” *Informes de La Construccion*. https://doi.org/10.3989/ic.14.100.

Tassios, T.P. 1988. “Meccanica Delle Murature.” In . Napoli: Liguori Editore.

———. 2004. “Recupero Di Murature Tri-Strato.” In *Evoluzione Nella Sperimentazione per Le Costruzioni*, 281–302. http://www.4emme.it/PDF/43.pdf.

———. 2013. “Centro Internazionale Di Aggiornamento Sperimentale – Scientifico.” In *EVOLUZIONE NELLA SPERIMENTAZIONE PER LE COSTRUZIONI*. Creta. http://www.cias-

italia.it/index.php?option=com_content&view=article&id=16&Itemid=163.

Tralli, A., C. Alessandri, and G. Milani. 2014. “Computational Methods for Masonry Vaults: A Review of Recent Results.” *The Open Civil Engineering Journal* 8 (1): 272–87. https://doi.org/10.2174/1874149501408010272.

Tung, S.H., M.H. Shih, and W.P. Sung. 2008. “Development of Digital Image Correlation Method to Analyse Crack Variations of Masonry Wall.” *Sadhana - Academy Proceedings in Engineering Sciences*. https://doi.org/10.1007/s12046-008-0033-2.

UNE-EN 772-1. 2016. “UNE-EN 772-1:2011+A1:2016. Methods of Test for Masonry Units - Part 1: Determination of Compressive Strength.”

UNE-EN 772-16. 2011. “UNE-EN 772-16:2011. Methods of Test for Masonry Units - Part 16: Determination of Dimensions.”

UNE EN 1015-11. 2014. “UNE EN 1015-11:2000/A1:2007. Methods of Test for Mortar for Masonry-Part 11: Determination of Flexural and Compressive Strength of Hardened Mortar.”

UNE EN 1052-1. 2014. “UNE EN 1052-1:1999. Methods of Test for Masonry-Part 1: Determination of Compressive Strength.”

Valluzzi, M.R., F. Da Porto, and C. Modena. 2004. “Behavior and Modeling of Strengthened Three-Leaf Stone Masonry Walls.” *Materials and Structures* 37 (April): 184–92. http://link.springer.com/article/10.1007/BF02481618.

Vintzileou, E. 2007. “Grouting of Three-Leaf Masonry: Experimental Results and Prediction of Mechanical Properties.” *Evoluzione Nella Sperimentazione per Le Costruzioni, …*, 171–90. http://scholar.google.com/scholar?hl=en&btnG=Search&q=intitle:GROUTING+OF+THREE-LEAF+MASONRY+:+EXPERIMENTAL+RESULTS+AND+PREDICTION+OF+MECHANICAL+PROPERTIES#0.

———. 2011. “Three-Leaf Masonry in Compression, Before and After Grouting: A Review of Literature.” *International Journal of Architectural Heritage* 5 (4–5): 513–38. https://doi.org/10.1080/15583058.2011.557137.

Vintzileou, E., and T.P. Tassios. 1995. “Three-Leaf Stone Masonry Strengthened by Injecting Cement Grouts.” *Journal of Structural Engineering* 121 (5): 848–56. https://doi.org/10.1061/(ASCE)0733-9445(1995)121:5(848).

Zucchini, A., and P.B. Lourenço. 2007. “Mechanics of Masonry in Compression: Results from a Homogenisation Approach.” *Computers and Structures* 85 (3–4): 193–204. https://doi.org/10.1016/j.compstruc.2006.08.054.